November 2016

Label-free and Aptamer-based Surface Enhanced Raman Spectroscopy for Detection of Food Contaminants

Shintaro Pang

LABEL-FREE AND APTAMER-BASED SURFACE ENHANCED RAMAN SPECTROSCOPY FOR DETECTION OF FOOD CONTAMINANTS

A Dissertation Presented

by

SHINTARO PANG

Submitted to the Graduate School of the
University of Massachusetts Amherst in partial fulfillment
of the requirements for the degree of

DOCTOR OF PHILOSOPHY

SEPTEMBER 2016

Department of Food Science

LABEL-FREE AND APTAMER-BASED SURFACE-ENHANCED RAMAN SPECTROSCOPY FOR DETECTION OF FOOD CONTAMINANTS

A Dissertation Presented

by

SHINTARO PANG

Approved as to style and content by:

_____
Lili He, Chair

_____
D. Julian McClements, Member

_____
Eric A. Decker, Member

_____
Wei Fan, Member

_____
Eric A. Decker, Department Head
Department of Food Science

DEDICATION

To my lovely wife, Mana, who supported me throughout my PhD studies.

ACKNOWLEDGMENTS

I would like to first thank my PhD advisor, Professor Lili He, for all the resources she provided me with to complete my PhD studies. Her cheerful personality and optimistic attitude towards research is remarkable, and I am constantly impressed by her innovative ideas to tackle project challenges. I am also very grateful to her for teaching me how to work "smart" and to maintain a good work-life balance. The lessons I have learnt from her will stay with me throughout my life and I hope to continue in her footsteps. I would also like to thank my committee members, Professors Eric Decker, Julian McClements and Wei Fan for their constructive feedback and advice on my research. It was an honor to discuss my projects with you and to tap on the "best minds" in their respective fields.

My next big thanks go out to all of my peers and collaborators, whom I enjoyed working with on a day-to-day basis. I would like to especially thank my lab colleagues, Changchu Ma, Jinkai Zheng, Wisiani Wijaya, Victoria Boushell, Tingting Lang, Ruyan Hou, Panxue Wang, Juhong Chen and Bin Zhao, who not only kept me company to discuss research-related topics, but worked diligently together to publish peer-reviewed scientific publications. I am also grateful to the rest of my collaborators, Drs. Theodore Labuza, Naijie Zhang and Paul Dornath whom I had the pleasure to work with. In addition, l would like to thank the many individuals in Professor He's lab, food science department, other departments (especially polymer science) and other institutions, who

provided the training and resources necessary for me to obtain the heaps of data contained in this theses.

I am also thankful for the guidance of my undergraduate research mentor, Dr. Michael Dunn, from Brigham Young University, who took me in as his research assistant when I was only a freshman; he laid the foundation for me to broaden my skills and interest in food science research. Special thanks to Dr. Frost Steele for his sound and non-judgmental career advice, which played a significant role in my decision to pursue a doctorate degree here.

I would also like to express my deepest gratitude to my parents, Meng Hock and Reiko Pang, for raising me with unconditional love and support. I thank them for stressing the importance of education and for providing the best resources to help me study. Next, I would like to thank my wife, Mana. Words cannot express how much I appreciate the love, care and moral support she gave me while I went to college and graduate school. Thank you for sacrificing all that you had, including your job and studies, to come to the United States to support me as a student while raising our three beautiful children, Kennosuke, Yuri and Daiki, who have been our joy and treasure. Your actions are a true representation of what charity, the pure love of Christ, means to me.

Last but not least, I thank my Heavenly Father for all the learning opportunities he has given me, including this research study experience.

ABSTRACT

LABEL-FREE AND APTAMER-BASED SURFACE-ENHANCED RAMAN SPECTROSCOPY FOR DETECTION OF FOOD CONTAMINANTS

SEPTEMBER 2016

SHINTARO PANG, B.S., BRIGHAM YOUNG UNIVERSITY

Ph.D., UNIVERSITY OF MASSACHUSETTS AMHERST

Directed by: Professor Lili He

The development of analytical methods to detect food contaminants is a critical step for improving food safety. Surface enhanced Raman spectroscopy (SERS) is an emerging detection technology that has the potential to rapidly, accurately and sensitively detect a wide variety of food contaminants. However, SERS detection becomes a challenge in real complex matrix, such as food, since non-specific matrix signals have the potential to drown out target associated Raman peaks. In this dissertation, we focused on the development and application of label-free, aptamer-based SERS in order to improve the accuracy and specificity of target contaminant detection in food. To accomplish this, different types of aptamer-modified SERS substrates (i.e. thiolated or non-thiolated ssDNA aptamers conjugated onto silver dendrites, gold-coated magnetic nanoparticles, gold nanoparticles and gold nanoparticles coated magnetic nanoparticles) were tested in liquid foods (e.g. apple juice and milk) to detect a variety of food contaminants including pesticides, antibiotics and foodborne pathogens. Next, an integration of aptamer-based SERS and aptamer-assisted colorimetric detection was attempted using gold nanoparticles as the substrate to create a rapid detection-validation protocol. Finally, we attempted to create a simple SELEX method that could be used to design aptamers for

food safety applications. Our results demonstrate that aptamer-based SERS is capable of detecting a variety of aptamer-specific food contaminants while drastically reducing Raman signal interference from food matrix. Thus, this method shows great potential as a rapid detection method in food, especially since sample extraction procedure can be simplified. Aptamer-based SERS method can also be used to validate results from the gold nanoparticles based colorimetric assays. It can help us understand the intermolecular interactions that govern the mechanism and successful interpretation of the colorimetric results, which can then reduce false positive and false negative results. Lastly, several breakthroughs were achieved using the developed "gold nanoparticle-assisted SELEX" procedure. This is promising to design a wider variety of target specific aptamers without the need for large, specialized equipment. By advancing the completion of this SELEX method, there is great potential for creating more label-free, aptamer-based SERS methods for food contamination detection and to improve food safety as a whole.

TABLE OF CONTENTS

Page

ACKNOWLEDGMENTS v

ABSTRACT vii

LIST OF TABLES xiii

LIST OF FIGURES xiv

CHAPTER

1. INTRODUCTION 1

    1.1 Background 1

    1.2 Objectives 3

2. LITERATURE REVIEW 6

    2.1 Surface-enhanced Raman Spectroscopy 6

        2.1.1 Background 6

        2.1.2 Factors to Consider in SERS detection 9

        2.1.3 Application of SERS in food contaminant detection 14

    2.2 Aptamer-based biosensing 23

3. DEVELOPMENT OF A SINGLE APTAMER-BASED SURFACE ENHANCED RAMAN SCATTERING METHOD FOR RAPID DETECTION OF MULTIPLE PESTICIDES 26

    3.1 Abstract 26

    3.2 Introduction 27

    3.3 Materials and Method 30

        3.3.1 Materials 30

        3.3.2 Preparation of dendritic silver (Ag) nanoparticles 30

        3.3.3 Conjugation of deprotected aptamer onto Ag dendrites 31

3.3.4 Addition of blocker molecule (i.e. 6-mercaptohexanol) onto silver-aptamer complex (Ag-Ap) 32
3.3.5 Detection of multiple specific pesticides using aptamer-based SERS 32
3.3.6 Raman instrumentation 33
3.3.7 Data analysis 33
3.4 Results and Discussion 34
3.4.1 Optimization of aptamer conjugation with Ag 34
3.4.2 Optimization of MH concentration and incubation time with Ag-Ap 36
3.4.3 Detection of multiple pesticides using Ag-(Ap+MH) 39
3.4.4 Determination of the limit of detection and quantitative capability of this method 42
3.4.5 Method validation in apple juice to ensure elimination of non-specific binding and applicability in food matrix 44
3.5 Conclusion 46
3.6 Supplementary Figures 47
4. LABEL-FREE, APTAMER BASED SERS DETECTION OF *SALMONELLA ENTERITIDIS* AND *LISTERIA MONOCYTOGENES* FOR FOOD SAFETY APPLICATIONS 52
4.1 Abstract 52
4.2 Introduction 53
4.3 Materials and Method 56
4.3.1 Materials 56
4.3.2 Nanoparticle Preparation 56
4.3.3 Aptamer preparation 56
4.3.4 Bacteria Preparation 57
4.3.5 SERS measurements 58
4.3.6 Data analysis 58
4.3.7 Preparation of aptamer-conjugated SERS substrate 59
4.4 Results and Discussion 60
4.4.1 Selection of appropriate aptamer-SERS substrate 60
4.4.2 Influence of Food Matrix on aptamer-conjugated Ag dendrites 63
4.4.3 Specificity of aptamer-modified SERS substrate 65
4.4.4 Detection Limit of the aptamer-based SERS method 67
4.5 Conclusions 68

4.6 Supplementary Figures 69
5. UNDERSTANDING THE COMPETITIVE INTERACTIONS IN THE APTAMER−GOLD NANOPARTICLE BASED COLORIMETRIC ASSAYS USING SURFACE ENHANCED RAMAN SPECTROSCOPY (SERS) 71
5.1 Abstract 71
5.2 Introduction 72
5.3 Materials and Methods 76
5.3.1 Chemicals and Reagents 76
5.3.2 Synthesis of citrate-stabilized AuNPs 76
5.3.3 Aptamer preparation 77
5.3.4 Procedure of aptamer-AuNPs based colorimetric assay 77
5.3.5 SERS study of molecular interactions in matrix 78
5.4 Results and Discussion 80
5.4.1 Target-Aptamer Interactions 80
5.4.2 Optimization of Concentration-Ratios 82
5.4.3 Competitive Interactions Influencing the Detection of Ampicillin 84
5.4.4 Competitive Interactions Influencing the Detection of Kanamcyin 88
5.5 Conclusions 91
5.6 Supplementary Figures 93
6. SELECTION OF APATMERS USING GOLD NANOPARTICLES-ASSISTED SELEX FOR THE DETECTION OF FOOD CONTAMINANTS 96
6.1 Abstract 96
6.2 Introduction 97
6.3 Materials and Method 104
6.3.1 Materials 104
6.3.2 Design 104
6.3.3 Selection 105
6.3.4 Partition 107
6.3.5 Amplification 108
6.4 Results and Discussion 112
6.4.1 Optimization of target capture and separation 112
6.4.2 Amplification and Extraction of ssDNA 115

6.4.3 Other considerations for using gold nanoparticles-assisted SELEX for the selection of aptamers 119

6.5 Conclusion 120

7. SUMMRARY AND OUTLOOK 121

APPENDICES

A. dPAGE for separating ssDNA from PCR product 124

B. PEER-REVIEWED MANUSCRIPTS THAT HAVE BEEN PREPARED AND/OR PUBLISHED DURING THIS PH.D. STUDY 128

REFERENCES 130

LIST OF TABLES

Table Page

Table 2.1 Quantification parameters of the four insecticides using SERS[a] 18

Table 6.1 List of characteristic differences between aptamers and antibodies 99

Table 6.2 PCR cocktail used in the first step of PCR optimization 108

Table 6.3 PCR protocol used in the first step of PCR optimization 109

Table 6.4 PCR cocktail used in the second step of PCR optimization 109

LIST OF FIGURES

Figure Page

Figure 2.1(a) Second derivative SERS spectra of the control water:methanol solution at 50 µg/mL (light blue line) vs the second derivative SERS spectra of acetamiprid at 0, 3, 10, and 50 µg/mL in apple juice (average of all data points); (b) Second derivative SERS spectra of acetamiprid in apple juice zoomed in the range of 610 to 640 cm^{-1} at full scale; (c) PCA plot of different acetamiprid concentrations in apple juice analyzed [33].....16

Figure 2.2 The SERS spectrum of fungicide ferbam taken on handheld Raman spectrometer. (A) Illustration of the use of a handheld Raman spectrometer to point and shoot the Ag dendrites on a glass slide. (B) The SERS chemical structure of the pesticide ferbam taken by handheld Raman spectrometer. Blank Ag dendrites were used as the negative control and compared with ferbam at the concentration of 50 ppm on Ag dendrites. 20

Figure 2.3 Principal Component Analysis (PCA) plot of Ag-Ap, Ag-Ly and Ag-Ap-Ly. 22

Figure 3.1 SEM image of (A) silver dendrites and (B) thiolated aptamer (S2-55) conjugated onto silver dendrites 31

Figure 3.2 The schematic illustration of the development of the single aptamer-based SERS method for the detection of four specific pesticides (isocarbophos, omethoate, phorate, profenofos) 34

Figure 3.3 Raman spectra showing the concentration optimization of thiolated aptamer (S2-55) on 100 µl Ag dendrites in 1M phosphate buffer, pH 7. As the thiolated aptamer concentration increased, the aptamer peaks, notably around 1330 cm^{-1}, increased up to 5 µM. At the same time, the Raman intensities of other competing molecules in the buffer decreased. At 5 µM, the buffer peak 970 cm^{-1} is no longer reflected on the Raman spectra, suggesting complete displacement by the thiolated aptamer.....36

Figure 3.4 Raman spectra of Ag-Ap and Ag-(Ap+MH). 40 µM MCH was incubated for 1 h with Ag-Ap and analyzed to produce the Raman spectra for Ag-(Ap+MH). The Raman peaks at 680 and 1080 cm^{-1} are both attributed to the capture of MH. The decrease in aptamer peaks (e.g. 1330 cm^{-1}) is inevitable due to the strong binding dissociation nature of MH 38

Figure 3.5 (A) Chemical structure of the four pesticides that is specific to the aptamer being used. (B) Second derivative transformation of the Raman spectra of an isocarbophos capture peak and the control between 1220-1170 cm^{-1}; a profenofos capture peak and the control between 1110-1060 cm^{-1}; a phorate capture peak and the control between 545-510 cm^{-1}; an omethoate capture peak and the control between 425-375 cm^{-1}. The control was the modified Ag dendrites [Ag-(Ap+MH)]. The spiked concentration for the four pesticides was 0.5 mM. All samples were conducted in a capture buffer with a 20 min incubation period. (C) A second derivative Raman spectra reflecting the capture of all four pesticides (isocarbophos, profenofos, phorate, omethoate) by Ag-(Ap+MH). 125 µM of each pesticide was added. Distinct Raman peaks were produced at different Raman shifts that correlated with each individual pesticide capture peak. 40

Figure 3.6 PCA plot comparing the second derivative Raman spectra of each pesticide (0.5 mM) captured by modified Ag dendrites [Ag-(Ap+MH)] as well as the control. This result shows significant differences between each pesticide capture, proving the detection and discrimination of the four pesticides 42

Figure 3.7 (A) Second derivative Raman spectra of the phorate capture peak between 645-600 cm^{-1} when 0, 0.04 µM, 0.4 µM, 4 µM and 40 µM phorate were exposed to the modified Ag dendrites [Ag-(Ap+MH)]. This result shows an increase in peak intensity around 625 cm^{-1} as phorate concentration increases; (B) PCA plot for Raman spectra of phorate at 0 µM-Control (○), 0.04 µM (+), 0.4 µM (△) , 4 µM (□) and 40 µM (●). A significant difference was seen beginning at 0.4 µM. 44

Figure 3.8 Raman spectra of modified Ag dendrites [Ag-(Ap+MH)] mixed with (from top to bottom) capture buffer, apple juice (diluted 1:10) (AJ), and phorate (Ph) (0.5 mM) spiked in AJ. Spectral results show no differences between Ag-(Ap+MH) exposed to buffer and AJ, suggesting nonspecific binding has been eliminated. However, when Ag-(Ap+MH) was exposed to Ph & AJ, huge spectral change was observed, proving the capture of phorate 45

Figure 3.9 Raman spectra of various concentrations of thiolated aptamer (S2-55) mixed with Ag dendrites in double distilled water. The largest peak intensities were produced at the smallest concentration (0.128 µM). As the thiolated aptamer concentration introduced was increased, the Raman peaks kept falling, suggesting a mechanism that was making less aptamer have access to the surface of the Ag dendrites 47

Figure 3.10 Raman spectra of silver-aptamer complex (Ag-Ap) with various incubation times to assess the binding time optimization of thiolated aptamer (5 μM) onto Ag. The aptamer capture peaks, such as the one in 1330 cm^{-1} was maximized after four hours incubation, which was the incubation time used for further analysis 48

Figure 3.11 Second derivative Raman spectra of modified nanoparticles [Ag-(Ap+MH)] with iscarbophos, omethoate, phorate and profenofos respectively and the four pesticides mixed together at even concentrations. Total pesticide concentration for each sample was 0.5 mM. The distinct Raman peaks produced by each pesticide at different Raman shifts allows for simultaneous detection of the four specific pesticide 49

Figure 3.12 (a) Second derivative Raman spectra and (b) PCA plot of isocarbophos between 530-480 cm^{-1} for 0 μM, 3.4 μM (1 ppm) and 17 μM (5 ppm); (c) Second derivative Raman spectra and (d) PCA plot of omethoate between 630-610 cm^{-1} for 0 μM, 4.8 μM (1 ppm), 24 μM (5 ppm) and 48 μM (10 ppm); (e) Second derivative Raman spectra and (f) PCA plot of profenofos between 1490-1460 cm^{-1} for 0 μM, 2.7 μM (1 ppm) , 14 μM (5ppm) and 27 μM (10 ppm). A gradual increase in Raman peak intensities was seen when the spiked pesticide was introduced at increasing concentrations. Significant difference against the control (0 μM) was seen at 3.4 μM (1 ppm) for isocarbophos, 24 μM (5 ppm) for omethoate, and 14 μM (5 ppm) for profenofos 50

Figure 3.13 Partial Least Square analysis (PLS) of phorate spiked at 0 μM, 0.04 μM (0.01 ppm), 0.4 μM (0.1 ppm), 2 μM (0.5 ppm), 4 μM (1 ppm). This result shows a linear relationship between the spectral peak intensities (i.e. calculated value) and the actual phorate concentration. Quantitative analysis of phorate was possible within this range. The root mean square error calibration (RMSEC) was 0.101 and the correlation coefficient was 0.9628..... 51

Figure 4.1 SERS substrates tested in this study: (a) Ag dendrites; (b) Au coated magnetic NPs; (c) Au nanoparticles-coated magnetic NPs. 60

Figure 4.2 SERS spectra of *salmonella enteritidis* capture (10^7-10^8 cfu/mL) using various aptamer-functionalized SERS substrates. Their corresponding principal component analysis (PCA) plot is shown on the right where (○) symbolizes the substrate control and (+) symbolizes the substrate + *salmonella enteritidis* 62

Figure 4.3 SERS spectra aptamer modified Ag dendrites at 10 µM aptamer and the principal component analysis plot of aptamer modified Ag dendrites with various aptamer concentration coverage. 63

Figure 4.4 Two methods were proposed for using Ag dendrites, one that solely depends on centrifugation while the other largely depended on the use of a double sided tape to stick the Ag dendrites onto the cap of a microcentrifuge tube. 64

Figure 4.5 SERS spectra and principal component analysis (PCA) plots showing the influence of 1% fat milk on Ag dendrites and aptamer-modified Ag dendrites. 65

Figure 4.6 Specificity of salmonella aptamer and listeria aptamer based on the signals given by SERS analysis. 66

Figure 4.7 The limit of detection of aptamer based SERS on the detection of bacteria (i.e. Salmonella enteritidis). 67

Figure 4.8 Irregularities in reproducibility seen in both gold nanoparticles coated magnetic nanoparticles (above) and gold coated magnetic nanoparticles below. 69

Figure 4.9 Raman map of salmonella enteritides at different concentrations using aptamer modified Ag dendrites. 70

Figure 5.1 Chemical structures of target antibiotics and aptamers used (i.e. circled regions on aptamer structures indicate conserved motifs) [aptamers obtained from Song et. al.[111,114] Used with permission from Elsevier] 80

Figure 5.2(a) Schematic Illustration of a suitable aptamer-based colorimetric assay; (b) Optimization of aptamer and NaCl concentrations using absorbance ratio (i.e. 640/520); (c) Relative binding affinity (Kd) requirements for successful implementation of the aptamer-based colorimetric assay (Ap = aptamer; T = target; Au = gold nanoparticle) 82

Figure 5.3(a) UV-vis absorbance of aptamer-based colorimetric samples with various ampicillin concentrations; (b) Absorbance ratio (640/520) based on UV-vis absorbance; (c) Optical image of aptamer-based colorimetric samples with increasing concentrations of ampicillin (left to right). 84

Figure 5.4 Second derivative SERS spectra and principal component analysis chart of aptamer-based colorimetric samples at low (i.e. 30 nM) and high (600 nM) ampicillin concentrations. Aptamer and ampicillin peaks are represented by orange lines on the spectra. Other specific peaks can be located by referring to Fig. 8. 86

Figure 5.5 (a) UV-vis absorbance of aptamer-based colorimetric samples with various kanamycin concentrations; (b) Absorbance ratio (620/520) based on UV-vis absorbance; (c) Optical image of aptamer-based colorimetric samples with increasing concentrations of kanamycin (left to right). 89

Figure 5.6 Second derivative SERS spectra and principal component analysis chart of aptamer-based colorimetric samples at low (i.e. 30 nM) and high (600 nM) kanamycin concentrations. Aptamer and kanamycin peaks are represented by dotted lines on the spectra. Other specific peaks can be located by referring to Fig. 5.9. 90

Figure 5.7 TEM image of synthesized AuNPs with an average diameter of 13 nm. 93

Figure 5.8 Raw SERS spectra of ampicillin at different concentrations (0, 30, 300, 600, 1200 nM) mixed with AuNPs or Aptamer + AuNPs 94

Figure 5.9 Raw SERS spectra of kanamycin at different concentrations (0, 30, 300, 600, 1200 nM) mixed with AuNPs or Aptamer + AuNPs. 95

Figure 6.1 Description of the SELEX process. 100

Figure 6.2 Schematic Illustration of the aptamer selection process using AuNPs 105

Figure 6.3 Partitioning of target bound/unbound ssDNA and their subsequent step. 107

Figure 6.4 Schematic Illustration of the separation of dsDNA after PCR amplification 111

Figure 6.5 Absorabance ratio (720/520) and color of gold nanoparticles exposed to different concentrations of ssDNA after the addition of 75 mM NaCl. 113

Figure 6.6 SERS spectra and principal component analysis score of the supernatant after AuNPs-based SELEX selection. 114

Figure 6.7 Agarose gel results showing DNA bands at the appropriate distance corresponding to its length. Also, 10+16 cycles is shown to have the clearest peak. 115

Figure 6.8 Agarose electrophoresis gel image of DNA library (50 bp ladder), DNA products after PCR, and supernatant (SUP) after streptavidin (STV) beads exposure. 116

Figure 6.9 dPAGE gel showing three clear bands, representing ssDNA with 86, 66 and 38 base lengths respectively 118

CHAPTER 1

INTRODUCTION

1.1 Background

Adulteration of food products is a major source of distress for consumers and food companies. The US FDA and EPA give certain limits as to how much unintended materials, i.e. physical, chemical, or microbial, are allowed in specific food products and fresh produce. In order to enforce this regulation, governmental agencies routinely check the food supply for these foreign matters and food manufacturers are expected to have a system in check to detect these substances. As such, the methods used to detect these contaminants have to be reliable and efficient to meet the demands of government and consumers. The traditional methods for detecting food chemical contaminants have been primarily HPLC and GC/LC-MS. Although these methods can give accurate and sensitive data, they have some limitations, including high start-up cost, need for highly skilled labor, long and laborious sample preparation and analysis, and a dedicated lab space to store bulky instrument. For food microbial contaminant detection, the plate count method has traditionally been used. Again, this method offers considerably accurate and sensitive data, but carries certain limitations such as long incubation times, and being incapable of distinguishing dead and live cells.

There is a great amount of interest in developing new technology and methods to improve the detection of food contaminants. Many factors have been considered for improvement. They include improving the accuracy and sensitivity, decreasing analysis time, simplifying the analytical procedure, increasing specificity to target, discrimination of similar substances, portability, minimizing space and waste, etc.

Surface enhanced Raman spectroscopy (SERS) is an emerging detection technology that has the potential to rapidly, accurately and sensitively detect a wide variety of food contaminants. Label-free SERS is particularly useful because it relies on the unique molecular fingerprints of each target molecule instead of the label dyes that produce Raman signals. However, label-free SERS detection becomes a challenge in real complex matrix, such as food, since non-specific matrix signals have the potential to drown out target associated Raman peaks. One way to overcome this limitation is by coupling target-specific capture agents, such as aptamers, to SERS substrates.

Aptamers are artificially engineered oligonucleotides that bind to their targets with high affinity, and has advantages over other biologically-derived capture agents such as antibodies because it is thermostable, chemically modifiable, easily amplifiable, and do not require animals for selection and production. The increase in use of aptamers for biomedical diagnostics has prompted us to explore the feasibility of its use for food safety applications.

1.2 Objectives

In this dissertation, we demonstrate the development and application of label-free, aptamer-based SERS for the detection of food contaminants. To achieve this **overall objective**, we conducted the following **specific aims**:

- ***Aim 1 – Fabricate an aptamer-modified SERS substrate that can be used to detect and differentiate multiple chemical contaminants in food***. Previous research has shown it is possible to detect single target molecules with aptamers using SERS as a signaling tool. For detection methods, it would be advantageous to screen multiple contaminants at the same time. Hence, this study employed a novel, multi-pesticide specific aptamer integrated with SERS to evaluate the feasibility of detecting four different pesticides simultaneously using our developed SERS substrate. The limit of detection and the ability to differentiate each pesticide in a mixture during detection were then investigated in apple juice.
- ***Aim 2 – Develop an aptamer-based SERS method that will detect pathogens in food***. Unlike pesticides and many chemical compounds, pathogens are typically larger in size. Hence, in addition to reducing non-specificity, physical separation of target pathogens from large food compounds, such as proteins and carbohydrates, need to be addressed in order to obtain clear SERS signals. In this study, we tested several fabricated SERS substrates to determine the best method to separate and detect two foodborne pathogens, *salmonella enteritidis* and *listeria monocytogenes*, in milk. The Raman spectra obtained were used to

evaluate the limit of detection, reproducibility and specificity by comparing it with other non-specific bacteria.

- ***Aim 3 – Integrate aptamer-based SERS with aptamer-assisted gold nanoparticle based colorimetric detection to create a rapid detection-validation protocol.*** Gold nanoparticles are one of the most widely used SERS substrates available. Their ability to change color upon induced aggregation can also be exploited to signal the presence of a given target. Although previous studies have shown the effectiveness of using aptamers in a gold nanoparticle based colorimetric detection method, the intermolecular interactions that causes the change in optical properties is not well understood. Therefore, this study focused on characterizing the competitive interactions that occur between gold nanoparticles, aptamers, and target molecules using SERS. This detection-validation study was conducted using two food-related antibiotics, ampicillin and kanamycin, as target models.
- ***Aim 4 – Develop a suitable aptamer selection SELEX procedure that will enhance the application of aptamer-based detection technology for food safety***. One of the main hindrances for the application of aptamer-based SERS and other aptamer-based detection methods for food safety is due to the lack of aptamers. This is likely due to the sophisticated, specialized procedure, i.e. systematic evolution of ligands by exponential enrichment (SELEX), currently being used to design new aptamer sequences. In an attempt to provide more food contaminant specific aptamers, the feasibility of developing a simple SELEX method was

explored using gold nanoparticles as a non-specific binding substrate and signaling tool.

The completion of these projects will help us better understand the feasibility and usefulness of label-free, aptamer-based SERS as a detection method for food contaminants in food matrix. It will also have the potential to assist the development of other types of analytical methods pertaining to food safety. To give the reader an informative background of the topics being discussed in this dissertation, a literature review of recent advances in SERS and aptamer-based technology will first be given. The details of each specific aim will then be addressed in subsequent chapters, and concluded with an overall summary.

CHAPTER 2

LITERATURE REVIEW[1]

2.1 Surface-enhanced Raman Spectroscopy

2.1.1 Background

Surface enhanced Raman spectroscopy (SERS) is essentially an agglomeration of two fields, namely Raman spectroscopy and nanotechnology. Raman scattering was first discovered in 1928 by Raman and Krishnan[1], who observed the inelastic scattering of light which constitutes only about one in a million photons of incident light striking a surface. The rest reflect elastically, commonly known as Rayleigh scattering. It was further discovered that the frequency changes that occurred due to the inelastic scattering of light matched precisely with the differences in vibrational energy levels. This enables the molecule to yield distinct Raman spectral profiles since different functional groups possess different characteristic vibrational energies. Thus, Raman spectroscopy is capable of molecular fingerprint specificity for every distinct molecule/analyte. However, this method was not applicable for sensitive detection due to the inherently weak Raman signals. In the 1970s, researchers discovered that Raman signals were enhanced by 10^4 –

[1] A part of this literature review is adapted from an invited review paper that has already been submitted: Pang, Shintaro and Lili He. 2016. "Recent Advances in Surface Enhanced Raman Spectroscopic (SERS) Detection of Synthetic Chemical Pesticides." *Trends in Analytical Chemistry*

10^5 if the target analyte was placed in close proximity to a roughened noble metal nanostructure [2]. Although the exact mechanism for this phenomenon is not yet fully understood, two sets of theories have become well-agreed upon by the scientific community; namely the electromagnetic and chemical theory. Briefly, in the electromagnetic theory, the enhancement of Raman signals is thought to be due to the excitation of the localized surface plasmon resonance (LSPR) of nanoparticles when an incident light hits the surface of the target analyte close to the nanomaterial. In order to maximize the enhancement of Raman signals, the excitation frequency of the nanomaterials used has to resonate with that of the incident light (i.e. for noble metals, this is in the UV-vis range). In the chemical theory, the Raman signal enhancement occurs based on the assumption that the target analyte is adsorbed on the metal surface and that a charge transfer is in effect. Because of the chemisorption of target analyte on the nanosubstrate, the electronic state of the complex is shifted to a new absorption maximum, which allows it to resonate with the laser excitation frequency, and thus enhance the Raman signals. To get a deeper understanding of the mechanisms and theory of SERS, the following review articles are highly recommended [3,4].

SERS has several merit-worthy properties over other analytical techniques that make it an excellent detection tool. First, SERS is able to detect extremely low levels of analytes, even down to a single molecule level [5,6]. Second, SERS is able to provide distinct molecular fingerprints and overall spectra based on the inherent chemical

structure of the target molecules[4]. Furthermore, it provides other information such as the surface chemistry and interface reactions of the analytes being examined [7,8]. Third, SERS is a rapid and convenient detection method as it typically takes a few seconds or less to obtain a spectrum. Sample preparation can be minimal and only a tiny speck (few micrometer size) is needed for analysis since the laser spot size is usually in that size range. Fourth, samples can be analyzed in aqueous solutions without interference from the solvent since water is a Raman scatterer. Because of this, SERS opens the door to a wider scope of application studies such as cells and bacteria that may not survive well in dry environments [9,10]. Fifth, SERS can be used to detect a wide variety of substances including small molecule, DNA, proteins, viruses, bacteria, etc. Lastly, SERS can be a cost effective alternative for many analytical techniques as only tiny amounts of nanosubstrates is required and these can potentially be fabricated at low cost. All of these outstanding properties of SERS have been recognized over the last two decades and has led to significant growth in SERS-based applications, including its use in food safety.

In order to apply SERS as a detection method for food contaminants, it is important to understand several critical determining factors: sensitivity, selectivity, reproducibility and portability. Hence, the following section will highlight some of the recent work that has been done to address these factors.

2.1.2 Factors to Consider in SERS detection

Sensitivity

Probably the main advantage of SERS is that it is capable of detecting ultra-low concentrations of molecules. This is very useful in food contaminant detection since certain harmful substances (e.g. pathogens, carcinogenic chemicals) are not tolerated at all. Many pesticides are also regulated with a maximum residue level of 10 parts per billion in fresh produce, which is difficult to achieve using many rapid detection tools. The high sensitivity of SERS is largely attributed to the nanosubstrate that is placed in close proximity to the target. The "hot spots" and surface area/morphology determine the enhancement factor of SERS. Thus, efforts have been made to increase hot spot locations and the surface area. For example, silver particles that have aggregated forms of nanosize shapes such as flowers and leaves have been fabricated to take advantage of their SERS enhancement capabilities [11,12]. By increasing the probability of the target landing at the centroid position of a hot spot, ultrasensitive detection even at a single molecule has been achieved under optimal SERS conditions.

Another way to increase the sensitivity of SERS is by preconcentrating the noble metal nanoparticles using an inducing chemical such as NaCl. In this way, the electric charges surrounding nanoparticles are neutralized by the salt and is able to pull both NPs and the adsorbed target together, which will subsequently enhance the SERS peak intensities [13]. Preconcentrating can also be done through physical means such as

filtration. Yu and White (2012) showed the concept by trapping silver nanoparticles on filter membranes in order to form a SERS active substrate, after which a large of volume of sample containing low levels of melamine was concentrated onto the filter [14]. Similarly, a membrane filter assisted SERS method was able to detect E.Coli 0157:H7 as low as 10 CFU/mL in 1 hr [15]. Lastly, the coupling of electrokinetic pre-concentration with SERS has been developed to detect polar molecules such as antibiotics and phenols [16,17].

The sensitivity of SERS is not the same for all molecules. Sometimes, chemical bonding characteristics, such as the affinity of the target to nanosubstrate, can be too weak for adequate adsorption. For example, hydrophobic molecules such as polycyclic aromatic hydrocarbons (PAH) and polychlorinated biphenyls (PCBs) will not adsorb well on citrate stabilized gold or silver colloids due to the incompatibility of the surface chemistry. Hence, attempts have been made to overcome this limitation by modification of the nanosubstrate surface. In the case of hydrophobic molecule detection, colloidal hydrophobic films have been placed onto gold nanoparticles immobilized onto silanized quartz substrates[18] to detect PAH. Alkylated thiols, graphene, proteins and DNA fragments have also been conjugated onto SERS substrate to modify the surface chemistry to enhance the sensitivity of SERS. Many of these studies show proof of concepts, but are not well studied in complex matrix such as food, hence, there is still a need for application based studies to take SERS into food industrial applications.

Selectivity

For any detection method development that will eventually be used in applications, the medium in which the target is embedded in plays a crucial factor in influencing the sensitivity of the result. For detection of food contaminants, the matrix could be aqueous (e.g. milk, fruit juices, drinking water) or solids (e.g. meat, fruits, vegetable, cereal). Depending on the food matrix, the interference of SERS signals can differ greatly. Since SERS detects virtually any substance that is in close proximity to the nanosubstrate, nontargeted substances may produce substantial noise peaks to lower the sensitivity of the target analyte. Furthermore, several molecules may produce strong Raman peaks that are similar to the target, making it challenging for qualitative and quantitative detection.

To improve the selectivity of SERS in actual food matrix, one can modify the SERS substrates with specific receptors such as molecular imprinted polymers (MIPs), antibodies and aptamers to block out the unwanted Raman signals. In fact, this approach has been used before to detect a variety of substances including food allergens. In this case, antibodies were used in ELISA methods to capture specific immunogenic protein targets [19,20].

Another way to improve the selectivity of SERS is to integrate SERS with a separation technique. This method essentially builds in a sample preparation step that

cleans up the matrix good enough for there to be minimal noise. Examples of separation methods used include capillary chromatography, thin layer chromatography, ion-pair chromatography and ion-pair electrophoresis. Indeed, these sample preparation techniques provide increased sensitivity and selectivity, while reducing false positive or negative results. However, the addition of a separation step may generate limitations to SERS, such as increased analysis time and lack of portability.

Portability

One of the popular aspects of SERS development is the potential for it to become a field detection method. In order to have a portable detection system, it has to be rapid, light, easy-to-use and small. Furthermore, the application of field detection methods will only be realized if it is cost-effective.

The miniaturization and commercialization of hand-held Raman spectrometers has enabled portable SERS detection to become a reality. However, just as crucial as the instrument is the development of suitable nanosubstrates. For portable applications, traditional colloidal based substrates may not work well due to the additional steps needed deposit the nanoparticles on a solid surface and concentrating/aggregating the substrate. Hence, solid SERS substrates are more suitable for detection that requires portability. A few SERS substrates have been developed to meet this need. One strategy is by using electron beam lithography (EBL) to graft the nanomaterials onto a solid

support, which allows for accurate control and precise spacing of nanoparticles [21]. Although this method can produce very reproducible and sensitive results, a major limitation is its cost. Commercial substrates such as Klarite^{TM} is based on this technique but they are still very expensive to manufacture and therefore may not be suitable for routine testing.

Another approach has been the development of paper-based [22–24] or fiber-based [25,26] SERS sensors. For example, one study screen printed SERS active NPs onto a filter paper, which could then be used to screen many samples using high throughput analysis in a portable setting [24]. Not only were these substrates cost-effective, but they were able to exhibit reproducible results with less than 10% spot-to-spot variation. In another study, a template guided self-assembly of gold nanoparticles into ordered arrays of uniform clusters was prepared on an optic fiber faucet [26]. These SERS enabled optic fiber showed high-performance of SERS as demonstrated by using crystal violet. This batch method approach may pave a way for low-cost, efficient SERS nanosubstrates. Continued research will be needed to examine the stability of the substrates and to apply it with wider varieties of target analyte.

Reproducibility

Despite the numerous advantages of SERS as an ultrasensitive detection tool, one of the main limitations that continue to be addressed in SERS studies is the reproducibility

of results, particularly with regards to peak intensities. Thus, quantitative studies remain a challenge in SERS if the wrong type of SERS substrates is being used. Colloidal nanoparticle solutions may not be as ideal for reproducibility due to uncontrolled aggregation and its lower stability. Well-ordered nanostructures are more promising as they are able to maintain even gaps between nanoparticles that give consistent hot spots exposed to target. Electron beam lithography (EBL) has been used to produce well-defined arrays, and has shown highly reproducible SERS performance [27]. However, they are expensive to fabricate, therefore, it might not be suitable for frequent food industrial applications.

A lower cost alternative to more reproducible SERS enhancement substrates is the fabrication of silver dendrites. These leaf-like dendritic nanostructures consist of colloidal sphere approximately 50 nm in diameter linked closely together. Because of the close proximity of each nanosphere, adsorbed analytes can produce strong and consistent Raman signals [28]. Other studies that have shown to control the uniformity of nanoparticles into uniform patterns include incorporation of colloids into a sol-gel [29,30] and integration with a microfluidic device [31,32]

2.1.3 Application of SERS in food contaminant detection

Many of the SERS studies described in literature are focused on nanosubstrate development to improve the factors described above, and typically use highly SERS

active molecules for detection as a proof-of-concept. However, in order to bring the technique into industrial applications, more application studies have to be performed with a wide variety of target molecules and food matrix. In this section, several research studies that I collaborated on will be described to show how SERS has been applied to detect food contaminants.

Acetamiprid on apple peel and in apple juice

This study describes a simple method and high sensitivity of SERS application for detection of food contaminants. Briefly, a simple, rapid method was developed to detect acetamiprid on apple peels and in apple juice by using silver dendrites coupled with SERS [33]. Acetamiprid is a neonicotinoid pesticide that is frequently used in modern farming. The US Environmental Protection Agency (EPA) sets tolerance levels between 0.01 and 50 ppm of acetamiprid residue, depending on the type of food (Electronic Code of Federal Regulations 2013). For apples, the tolerance level is 1.0 parts per million (1000 μg/kg) [34]. Although there have been previous studies focusing on SERS detection of pesticides, most of them were focused on substrate development by testing simple pesticide solutions [35–39], and spectral characterization [40]. For applications in food matrices, many of the SERS studies still used a complex extraction procedure, which increased the analytical time [38,41,42], or achieved unsatisfactory sensitivity [35,36]. In this study, the focus was on detection sensitivity of the method in food matrix.

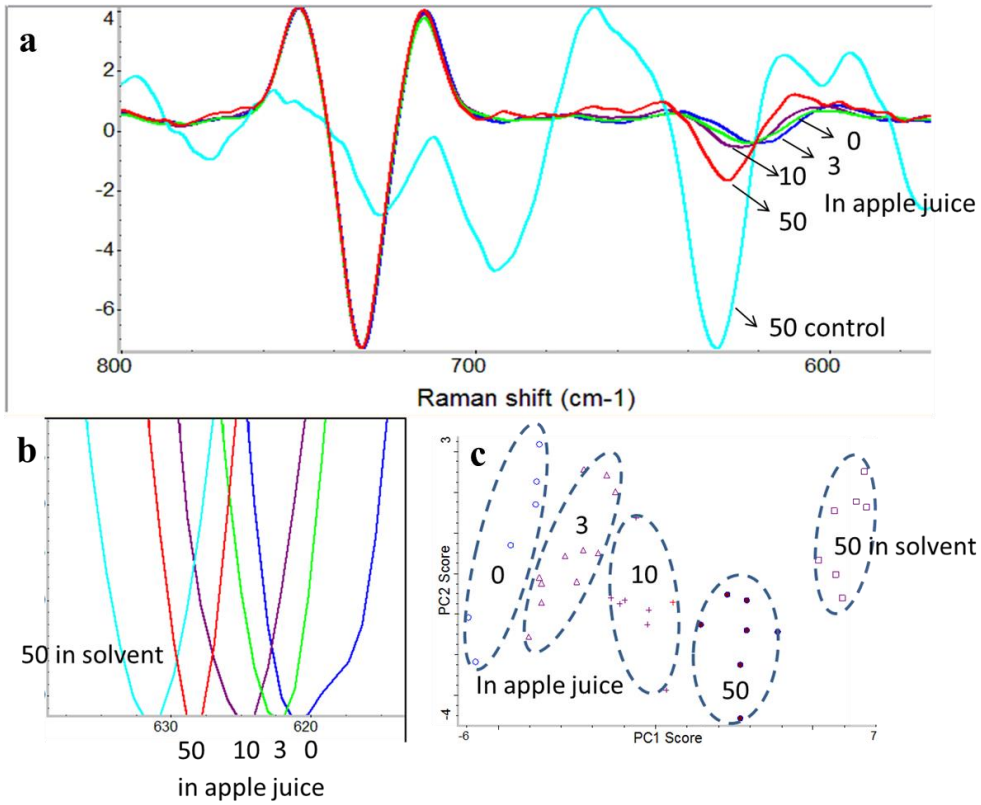

Figure 2.1(a) Second derivative SERS spectra of the control water:methanol solution at 50 µg/mL (light blue line) vs the second derivative SERS spectra of acetamiprid at 0, 3, 10, and 50 µg/mL in apple juice (average of all data points); (b) Second derivative SERS spectra of acetamiprid in apple juice zoomed in the range of 610 to 640 cm^{-1} at full scale; (c) PCA plot of different acetamiprid concentrations in apple juice analyzed [33].

Acetamiprid was detected in water, apple juice and on apple peel. For apple juice, no sample preparation was done. For apple peel, a simple swab method was used. By using the highest acetamiprid peak at 634 cm^{-1}, the SERS method was able to successfully detect acetamiprid at 0.5 µg/mL (0.5 ppm) in solvent, 3 µg/mL (3 ppm) in apple juice, and 0.125 µg/cm^2 on apple surfaces. The longest it took to detect the samples was 15 min for total 5 samples on apple peel. The spectral data was then analyzed statistically using

principal component analysis (PCA). In Figure 1, the spectra show that with increasing concentration of acetamiprid, the acetamiprid "fingerprint" peak intensity increased, noticeably at high concentration (50 μg/mL) while there were no intensity differences at low concentrations (3 and 10 μg/mL). However, the acetamiprid concentration correlated with the shifting of the acetamiprid peak as well. By zooming into around 610 to 640 cm^{-1} at full scale (Figure 1B), it is clear that the apple juice samples that contain different concentrations of acetamiprid were "sandwiched" in between the pure apple juice peak (negative control) and 50 μg/mL acetamiprid in solvent peak (positive control). Although more studies will be needed to understand the mechanistic detail of this phenomenon, this study showed the feasibility of detecting acetamiprid in real apple juice at low concentrations.

Multi-class insecticides on plant surfaces

The next study illustrates the potential for detecting multiple target contaminants on a food plant surface. In this study, a rapid SERS detection method was developed to examine four insecticides (i.e. Isocarbophos, Phorate, Detlamethrin, Imidacloprid) representing three different classes (i.e. organophosphate, pyrethroid, neonicotinoid) on tea leaves and apple peels. This study was also done to address the issue of complex extraction procedure [38,43,44] performed in most food matrix studies. In our previous studies, SERS methods had been established for acetamiprid[33] and thiabendazole [45] on apple surfaces after a swab method. In our previous studies, SERS methods had been

established for acetamiprid[33] and thiabendazole [45] on apple surfaces after a swab method. However, until now, only a few studies had been reported on the in situ detection of pesticides residues on several plant surfaces using homemade SERS substrates [46,47]. These studies used very SERS active compounds such as thiram, methyl parathion and parathion. Therefore, further studies were urgently needed to investigate the in situ SERS methods for more pesticide residues on various plant surfaces.

The results as summarized in Table 1 show that these pesticides can be detected at very low concentrations. The limits of detection (LODs) of isocarbophos, phorate, imidacloprid and deltamethrin were 0.25, 0.25, 0.5 and 0.5 mg kg^{-1} on fresh tea leaves, and 0.01, 0.01, 0.02, 0.02 mg kg^{-1} on apple peels, respectively. Furthermore, principal component analysis showed that all four pesticides were distinguishable from each other based on their distinct Raman fingerprint. Hence, this study was able to show that not only was SERS capable of detecting a variety of pesticides at low concentrations, but it was able to detect them simultaneously and discriminate them based on their spectral peaks.

Table 2.1 Quantification parameters of the four insecticides using SERS[a]

Insecticide	Linear conc. range, µg mL^{-1}	Corr. coeff.	RMSEC	LOD,[b] µg mL^{-1}	LOD,[c] mg kg^{-1} (µg cm^{-1})	
				In solvent	Tea	Apple

Insecticide	Linear conc. range, μg mL^{-1}	Corr. coeff.	RMSEC	LOD,[b] μg mL^{-1}	LOD,[c] mg kg^{-1} (μg cm^{-1})	
				In solvent	Tea	Apple
a RMSEC, the Root Mean Square Error of Calibration, got from PLS analysis. b Limit of detection of insecticides in methanol (1 : 1). c Limits of detection on plant surface.						
Isocarbophos	0–5.0	0.9993	0.0654	0.005	0.25 (0.01)	0.01 (0.01)
Phorate	0–10.0	0.9923	0.0443	0.005	0.25 (0.01)	0.01 (0.01)
Imidacloprid	0–1.0	0.9678	0.0904	0.005	0.5 (0.02)	0.02 (0.02)
Detlamethrin	0–10.0	0.9966	0.283	0.005	0.5 (0.02)	0.02 (0.02)

Semi-quantification of Ferbam using Portable SERS

This study was conducted to illustrate the compatibility of SERS for on-site detection of food contaminants and the feasibility of semi-quantification using a handheld Raman spectrometer traditionally used for a straightforward “Yes/No” detection of bulk materials. In order to do this, silver dendrites were used as the SERS susbtrate and ferbam was used as the pesticide of interest.

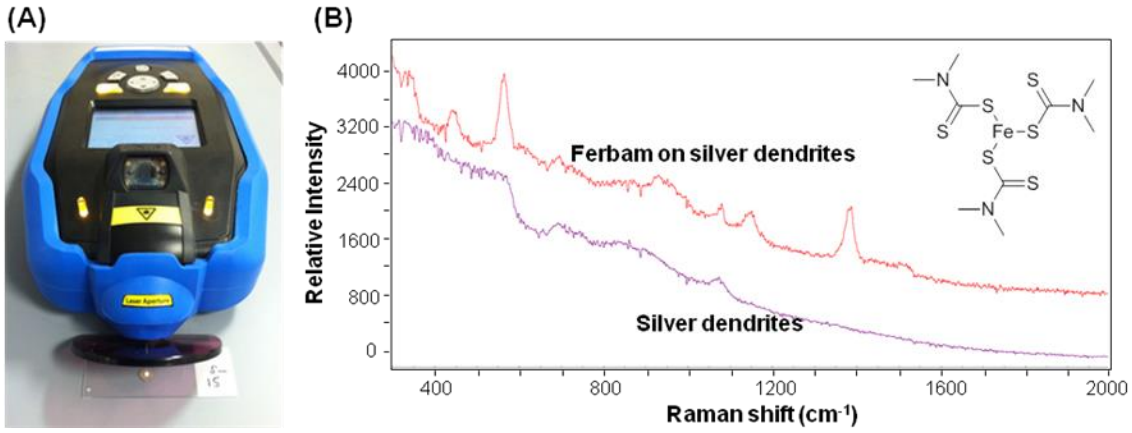

Figure 2.2 The SERS spectrum of fungicide ferbam taken on handheld Raman spectrometer. (A) Illustration of the use of a handheld Raman spectrometer to point and shoot the Ag dendrites on a glass slide. (B) The SERS chemical structure of the pesticide ferbam taken by handheld Raman spectrometer. Blank Ag dendrites were used as the negative control and compared with ferbam at the concentration of 50 ppm on Ag dendrites.

As shown in Figure 2, the setup of the detection method was such that the silver dendrite was placed on a plain glass slide, and a handheld Raman spectrometer was placed above so that the laser pointed directly at the sample. The pesticide showed clear Raman peaks at several Raman shifts, notably at 1384 cm^{-1}, which was likely due to the γ(C–N) stretching coupled to the symmetric $\delta(CH_3)$ motion. The instrument parameters were optimized with four "reference" concentration levels chosen to represent "No risk" (0 ppm), "Low risk" (4 ppm, about a half of risk level), "Risk" (7 ppm, risk level), and "High risk" (14 ppm, double of risk level) and because the technique was capable of distinguishing these concentrations clearly using principal component analysis. After inputting those spectra as reference points in the software library, nine different concentrations were tested to see if they were able to match the reference concentration

spectra most closely representing it. A p-value of greater than 0.05 was considered a positive result when comparing it against the reference. A p-value between 0.001 and 0.05 was considered negative as they would not resemble the reference. The results worked flawlessly and showed the feasibility of using handheld Raman spectrometers as detection tools for on-site detection.

Integration of colorimetric and SERS detection of melamine in milk

Rapid detection methods typically require another method to check the validity of the results when there is a positive sample. For example, although colorimetric methods look promising for on-site measurements of melamine, they can be greatly influenced by the sample matrices, resulting in high rates of false positive and false negative data. In this study, the intrinsic properties of gold nanoparticles were employed to integrate both colorimetric and SERS assays so that the benefits of both methods could be realized [48]. To do this, the size of gold nanoparticles and a simple sample extraction method was developed to be compatible for both methods. The change in color from red to purple indicated that melamine was potentially present due to the bridging effect induced by its three amine groups that bind to Au surfaces. A small portion of the sample is then transferred onto a gold slide and detected using SERS. The developed colorimetric–SERS method was able to rapidly screen and validate as low as 0.25 ppm melamine in milk within 20 min, displaying its advantageous as a rapid dual validation method for food contaminant detection.

Aptamer-based SERS substrate for detecting lysozyme on food handling surface

In order to address the issue of low selectivity when using unmodified SERS substrates, a study was conducted to target the egg allergen, lysozyme, using aptamers by modifying silver dendrites with a thiolated aptamer. After optimizing the surface coverage of silver dendrites with aptamers, a stainless steel surface representing a food handling surface was spiked with lysozyme at low concentrations.

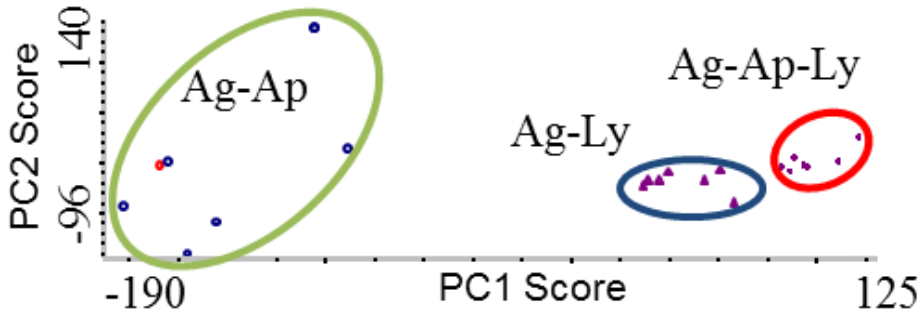

Figure 2.3 Principal Component Analysis (PCA) plot of Ag-Ap, Ag-Ly and Ag-Ap-Ly.

Figure 2.3 shows the principal component analysis of the lysozyme detection using aptamer-based SERS. It shows successful capture of the lysozyme by the aptamer. The limit of detection for lysozyme was 0.1 µg/mL in water and 5 µg/mL on a stainless steel food-handling surface. Quantification of lysozyme target was also shown from 0 to 6 µg/mL and the overall method took less than 40 min. This provided an extra step of using SERS as a selective and sensitive tool to detect food allergens.

2.2 Aptamer-based biosensing

Many rapid detection assays use a biological capture agent as a probe coupled with a transducing mechanism for analysis. Depending on the target of interest, the capture probe can be a protein (i.e. antibody, enzyme) or oligonucleotide (i.e. DNA, RNA). Over the last two decades, aptamers have begun to emerge as a popular alternative to other biological capture agents as the analytical tool of choice for many target analytes, including food contaminants.

Aptamers are a class of oligonucleotides that have been designed using an in-vitro method. The term "aptamer" is derived from the root Latin word "aptus", which means "to fit" [49,50]. Although aptamers are artificially engineered molecules, similar compositional structure and functions have been found in molecules found in nature known as riboswitches [51,52]. In both of these cases, it is a single stranded RNA or DNA that possesses high binding affinity to their target of interest.

The underlying molecular interaction between aptamers and their target is largely due to the following: hydrogen bonding, electrostatic interactions, stacking of aromatic rings and van der Waals interaction. They typically follow an induced fit model, whereby the aptamer changes its 3-D structure in order to interact fully with their target. Their secondary structure is also characterized by stems, internal loops, bulges, hairpins, tetra

loops, pseudoknots, triplicates, kissing complexes, or G-quadruplex; these specific structures influences the binding sites of the target.

Today, aptamers have been selected for a wide variety of targets including proteins, peptides, nucleotides, amino acids, small molecules, low-molecular organic and inorganic compounds, and even whole cells. The process of designing aptamers for specific targets originated from 1990 by three separate labs [50,53,54]. They all described a similar selection procedure that isolated functional oligonucleotides having high binding affinity to their target molecules that started from a randomly synthesized oligonucleotide library starting with more than 10^{15} sequences. This procedure is commonly known as "systematic evolution of ligands by exponential enrichment", or "SELEX".

Briefly, SELEX can be broken down into five essential steps: Design, Selection, Partition, Amplification and Acquisition. The design stage requires thoughtful planning on the ssDNA or ssRNA sequence, which typically consists of at least one random sequence flanked between two constant primer binding sites. In the selection stage, the target and oligonucleotide library is exposed to each other. In the partition stage, the target bound oligonucletoides are separated from the remaining oligonculeotides and subsequently eluted from the target. The amplification stage uses polymerase chain reaction (PCR) to amplify the sequences obtained which is then separated from its complementary strand. The obtained ssDNA or ssRNA is then subjected to a repeat of the

selection, partition and amplification procedure until the proportion of the oligonucleotide library binding to the target remains high and constant. In the last step, the acquired ssDNA or ssRNA is cloned in bacteria and then several colonies are selected for DNA sequencing. The sequences are then analyzed using m-fold software to understand its secondary structure and to predict binding site. Lastly, the sequences of interest will be tested for its binding affinity to target.

The dissociation constants (K_d) of aptamers to their target is usually between the micromolar to picomolar range, making it a highly specific capture probe. In addition to their high specificity, aptamers carry several advantageous over antibodies as capture receptors. The main important factors are listed below:

1. Aptamers are thermally stable, hence they can be regenerated easily after denaturation.
2. Aptamers can be easily modified, hence they can be labeled with a dye or immobilized onto a solid surface using thiol or biotin functional groups.
3. Aptamers can be selected for virtually any type of molecules, including toxic or nonimmunogenic susbtances.
4. Aptamers can be amplified easily using PCR, hence it can be reproduced rapidly with large amounts.
5. Aptamers do not require scarification of live animals or in vivo immunization, hence getting rid of any ethical issues associated with animal-related experiments.

CHAPTER 3

DEVELOPMENT OF A SINGLE APTAMER-BASED SURFACE ENHANCED RAMAN SCATTERING METHOD FOR RAPID DETECTION OF MULTIPLE PESTICIDES[2]

3.1 Abstract

The objective of this study was to develop a simple and rapid method that could detect and discriminate four specific pesticides (isocarbophos, omethoate, phorate, and profenofos) using a single aptamer-based capture procedure followed by Surface Enhanced Raman Spectroscopy (SERS). The aptamer is a single stranded DNA sequence that is specific to capture these four pesticides. The thiolated aptamer was conjugated onto silver (Ag) dendrites, a nanostructure that can enhance the Raman fingerprint of pesticides, through Ag–thiol bonds. It was then backfilled with 6-mercaptohexanol (MH) to prevent nonspecific binding. The modified SERS platform [Ag–(Ap + MH)] was then mixed with each pesticide solution (P) for 20 min. After capturing the pesticides, the Ag–(Ap + MH)–P complex was analyzed under a DXR Raman microscope and TQ Analyst software. The results show that the four pesticides can be captured and detected using principal component analysis based on their distinct fingerprint Raman peaks. The limits

[2] The contents of this study have been published: Pang, Shintaro, Theodore P Labuza and Lili He. 2014. "Development of a Single Aptamer-based Surface Enhanced Raman Scattering Method for Rapid Detection of Multiple Pesticides." *The Analyst*. doi:10.1039/C3AN02263C.

of detection (LODs) of isocarbophos, omethoate, phorate, and profenofos were 3.4 μM (1 ppm), 24 μM (5 ppm), 0.4 μM (0.1 ppm), and 14 μM (5 ppm) respectively. This method was also validated successfully in apple juice. These results demonstrated the super capacity of aptamer-based SERS in rapid detection and discrimination of multi-pesticides. This technique can be extended to detect a wide range of pesticides using specific aptamers.

3.2 Introduction

The development of rapid detection techniques for pesticide residual analysis has become a hot topic in recent years due to increased application of pesticides and fear of its health deteriorating effects.[41,55] This field of analysis is termed "QuEChERS" for finding methods that include making the process to be Quick, Easy, Cheap, Effective, Rugged, and Safe.[56] Traditional/currently-used methods mostly apply chromatography (i.e. GC or LC) coupled with MS.[57–59] Despite its sensitivity and capability to detect multiple residues quantitatively, this method carries several disadvantages including extensive sample preparation (i.e. extraction, filtration, etc.), need for technical expertise and high cost.

Many alternative methods, such as ELISA,[60–62] radioimmunoassay[63,64] and multiarray biosensor methods,[65] have been developed for rapid and sensitive detection of pesticide residues. In these cases, a recognition element captures the target

analyte, and in doing so, the receptor-analyte complex produces a biochemical signal (i.e. change in pH, color, radioactivity, charge potential, etc.) that can be qualitatively or quantitatively determined by an appropriate transducer (i.e. signal probe).[66] However, these methods are not without drawbacks. For example, the recognition element might exhibit broad specificity, potentially capturing substrates that are unrelated. The signals produced by the transducer are also often secondary, meaning that the output can only tell us if something was captured. This can be disadvantageous as the analyst will not be sure if the signal came from the target analyte or from some other compound that triggered a similar signal.

Surface-enhanced Raman scattering (SERS) is a powerful spectroscopic technique utilizing nanotechnology and Raman spectroscopy that can detect traces of closely adsorbed molecules on metallic nanostructures (often gold or silver).[67] Even though SERS methods can be conditioned to be sensitive enough to detect a single molecule, SERS alone will not single-handedly separate compounds present in a sample. This might prove to be disadvantageous, especially when detecting trace amounts of a target in a complex matrix like food. In this case, Raman signals from the target analyte will be drowned out by the signal of other ingredients/compounds present, thus making it impossible to detect anything.

To overcome the non-specific nature of SERS, aptamers can be deployed as suitable capture agents. Aptamers are single stranded oligonucleotides that can be synthesized in vitro to capture target molecules. They have become increasingly popular as a capture agent because it is adaptable to various targets, convenient in screening, reproducible for synthesis, versatile in labelling, immobilizing, signalling and regenerating.[68,69] In addition, recent technological advancements have made it faster and cheaper to create new aptamers, particularly through the SELEX (Systemic Evolution of Ligands by Exponential Enrichment) protocol.[49]

Aptamer based SERS method has been previously evaluated on proteins in liquid foods.[70] However, the problem of non-specific binding by other food components has not been solved. The objective of this study was to evaluate the feasibility of an aptamer-based SERS technique for pesticide detection in a complex liquid food (e.g. apple juice) using a single aptamer that was previously synthesized to be specific to not one, but four commercially available pesticides (isocarbophos, omethoate, profeonofos, phorate).[71] The optimization of aptamer conjugation to eliminate the nonspecific binding in apple juice as well as the feasibility of multi-detection was emphasized and discussed. To the best of our knowledge, very few studies have been published on aptamer-based SERS for small molecule detection.[72,73] No similar study has been reported for detection in a complex food matrix.

3.3 Materials and Method

3.3.1 Materials

All the chemicals were of analytical reagent grade and were purchased through Fisher Scientific unless otherwise noted. The multiple pesticide binding aptamer (SS2-55) reported previously[71] with the sequence 5'-AAG CTT GCT TTA TAG CCT GCA GCG ATT CTT GAT CGG AAA AGG CTG AGA GCT ACG C-3' with disulfide (S-S) modification at the 5' end was purchased through Eurofins Operon MWG (Ebersberg, Germany). Apple Juice (Stop N Shop, MD, USA) was purchased from a local grocery store.

3.3.2 Preparation of dendritic silver (Ag) nanoparticles

Silver (Ag) dendrites were synthesized in accordance with previously published methods.[11,28] Briefly, a zinc metal plate was rinsed with 1M HCl to remove any metal oxides forming on the outer layer, then rinsed with double distilled water and dried. The zinc plate was then immersed in a 200 mmol $AgNO_3$ (aq) solution for exactly 1 min, which produced nanoparticle size diameters of ≈50 nm. After incubation, the silver dendrites formed on the surface of the zinc plate was gently peeled off and washed with double distilled water several times. SEM images obtained from FEI Magellan 400 (FEI, Oregon, USA) confirmed consistent nanoparticles sizes of ≈50 nm in diameter were crystallized and form a dendritic structure (Fig. 3.1a). This unique structure can provide locally consistent enhancement factor and have been previously demonstrated as a sensitive and reliable SERS substrate. [28,74,75]

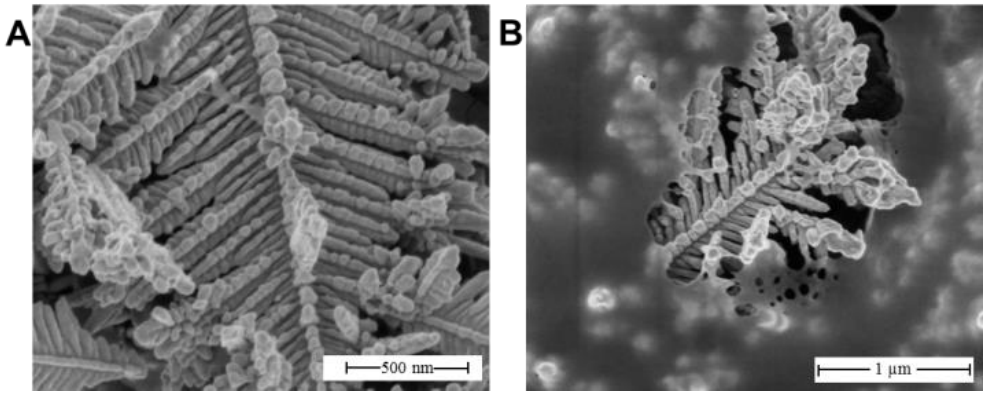

Figure 3.1 SEM image of (A) silver dendrites and (B) thiolated aptamer (S2-55) conjugated onto silver dendrites

3.3.3 Conjugation of deprotected aptamer onto Ag dendrites

The step by step sequence for developing this single aptamer-based SERS method is illustrated in Fig. 3.2. Aptamer was first dissolved in a 1xTE buffer (pH 7.4) to give a stock concentration of 129 µM. 100 µl of the aptamer stock solution was then added to 10 mM Tris (2-carboxyethyl) phosphine hydrochloride (TCEP) (i.e. concentration ratio was 1:77) and incubated for 1 hour in order to reduce the disulfide (S-S) to thiol (SH) groups, which has stronger binding affinity to the Ag surface. Then, 30 µl of the aptamer solution was mixed with 370 µl of 1 M phosphate buffer (pH 7), after which 100 µl (≈400 µg) Ag was added. This mixture was homogenized by mixing them together briefly with a micropipette tip. The mixture was then incubated at room temperature for 4 hours on a Nutating mixer (Fisher Scientific) at the speed of 24 rpm to allow the aptamer to conjugate onto the Ag through Ag-thiol binding interaction.

3.3.4 Addition of blocker molecule (i.e. 6-mercaptohexanol) onto silver-aptamer complex (Ag-Ap)

In order to eliminate all forms of non-specific binding interactions with Ag, 40 µM 6-mercaptohexanol (MH) was incubated with Ag-Ap for 1 hour, after which it was rinsed 3 times with double distilled water to fabricate our modified Ag dendrites [Ag-(Ap+MH)].

3.3.5 Detection of multiple specific pesticides using aptamer-based SERS

The pesticides (isocarbophos, omethoate, phorate, profenofos) were spiked in a buffer containing 300 mM NaCl, 50 mM KCl, 10 mM MgCl2, 50 mM Tris/HCl, pH 8.3. 5µl of Ag-(Ap+MH) was added to 400 µl of spiked buffer solution, stirred and incubated for 20 minutes. After incubation, the mixture was centrifuged at 6000 × g for 1 min to allow the modified Ag dendrites and the captured pesticides [Ag-(Ap+MH)-P] to settle to the bottom. The supernatant was then removed and Ag-(Ap+MH)-P was quickly rinsed with double distilled water twice before being deposited onto a glass slide to dry. If testing the pure pesticide solution, this washing and drying step can be minimized. But if the detection is in a complex matrix, i.e. apple juice, a quick wash step is necessary to remove food components.

3.3.6 Raman instrumentation

After drying, the samples were analyzed immediately using a DXR Raman Spectro-microscope (Thermo Scientific, Madison, WI) with the following conditions: 10× confocal microscope objective (3 μm spot diameter and 5 cm−1 spectral resolution), 780 nm excitation wavelength, 5 mW laser power and 50 μm slit width for 2 s integration time. OMNIC^{TM} software version 9.1 was used to control the Raman instrument. Eight spots were selected randomly for each sample within the range of 100-3300cm^{-1}.

3.3.7 Data analysis

SERS spectral data were analyzed using TQ Analyst software (version 8.0) from Thermo Scientific. The SERS spectra obtained from the multiple spots from each sample were averaged and compared against other samples. Second derivative transformation and smoothing were applied at times in order to reduce spectral noise and to separate overlapping bands. The variances of spectral data between spots and samples were then assessed using principal component analysis (PCA). This method focuses a multidimensional data set to the most dominant features while removing random variation so that the principal components can be used to capture the variation between spectra. This discriminant analysis is thus useful in evaluating SERS spectra for variance within a class and between classes. Generally speaking, if two data clusters (classes) do not overlap, then it means they are significantly different at the $p = 0.05$ level. The limit of detection LOD was determined to be the lowest concentration of the data cluster that

can be separated from the negative control in the PCA plot. Partial least square (PLS), a multivariate analysis model, was also applied to see if there was a linear relationship between the obtained spectral peak intensities and the actual spiked concentrations.

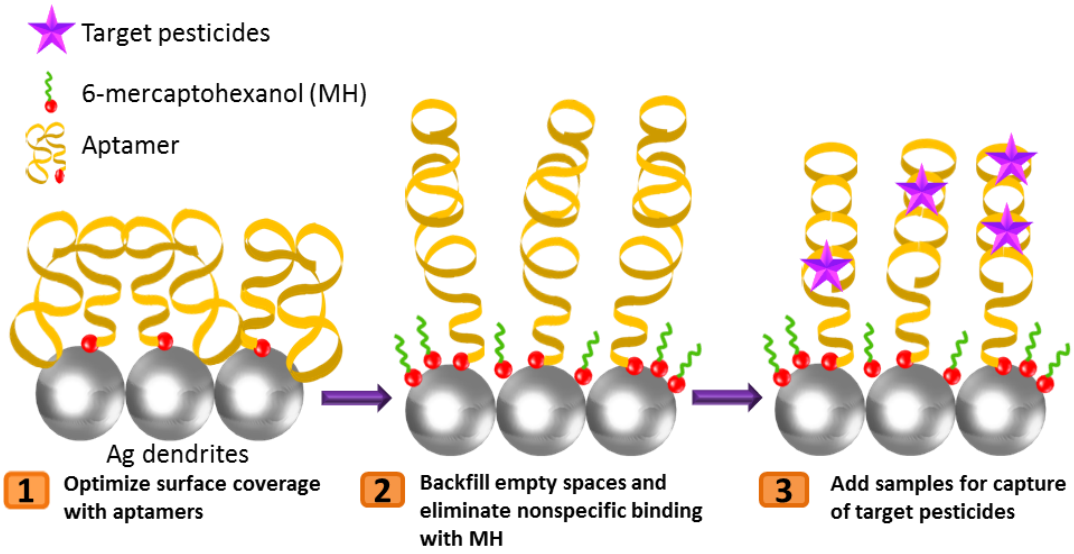

Figure 3.2 The schematic illustration of the development of the single aptamer-based SERS method for the detection of four specific pesticides (isocarbophos, omethoate, phorate, profenofos)

3.4 Results and Discussion

3.4.1 Optimization of aptamer conjugation with Ag

In order to maximize Ag-Ap conjugation, various concentrations of aptamers up to 0.512 µM were initially added to 100 µl Ag in water as the solvent. The SERS spectra were then analyzed to pick out the concentration with the highest aptamer peak (i.e. highest amount of aptamers bound to Ag).[76] Interestingly, the aptamer peak intensities started to decrease after 0.128 µM (Fig. 9). This could be explained due to the intermolecular electrostatic repulsion from the negatively charged ssDNA molecules. In

order to minimize the intermolecular electrostatic repulsion, 1 M phosphate buffer (pH 7) was used as a medium to increase the ionic strength, thus electrostatically shielding the charged oligonucleotides.[77] This caused the aptamer peak intensities to increase significantly at higher aptamer concentrations up to 5 μM (**Fig. 3.3**), thus proving the need for a higher level of salts to increase surface coverage. Other medium such as Tris buffers, chloride and nitrate salts were also tested to evaluate their effectiveness in increasing aptamer optimization, but they brought other problems (i.e. clumping/reaction of Ag nanoparticles), and subsequent reduction in SERS peak intensities. Incubation time to optimize aptamer surface coverage was also evaluated (up to 24 hours) and it was found that after 4 hours, the coverage was optimized (**Fig. 3.10**). This result was consistent with other findings that showed thiol-derivative oligonucleotide having optimized surface coverage after 4 hours.[77,78]

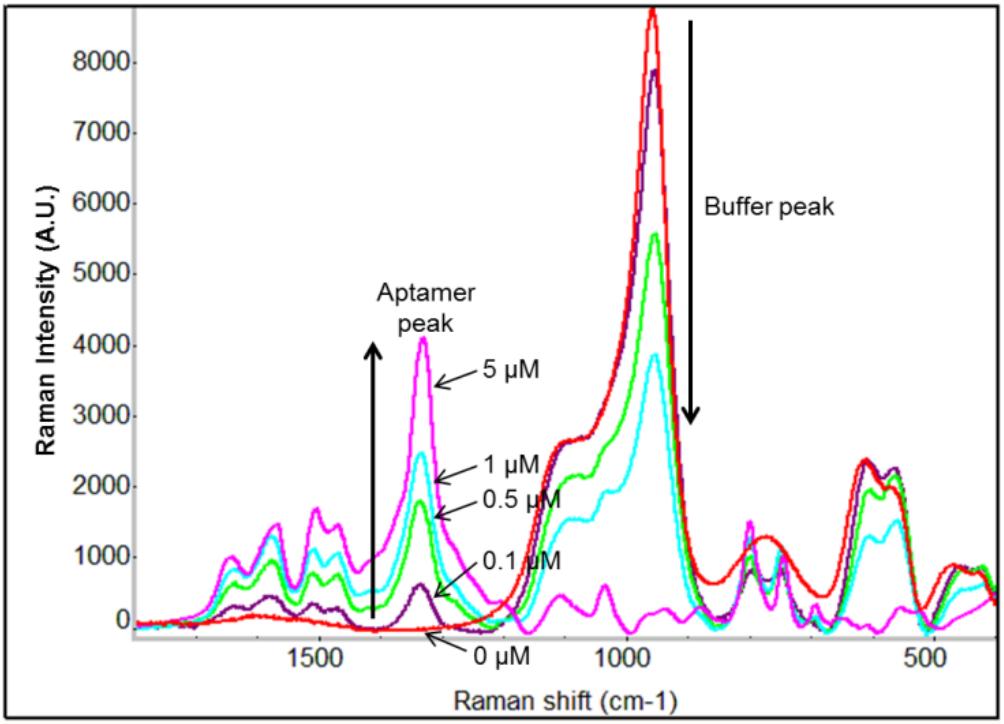

Figure 3.3 Raman spectra showing the concentration optimization of thiolated aptamer (S2-55) on 100 µl Ag dendrites in 1M phosphate buffer, pH 7. As the thiolated aptamer concentration increased, the aptamer peaks, notably around 1330 cm^{-1}, increased up to 5 µM. At the same time, the Raman intensities of other competing molecules in the buffer decreased. At 5 µM, the buffer peak 970 cm^{-1} is no longer reflected on the Raman spectra, suggesting complete displacement by the thiolated aptamer.

3.4.2 Optimization of MH concentration and incubation time with Ag-Ap

Since aptamers are relatively large molecules, maximizing its surface coverage on Ag does not ensure elimination of non-specific binding to Ag because steric hindrance can occur. The small, empty spaces between the aptamers can become non-specific binding sites for smaller molecules (e.g. pesticides, salts, food matrix). Furthermore, although aptamers can bind specifically to Ag with the thiolated 5' end, they can also interact non-

specifically with the N1 groups present on the A, T, G, C ring functional groups of the aptamer,[77,79] making them possibly incapable of capturing their target agents since their 3D conformation will be unable to change.

In order to eliminate non-specific binding and to ensure that the aptamer is free to change its 3D conformation during target capture, a small blocker molecule (i.e. 6-mercaptohexanol) was introduced.[80] Since this molecule is relatively very small, it does not interfere with the 3D conformational change that occurs when the aptamer is capturing its target. In addition, its thiol end has a strong binding affinity to Ag, thus enabling displacement of any non-specific binding of aptamers or other molecules (e.g. TCEP) that might be present in the Ag-Ap complex. Inadvertently, studies have shown that high concentrations and longer incubation times of MH can even displace thiolated oligonucleotides,[80,81] thus it was essential to optimize the time/concentration of added MH to fully cover the empty surface area and to displace non-specific binding, but at the same time, to minimize displacement of the thiolated aptamer. Varying concentrations (0-1 mM) of MH and varying incubation times (0-1 h) were tested and their Raman spectra were analyzed to monitor the appearance of MH peaks and aptamer peak intensities. As the MH concentration and incubation time increased, the Raman peaks attributed to MH increased, but at the same time, the peaks attributed to the aptamer decreased, albeit at a lower extent. The optimized time/concentration was determined to be 40 µM for 1 h because the Raman peaks from MH were visible while the aptamer peak intensities did

not drop drastically (**Fig. 3.4**). This observation was in line with another study that showed that when MH was introduced to thiolated oligonucleotides conjugated to gold nanoparticles, the oligonucleotides started to become displaced after using 10 µM of MH for 10 mins and a significant displacement was observed when 100 µM MH was incubated for 10 mins.[80]

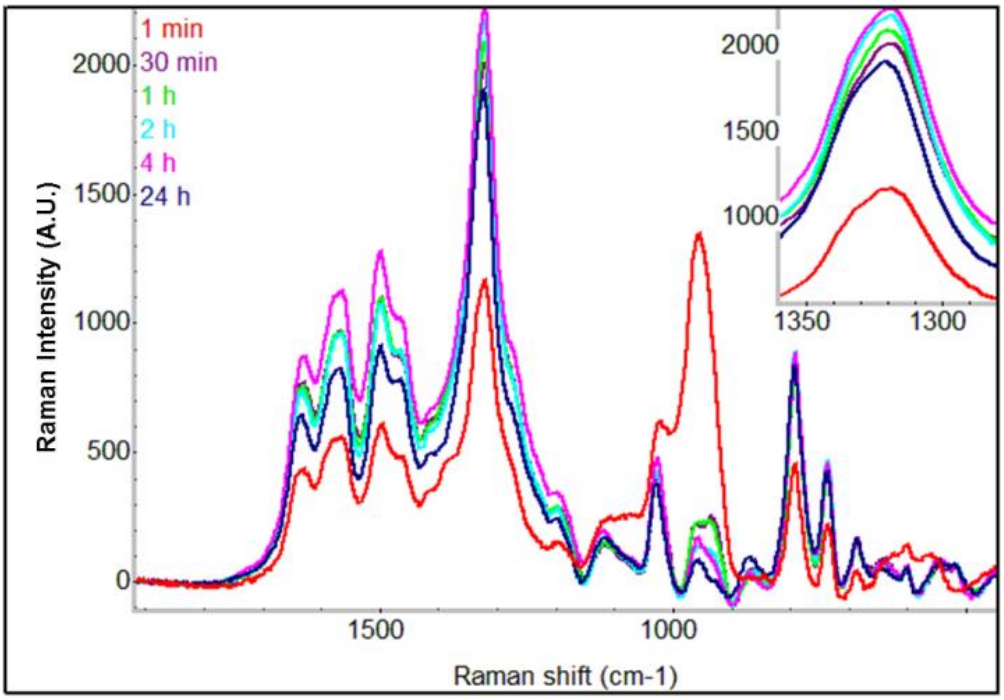

Figure 3.4 Raman spectra of Ag-Ap and Ag-(Ap+MH). 40 µM MCH was incubated for 1 h with Ag-Ap and analyzed to produce the Raman spectra for Ag-(Ap+MH). The Raman peaks at 680 and 1080 cm^{-1} are both attributed to the capture of MH. The decrease in aptamer peaks (e.g. 1330 cm^{-1}) is inevitable due to the strong binding dissociation nature of MH

One visual test to see if the nanoparticles had been fully covered with the aptamer and MH was by adding it into the capture buffer solution. When bare Ag dendrites were

added to the buffer, they aggregated immediately. When Ag-Ap was added to the buffer, it remained dispersed for a few minutes, but slowly started to aggregate as time went on. However, when the fully modified Ag dendrites [Ag-(Ap+MH)] was added to the buffer, it remained dispersed for as long as 20 min without any aggregation, thus proving that the Ag dendrites had been fully covered by the aptamer and MH (data not shown).

3.4.3 Detection of multiple pesticides using Ag-(Ap+MH)

The chemical structures of the four target pesticides are shown in **Fig. 3.5A**.

Pesticides at varying concentrations (0-0.5 mM) individually or as a mixture were initially spiked in water before Ag-(Ap+MH) was added. However, when the Raman spectra were measured, there was no noticeable capture of any of the pesticides. Furthermore, among the 8 replicates tested for each sample, the aptamer peaks were very inconsistent (data not shown). This could be due to the instability of the aptamers in a medium that does not have cations, as they are being introduced in the buffers used to select the aptamers.[71] In addition, some other aptamer papers have reported the dependency of cations to form stable 3D conformations to ensure the capture of their target agents.[82,83] Therefore, the aptamer selection buffer was then employed as a capture buffer.

Raman spectra show a huge difference in pesticide capture peaks when the capture buffer was used. As shown in **Fig. 3.5B**, each pesticide capture produces distinct peaks at

different Raman shifts, signifying the capture of the target pesticides. Fig. 5B highlights the most noticeable difference between each pesticide and the control. Their full spectra are shown in the supporting information (Fig. 11).

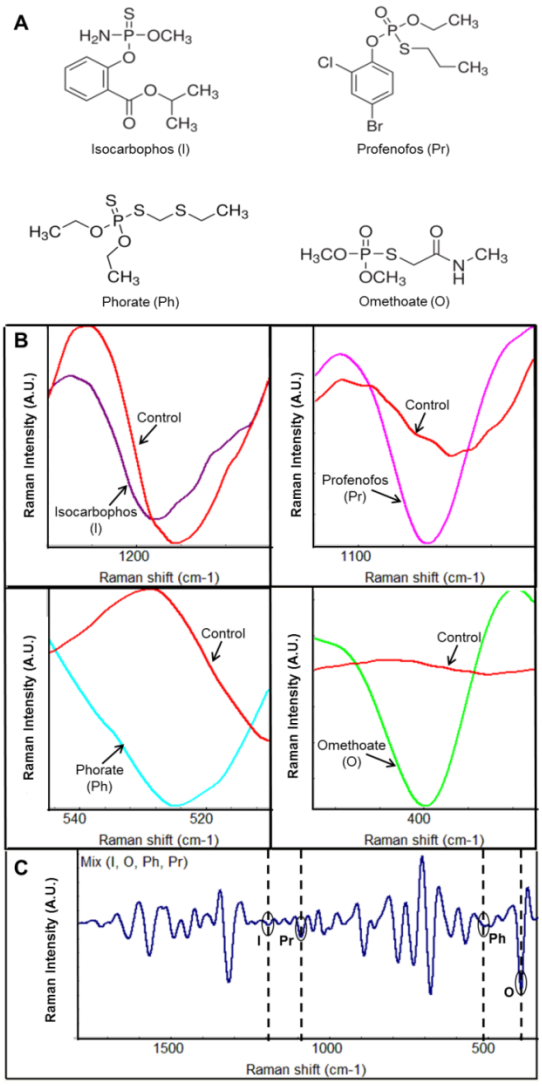

Figure 3.5 (A) Chemical structure of the four pesticides that is specific to the aptamer being used. (B) Second derivative transformation of the Raman spectra of an isocarbophos capture peak and the control between 1220-1170 cm^{-1}; a profenofos capture peak and the control between 1110-1060 cm^{-1}; a phorate capture peak and the control between 545-510 cm^{-1}; an omethoate capture peak and the control

between 425-375 cm^{-1}. The control was the modified Ag dendrites [Ag-(Ap+MH)]. The spiked concentration for the four pesticides was 0.5 mM. All samples were conducted in a capture buffer with a 20 min incubation period. (C) A second derivative Raman spectra reflecting the capture of all four pesticides (isocarbophos, profenofos, phorate, omethoate) by Ag-(Ap+MH). 125 µM of each pesticide was added. Distinct Raman peaks were produced at different Raman shifts that correlated with each individual pesticide capture peak.

Because each pesticide produces distinct Raman peaks, the type of pesticides being captured can be discriminated based on the peak intensities at various Raman shifts. Furthermore, by looking at the principal component analysis score, the whole spectrum can be analyzed to see if these peaks are significantly different from each other. In this case, all four pesticides that are specific to this aptamer produced significantly different Raman spectra peaks from each other and the control (i.e. no pesticide) (**Fig. 3.6**). The four pesticides were also added together as a mixture and measured to find out if they could all be detected at the same time (**Fig. 3.5C**). By looking at each distinct Raman peak from each pesticide capture, it was found to be correlated with a Raman peak that appeared in the mixture. Thus, this method provides a method that can identify four specific pesticides with one sample. On the other hand, when acetamiprid, a pesticide not specific to this apatamer was introduced, no visible pesticide capture peaks were seen (data not shown), thus validating the aptamer's high specificity.[71] The great advantage of this technique is not only that it can measure multiple target analytes, but it can also simultaneously validate that the captured molecules are the target analytes based on their specific signature peaks at certain Raman peak shifts. This unique "self-validation" method ensures great accuracy of this technique, superior to other sensor techniques that

are based on color, fluorescence or electrochemical signals and begins to satisfy many of the requirements of "QuChERS".

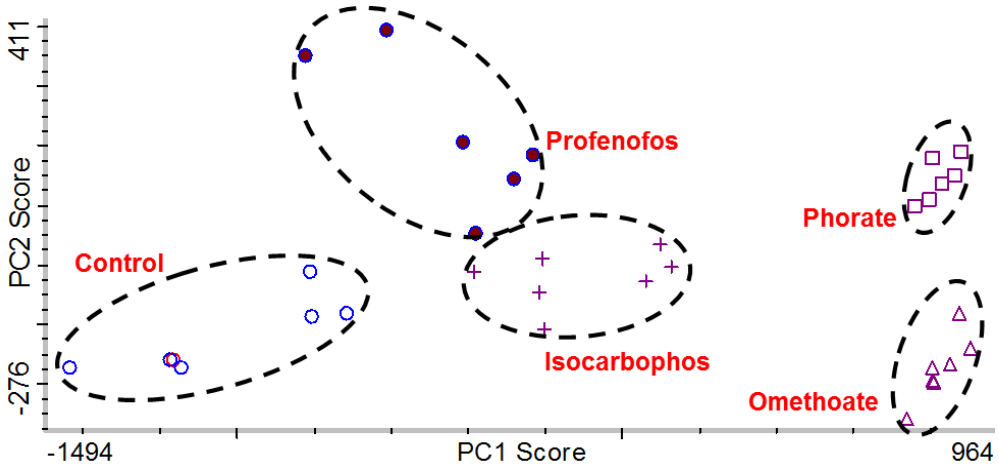

Figure 3.6 PCA plot comparing the second derivative Raman spectra of each pesticide (0.5 mM) captured by modified Ag dendrites [Ag-(Ap+MH)] as well as the control. This result shows significant differences between each pesticide capture, proving the detection and discrimination of the four pesticides

3.4.4 Determination of the limit of detection and quantitative capability of this method

Fig. 3.7A shows the relationship between the phorate capture peaks and the phorate concentration. The limit of detection (LOD) was determined to be 0.4 µM (0.1 ppm) by PCA (Fig. 7B). The LODs of other pesticides were also determined and are shown in Fig. 12. Compared with the LOD of phorate, the LODs of iscocarbophos (3.5 µM = 1 ppm), omethoate (24 µM = 5 ppm) and profenofos (14 µM = 5 ppm) were much higher, although the reported binding dissociation constants were similar for these four pesticides. One hypothesis is that the phorate molecules after being captured by the

aptamers were positioned in a distance closer to the surface of Ag-(Ap+MH) compared with other molecules or the interaction between phorate and aptamer resulted in a specific charge transfer mechanism that enhanced the Raman scattering of phorate. More studies are needed to understand this phenomenon. Nevertheless, the LODs mainly depend on the binding dissociation constants of the aptamer. Aptamers that are specific to smaller molecules tend to have a lower binding affinity due to the limited binding sites available for the aptamer to bind to the molecule.[84] Thus, this method can be further improved by selecting and applying an aptamer of higher binding dissociation constants.

The quantitative capability of this method to phorate was also evaluated. The partial least square line depicting the relationship between the calculated phorate concentration based on the phorate capture peak and the actual spiked phorate concentration added shows a linear relationship within the range of 0-3.8 μM (10 ppm) with a root mean square error coefficient of 0.9628 (**Fig. 3.13**). However, not all pesticides had such a linear response. It was found, at high concentrations (i.e. 0.5 mM), the captured omethoate produced the most profound peak intensities among the four pesticides. However, at lower concentrations (i.e. 4.8-48 μM), the captured omethoate produced little enhanced peaks compared to the other pesticides, suggesting that Raman peak intensities are not linearly correlated with omethoate concentration. Little is known about this relationship and more studies will be needed to understand the molecular mechanism behind this phenomenon.

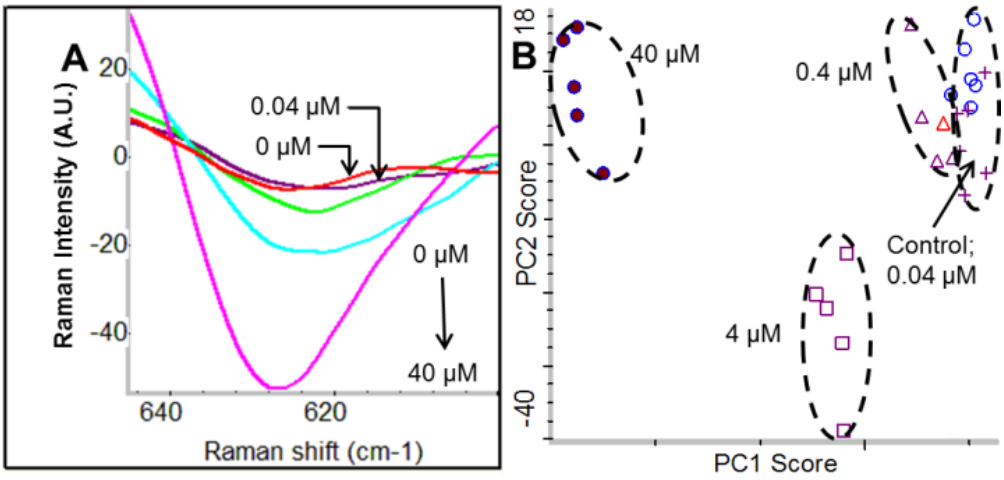

Figure 3.7 (A) Second derivative Raman spectra of the phorate capture peak between 645-600 cm^{-1} when 0, 0.04 µM, 0.4 µM, 4 µM and 40 µM phorate were exposed to the modified Ag dendrites [Ag-(Ap+MH)]. This result shows an increase in peak intensity around 625 cm^{-1} as phorate concentration increases; (B) PCA plot for Raman spectra of phorate at 0 µM-Control (○), 0.04 µM (+), 0.4 µM (△) , 4 µM (□) and 40 µM (●). A significant difference was seen beginning at 0.4 µM.

3.4.5 Method validation in apple juice to ensure elimination of non-specific binding and applicability in food matrix

When Ag was exposed to liquid foods (e.g. apple juice), nonspecific binding interaction occurred rampantly, causing multiple Raman peaks to form that easily drowned the target agent peaks. In order to validate the elimination of non-specific binding, the prepared complex [Ag-(Ap+MH)] was incubated with apple juice by adding 100 µL of apple juice into 900 µL of optimized Ag complex in buffer. The spectrum in apple juice showed no significant changes in peaks compared with the one in buffer (**Fig. 3.8**), proving that non-specific binding was eliminated. When phorate was added to apple juice, phorate intense capture peaks appeared, signifying the capture of phorate in apple

juice. It is worthy to note, however, that an optimized dilution of the apple juice was needed to produce the most intense phorate capture peaks (data not shown). At higher apple juice concentrations, the food components might alter the optimized condition for the Ag complex to function. Nevertheless, this method can be easily applied to other food and beverage samples for more effective capture and analysis.

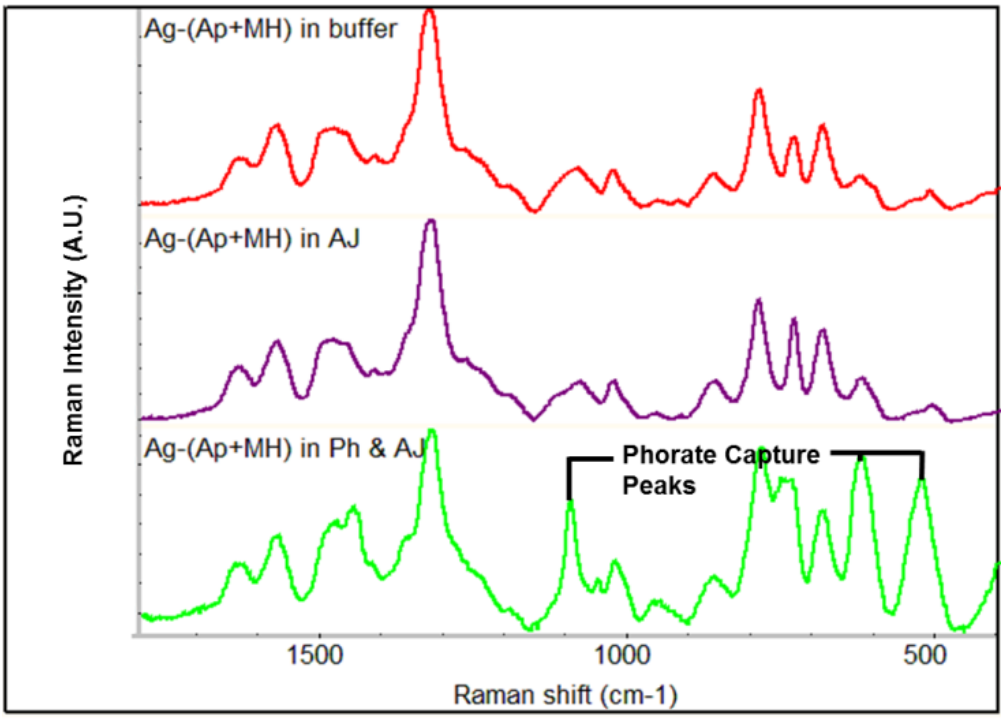

Figure 3.8 Raman spectra of modified Ag dendrites [Ag-(Ap+MH)] mixed with (from top to bottom) capture buffer, apple juice (diluted 1:10) (AJ), and phorate (Ph) (0.5 mM) spiked in AJ. Spectral results show no differences between Ag-(Ap+MH) exposed to buffer and AJ, suggesting nonspecific binding has been eliminated. However, when Ag-(Ap+MH) was exposed to Ph & AJ, huge spectral change was observed, proving the capture of phorate

3.5 Conclusion

In summary, a single aptamer based SERS method for detecting multiple specific pesticides in complex liquid food (i.e. apple juice) was established. The elimination of nonspecific binding was achieved by optimization of aptamer conjugation and with the blocker molecule MH to fill the empty spaces. The detection, discrimination, and validation of multiple pesticides using aptamer-based SERS method were achieved based on their distinct Raman fingerprint peaks. Furthermore, simultaneous detection of multiple pesticides was shown using the SERS spectra obtained. Total analytical time for measuring six samples was 40 min. The developed aptamer SERS method shows great potential to analyze pesticide residues in apple juice. Further experiment is needed to explore the application in other food matrices.

Supplementary Figures

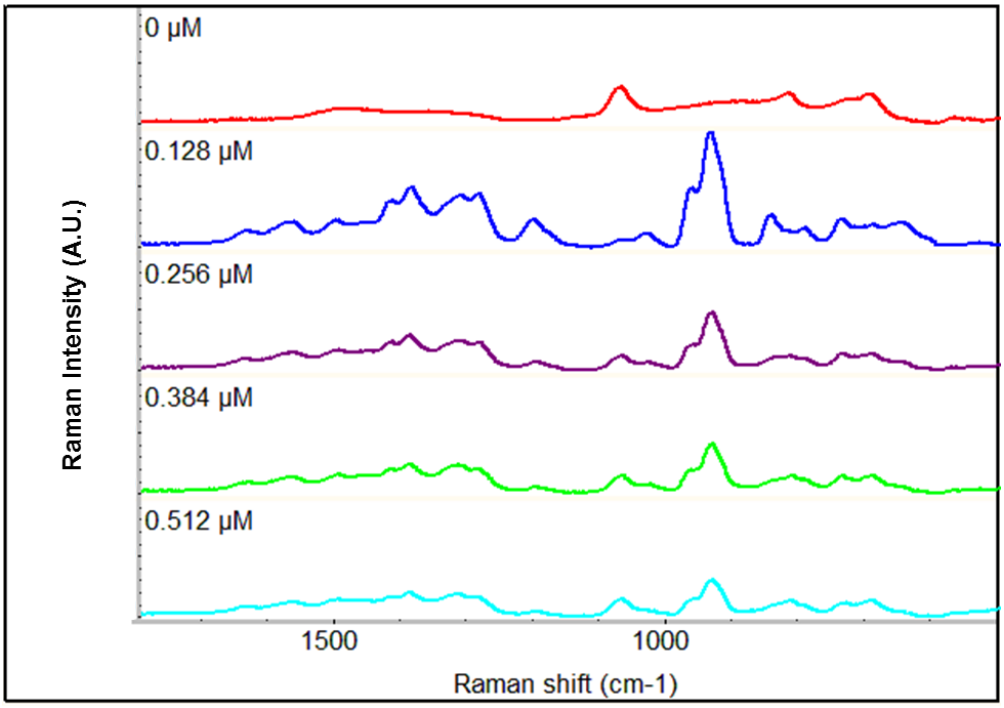

Figure 3.9 Raman spectra of various concentrations of thiolated aptamer (S2-55) mixed with Ag dendrites in double distilled water. The largest peak intensities were produced at the smallest concentration (0.128 µM). As the thiolated aptamer concentration introduced was increased, the Raman peaks kept falling, suggesting a mechanism that was making less aptamer have access to the surface of the Ag dendrites

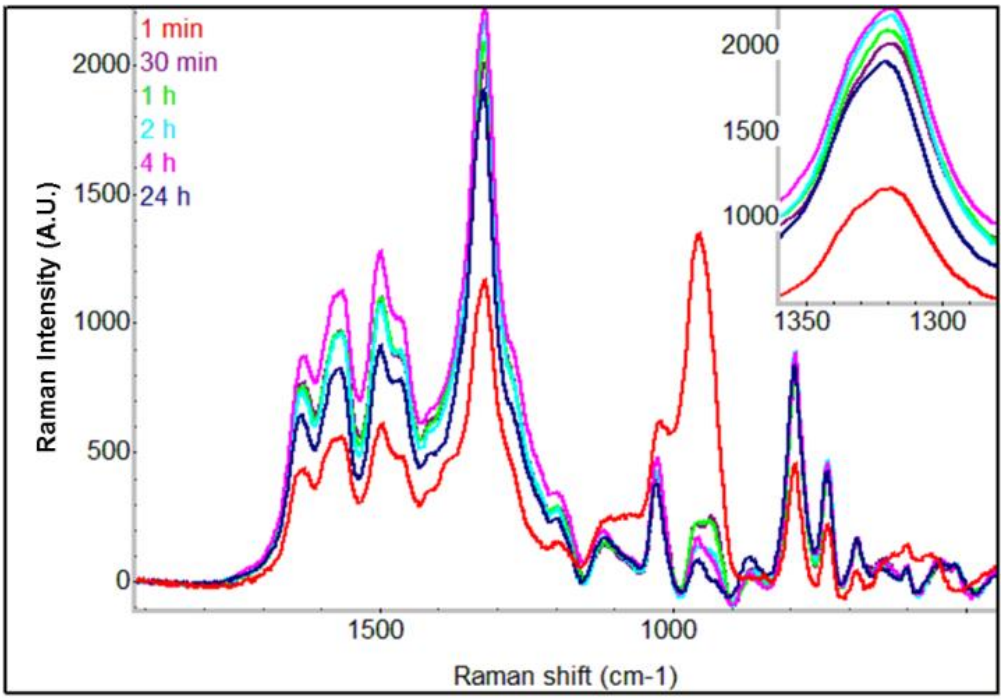

Figure 3.10 Raman spectra of silver-aptamer complex (Ag-Ap) with various incubation times to assess the binding time optimization of thiolated aptamer (5 µM) onto Ag. The aptamer capture peaks, such as the one in 1330 cm^{-1} was maximized after four hours incubation, which was the incubation time used for further analysis

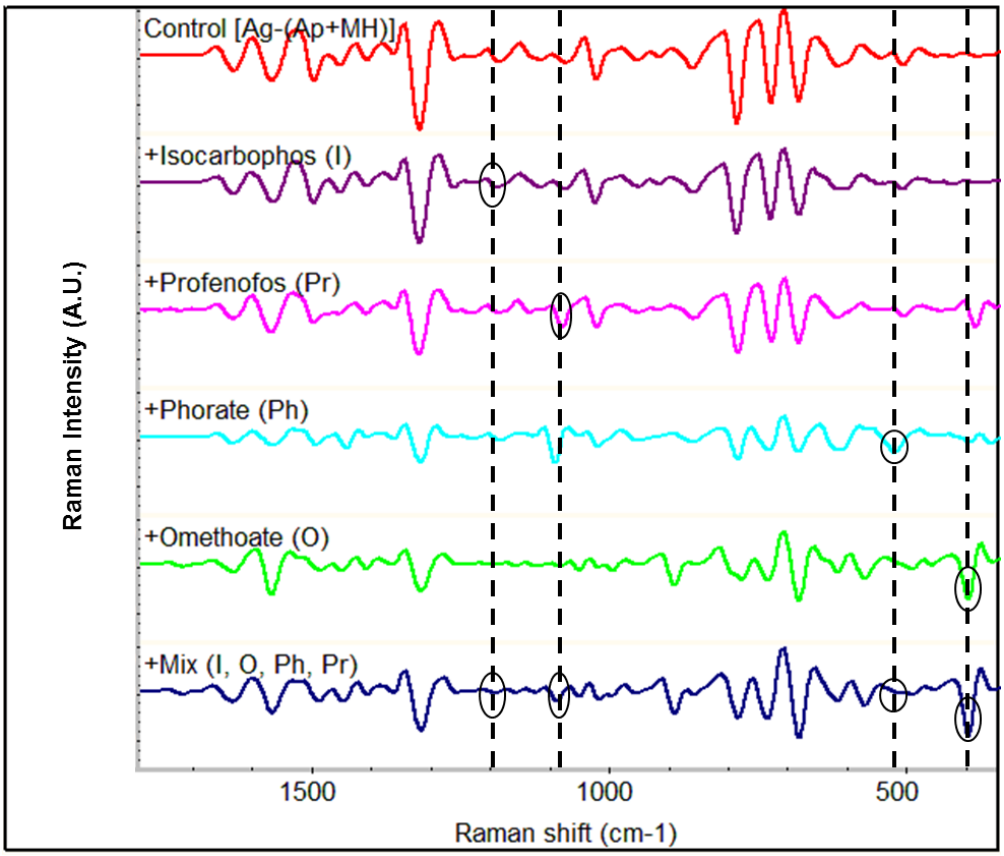

Figure 3.11 Second derivative Raman spectra of modified nanoparticles [Ag-(Ap+MH)] with iscarbophos, omethoate, phorate and profenofos respectively and the four pesticides mixed together at even concentrations. Total pesticide concentration for each sample was 0.5 mM. The distinct Raman peaks produced by each pesticide at different Raman shifts allows for simultaneous detection of the four specific pesticide

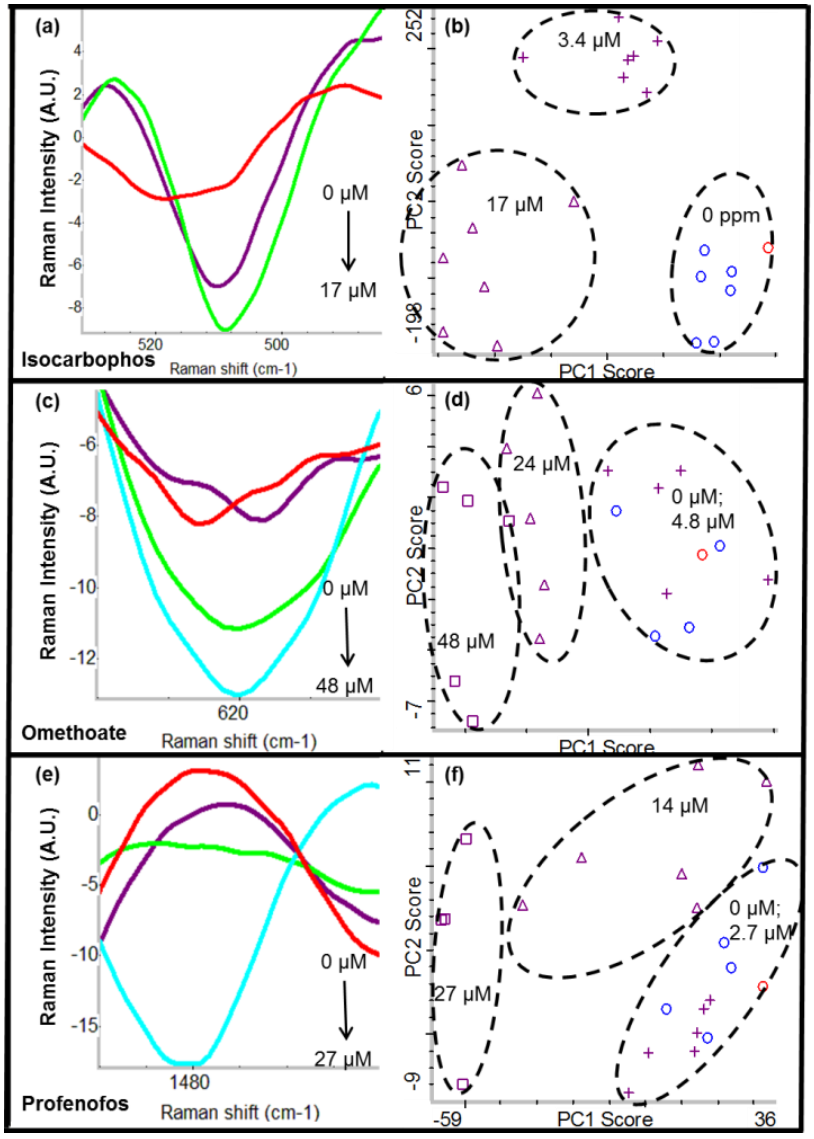

Figure 3.12 (a) Second derivative Raman spectra and (b) PCA plot of isocarbophos between 530-480 cm^{-1} for 0 µM, 3.4 µM (1 ppm) and 17 µM (5 ppm); (c) Second derivative Raman spectra and (d) PCA plot of omethoate between 630-610 cm^{-1} for 0 µM, 4.8 µM (1 ppm), 24 µM (5 ppm) and 48 µM (10 ppm); (e) Second derivative Raman spectra and (f) PCA plot of profenofos between 1490-1460 cm^{-1} for 0 µM, 2.7 µM (1 ppm) , 14 µM (5ppm) and 27 µM (10 ppm). A gradual increase in Raman peak intensities was seen when the spiked pesticide was introduced at increasing concentrations. Significant difference against the control (0 µM) was seen at 3.4 µM (1 ppm) for isocarbophos, 24 µM (5 ppm) for omethoate, and 14 µM (5 ppm) for profenofos

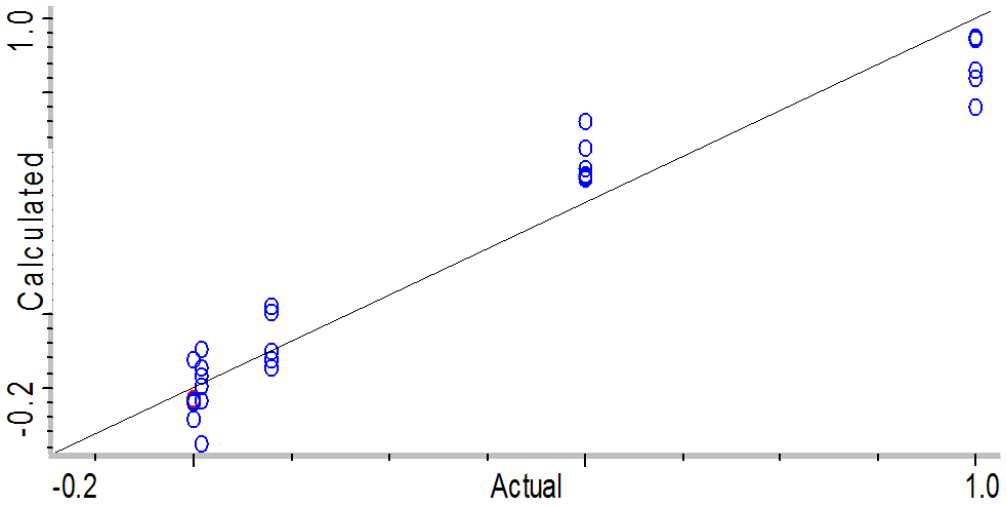

Figure 3.13 Partial Least Square analysis (PLS) of phorate spiked at 0 µM, 0.04 µM (0.01 ppm), 0.4 µM (0.1 ppm), 2 µM (0.5 ppm), 4 µM (1 ppm). This result shows a linear relationship between the spectral peak intensities (i.e. calculated value) and the actual phorate concentration. Quantitative analysis of phorate was possible within this range. The root mean square error calibration (RMSEC) was 0.101 and the correlation coefficient was 0.9628

CHAPTER 4

LABEL-FREE, APTAMER BASED SERS DETECTION OF *SALMONELLA ENTERITIDIS* AND *LISTERIA MONOCYTOGENES* FOR FOOD SAFETY APPLICATIONS[3]

4.1 Abstract

The overall objective of this study was to develop an aptamer-based SERS method that will improve the specificity of capture to salmonella enteritidis and listeria monocytogenes for detection in food matrix. In order to provide the best separation/specificity and SERS detection sensitivity, three types of fabricated SERS substrates, namely gold nanoparticles coated magnetic nanoparticles (Fe3O4@AuNPs), gold coated magnetic nanoparticles (Fe3O4@Au), and silver (Ag) dendrites were evaluated. Results show that although all three substrates can be separated from solution to detect bacteria, the aptamer-conjugated Ag dendrite was the only substrate having consistently, reproducible Raman intensities, and thus it was chosen as the SERS substrate for subsequent application studies. By conjugating onto Ag dendrites, aptamers were able to selectively capture their respective target bacteria, and increase aptamer related Raman peaks. The limit of detection for both salmonella enteritidis and listeria

[3] The contents of this study have not yet been submitted for peer-review and is under preaparation: Pang, Shintaro, Panxue Wang, Juhong Chen and Lili He. 2016. "Label-free, aptamer based SERS detection of *salmonella enteritidis* and *listeria monocytogenes* for food safety applications."

monocytogenes were 107cfu/mL in milk respectively. This method can be a promising tool to detect pathogens in real food matrix if combined with preenrichment of samples or by optimizing detection sensitivity.

4.2 Introduction

Salmonella enteritidis and *listeria monocytogenes* are two of the most common pathogens that cause foodborne illnesses [85]. In order to prevent these outbreaks, food manufacturers have the responsibility to monitor the microbial safety of their products to meet safety specifications. One of the challenges of current monitoring (detection) techniques is that they require lengthy times, typically over 24 h. This can lead to huge financial losses for the company, especially if microbial contamination is discovered after the product had been dispatched to market and a food recall has to be initiated.

To respond to this time sensitivity issue, many rapid detection methods have begun to emerge. These emerging techniques typically use sensors (e.g. colorimetric, electrochemical) that give simple readouts combined with biological agents (e.g. antibodies, enzymes, DNA) that selectively capture their target analyte [86,87]. To further improve the detection sensitivity of these assays, reporter molecules (e.g. fluorescein, dyes, MBA) are tagged to the target capture agent [88–90].

Surface enhanced Raman spectroscopy is an analytical tool that combines nanotechnology and Raman spectroscopy, and can be used to detect and characterize trace levels of analyte, including bacteria. Although Raman signals are relatively weak, the placement of nanoscale roughened noble metal nanosubstrates on the sample can enhance these signals by at least 10^4 times due to localized surface plasmon resonance and charge transfer mechanisms [3]. Hence, the main advantage of this detection method is that each target component which is in close proximity (< 10 nm) to the SERS substrate produces a strong, unique molecular fingerprint, making it much less likely for false positive or negative result to happen when compared to other emerging techniques.

Aptamers are an increasingly popular group of biosynthesized capture agents that can be fabricated easily to target a range of analytes, including bacteria. By definition, they are comprised of oligonucleotides (i.e. single-stranded DNA or RNA) and are pre-selected *in-vitro* based on their high binding affinity to their targets . These molecules can be easily modified chemically to attach probes such as thiol groups in order to conjugate it onto solid supports, and can be synthesized at high purity with low cost. When an aptamer is conjugated onto the SERS substrate, the method not only becomes more selective, but it can provide specific information of the chemical binding interaction between the target and capture agent. These characteristics make aptamer a promising capture agent, and have already become widely used in many applications such as diagnostic tools and drug discovery.

In this study, a label-free aptamer-based SERS technique was developed to detect two foodborne pathogens, *salmonella enteritidis* and *listeria monocytogenes* in milk. Recently, a study was reported based on an aptamer-based SERS technique using gold-coated magnetic nanoparticles as SERS substrates for bacterial detection [90]. Reporter molecules (i.e. Mercaptobenzoic acid and 5,5′-Dithiobis(2-nitrobenzoic acid)) were used as signal probes to enhance Raman peak intensity. It is worthy to note, however, that since the detection was solely based on the Raman peaks associated with the reporter molecule and not from the Raman fingerprint specific to the target bacteria, it cannot be used as a "self-validation" tool [91]. In other words, this method is unable to verify the true existence of the target analyte, which could have been done by comparing it against Raman spectral assignment associated with the target. In order to take advantage of the self-validation potential of aptamer based SERS, we attempted to perform aptamer-based SERS without the use of reporter molecules. A prominent focus of this study was to select the right kind of SERS substrate to improve the selectivity and specificity of the target pathogenic bacteria in food matrix. While the limit of detection of this assay was relatively high at10^7 cfu/mL for both target bacteria, this method was able to discriminate different bacteria based on the apatamer specificity, and drastically reduce the interference of food matrix, thus making this a potential way of detecting bacteria as a rapid detection method.

4.3 Materials and Method

4.3.1 Materials

All chemical reagents were purchased from Fisher scientific unless otherwise noted. The single stranded DNA aptamer sequences that were specific to capturing *salmonella enteritidis* and *listeria monocytogenes* were based on published literature [92,93], and purchased through Eurofins Scientific (Louisville, KY).

4.3.2 Nanoparticle Preparation

Different sizes of gold nanoparticles were synthesized using a standard procedure as outlined in published literature [94,95]. The nanoparticles were then coated onto ferrous oxide magnetic nanoparticles using another procedure as published in literature [96,97]. Silver dendrites were synthesized according previously published protocol [28,44].

4.3.3 Aptamer preparation

All aptamer sequences were obtained from published references with high binding dissociation constants to their respective targets [92,93]. The DNA sequences were then pre-ordered as salt-free, powder form, with a thiol-modification on the 5' end. The aptamer sequence selected for *salmonella enteritidis* was 5'- CTC CTC TGA CTG TAA CCA CGC ACA AAG GCT CGC GCA TGG TGT GTA CGT TCT TAC AGA GGT -3'

and the aptamer sequence for *listeria monocytogenes* was 5'-TAC TAT CGC GGA GAC AGC GCG GGA GGC ACC GGG GA -3'.

The aptamer stock solution was prepared by adding appropriate amounts of 1x Tris-EDTA buffer, pH 7.4 to make a 100 µM solution. Then, the thiol group was activated by adding 100x TCEP (i.e. reducing agent that breaks dithiol bonds) and incubated for 1 h with stirring. The prepared aptamer solution was then immediately added to nanoparticles in order to conjugate the aptamer.

4.3.4 Bacteria Preparation

All bacteria were obtained either from ATCC or from a microbiological lab at Cornell University. For this study, *Salmonella enterica subsp enterica* BAA1045 (SE1045) and *Listeria monocytogenes* (LM18) were used. E. Coli 0157:H7 (non-pathogenic strain) was also used for the specificity study. Initial frozen cultures were revived in tryptone soy agar and prepared fresh by transferring a single colony into a 10 mL soy broth at 37 ℃. This media was then incubated for 12 h, and centrifuged at 5000 X g for 5 min in order to collect the cells. The bacteria cells were washed three times with Dulbeco's phosphate buffer saline (DPBS) and resuspended in the same buffer.

4.3.5 SERS measurements

A DXR Raman Spectro-microscope (Thermo Scientific, Madison, WI) was used to analyze each sample spot. For silver dendrites, a 10× confocal microscope objective was used whereas 50× confocal microscope objective was used for gold nanoparticles for optimized enhancement (3 μm spot diameter and 5 cm−1 spectral resolution). 780 nm excitation wavelength was used with 5 mW laser power and 50 μm slit width at 2 s integration time. The OMNIC^{TM} software version 9.1 was used for this experiment with ten spots selected randomly for each sample within the range of 400-3300cm^{-1}.

4.3.6 Data analysis

SERS spectral data was analyzed using TQ Analyst software (version 8.0). The SERS spectra obtained from the multiple spots from each sample was averaged and then analyzed. Depending on the sharpness of the overall peaks, second derivative transformation and smoothing were applied at times in order to reduce spectral noise and to separate overlapping bands. Principal component analysis (PCA) was used to compare results against different bacteria/aptamer capture and concentrations. The accuracy and precision of the SERS data was compared using PCA as well. Generally speaking, if two data clusters (classes) do not overlap, then it means they are significantly different at the $p = 0.05$ level. The limit of detection LOD was determined to be the lowest concentration of the data cluster that can be separated from the negative control in the PCA plot.

4.3.7 Preparation of aptamer-conjugated SERS substrate

100 µL of magnetic nanoparticles solutions, gold nanoparticles coated magnetic nanoparticles (Fe_2O_3@AuNPs) or gold coated magnetic nanoparticles (Fe_2O_3@Au) (1 mg/mL) were expelled into a 0.6 ml centrifuge tube and a neodymium magnet (CMS Magnetics, Garland, TX) was used to gather the nanoparticles. 90 µL of supernatant was discarded and replaced with same volume of aptamer solution at varying concentrations (0, 1, 5, 10 µM). Then, the mixture was incubated overnight. After incubation, the magnet was placed next to the sample of nanoparticles to remove 90 µL of clear solution. The nanoparticles were then washed three times with water. Lastly, 1 mL of 40 µM 6-mercaptohexanol (MCH) was added and incubated for 1 hr to block any remaining uncovered surface, then 1 µL of nanoparticles were deposited on gold slide for Raman analysis to quantify aptamer coverage.

For Ag dendrites, 10 µL were deposited onto 1 mL of aptamer solution at varied concentrations (0, 1, 5, 10 µM) and incubated overnight over a nutating mixer, after which the solution was centrifuged at 2000 G for 30 seconds to separate the aptamer-Ag substrate from the supernatant. The substrate was then washed 3X with water, then 1 mL of 40 µM 6-mercaptohexanol (MCH) was added and incubated for 1 hr to block any remaining uncovered surface. Lastly, 1 uL of sample was deposited onto a gold slide for Raman analysis to quantify aptamer coverage.

4.4 Results and Discussion

4.4.1 Selection of appropriate aptamer-SERS substrate

The main objective of this study was to provide a selective detection method that could detect specific bacteria in a food matrix. To begin this study, three different nanoparticles were synthesized (**Fig. 4.1**). First, Ag dendrites was selected because we had previously discovered a strong SERS enhancement and reproducibility with its use in detecting other targets in both simple and complex food matrix[44,74,98]. Another rationale behind using this was that centrifugation could be used to separate the Ag dendrites from most food matrix. Gold coated magnetic nanoparticles (Fe_2O_3@Au) were selected as an alternative substrate because a magnet could be used to separate the magnetic nanoparticles from other non-specific materials not attached to the nanoparticles.

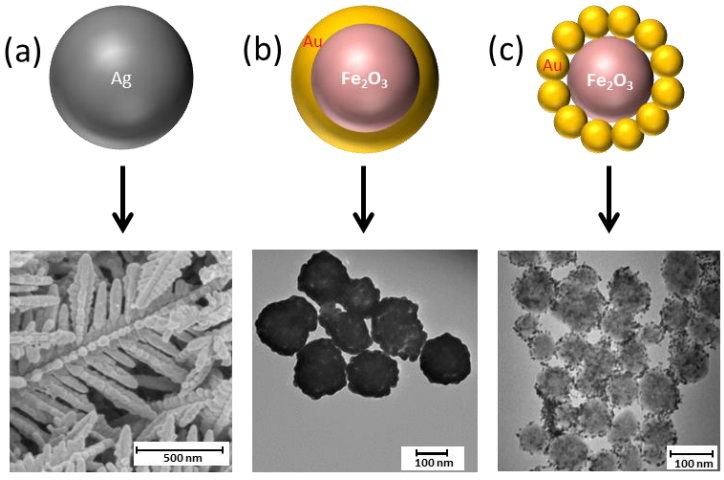

Figure 4.1 SERS substrates tested in this study: (a) Ag dendrites; (b) Au coated magnetic NPs; (c) Au nanoparticles-coated magnetic NPs.

Furthermore, the gold coating would allow for SERS enhancement [99]. Another type of magnetic nanoparticles (i.e. Fe_2O_3@AuNPs), were used to increase the surface area coverage, thus potentially increasing the aptamer coverage.

After the preparation of the three SERS substrates with conjugation to a salmonella specific aptamer, the target bacteria were inoculated for 30 min at 10^7 cfu/mL. As we can see from **Fig. 4.2**, all three SERS substrates showed a similar trend, which is, the overall Raman peak intensity from the aptamer-conjugated SERS substrates increased. This suggested that all three SERS substrates were sensitive enough to detect the aptamer-specific target bacteria at high concentrations.

However, upon looking closely at the reproducibility of the generated Raman spectra, we saw huge differences between the different SERS substrate. To begin, Fe_3O_4@AuNPs produced a darker red color in the supernatant after adding higher concentrations of aptamer with magnetic separation. This suggests that the AuNPs were released from the Fe_3O_4 core, likely because the binding affinity of thiolated end of the aptamer to the AuNPs was much stronger than Fe_3O_4 core's amine binding to AuNPs, thus displacing this bond. Consequently, the SERS results show discrepancies in spectral peaks and peak intensities, which make it hard to obtain consistent results.

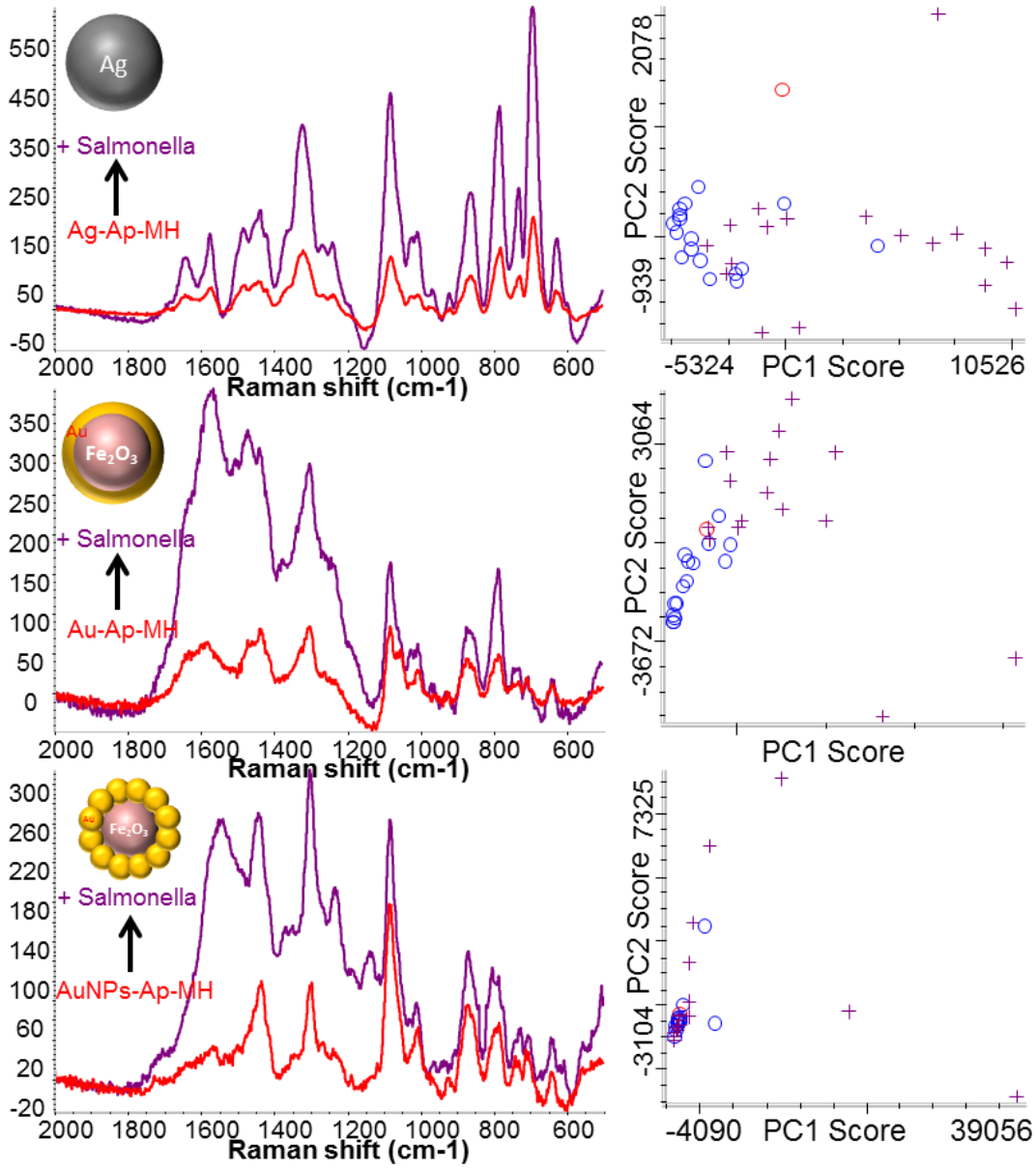

Figure 4.2 SERS spectra of *salmonella enteritidis* capture (10^7-10^8 cfu/mL) using various aptamer-functionalized SERS substrates. Their corresponding principal component analysis (PCA) plot is shown on the right where (○) symbolizes the substrate control and (+) symbolizes the substrate + *salmonella enteritidis*

For the Fe_3O_4@Au, there was no displacement of AuNPs from the Fe_3O_4 core, however, the peak intensities of the aptamer conjugated Fe_3O_4@Au varied widely, possibly because the aggregation of these nanoparticles between each other was not very consistent and/or synthesis of Au coating was not even. On the other, Ag dendrites were able to reproduce consistent Raman peak intensities (**Fig. 4.3**). Hence, based on the sensitivity and reproducibility of SERS, Ag dendrites were chosen as the most suitable SERS substrate.

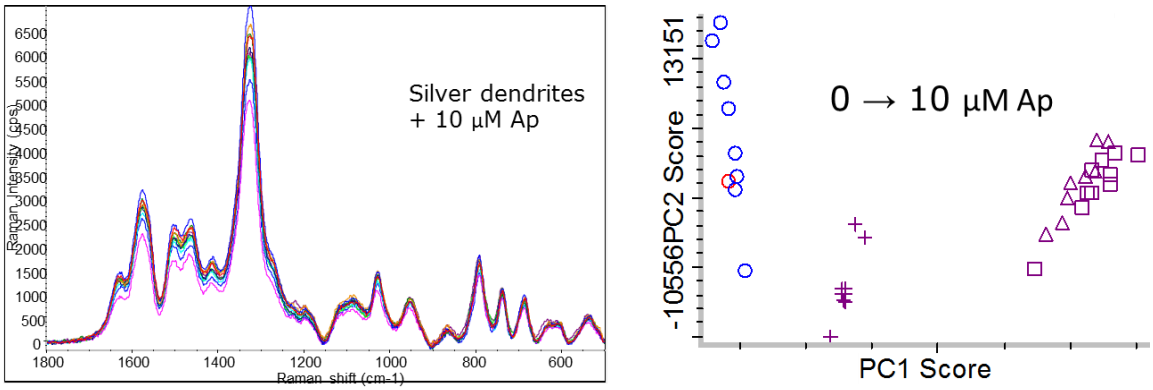

Figure 4.3 SERS spectra aptamer modified Ag dendrites at 10 µM aptamer and the principal component analysis plot of aptamer modified Ag dendrites with various aptamer concentration coverage.

4.4.2 Influence of Food Matrix on aptamer-conjugated Ag dendrites

One of the most challenging tasks of applying analytical techniques for bacteria detection is the interference of food matrix. Often, a laborious extraction method is used to purify the sample beforehand, which can take up valuable time and resources. In this study, our prepared SERS substrates were capable of removing noise signals coming

from food components. To do this, the first approach was to figure out a way to separate Ag dendrites physically from the food matrix. Since centrifugation can cause sedimentation of large molecules together with the Ag dendrites, a double sided tape was placed on the cap of a 2 mL microcentrifuge tube followed by deposition of Ag dendrites onto it. Hence, after mixing the sample solution with Ag dendrites in the tube, a short centrifugation (i.e. 2000 g for 3 sec) was sufficient to physically separate the larger food components from Ag dendrites (**Fig 4.4**).

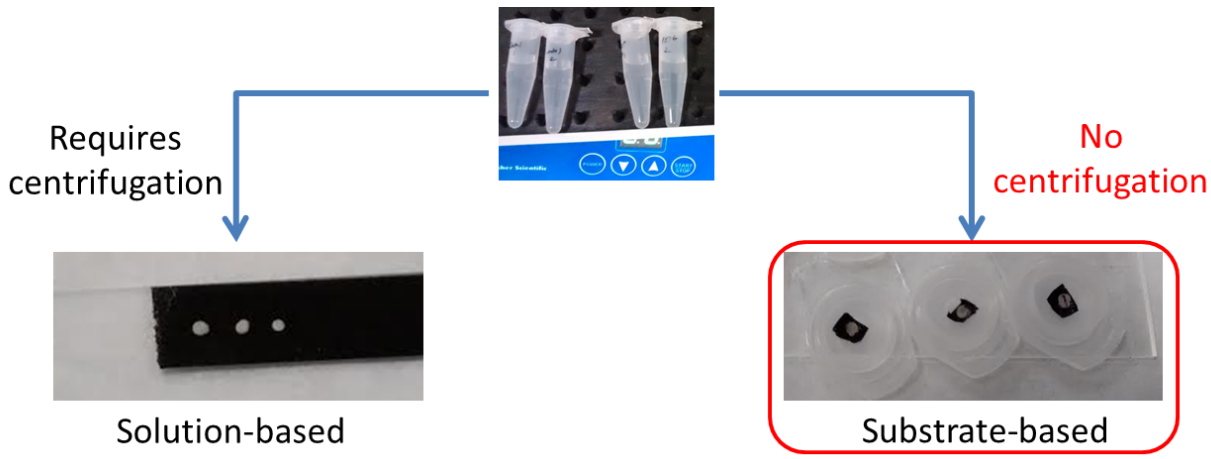

Figure 4.4 Two methods were proposed for using Ag dendrites, one that solely depends on centrifugation while the other largely depended on the use of a double sided tape to stick the Ag dendrites onto the cap of a microcentrifuge tube.

The optimal coverage of aptamer and the addition of blocker molecule (i.e. 6-mercaptohexanol) helped to remove influence of food components that might potentially bind to Ag dendrites (**Fig 4.5**). When 1 % fat milk was added to Ag dendrites, many sharp, Raman peaks were produced. However, when a similar milk sample was added to the aptamer-modified Ag dendrites, hardly any new peaks appeared. This suggests that

the aptamer coverage and MCH successfully eliminated the non-specific binding of food component molecules onto the SERS substrate.

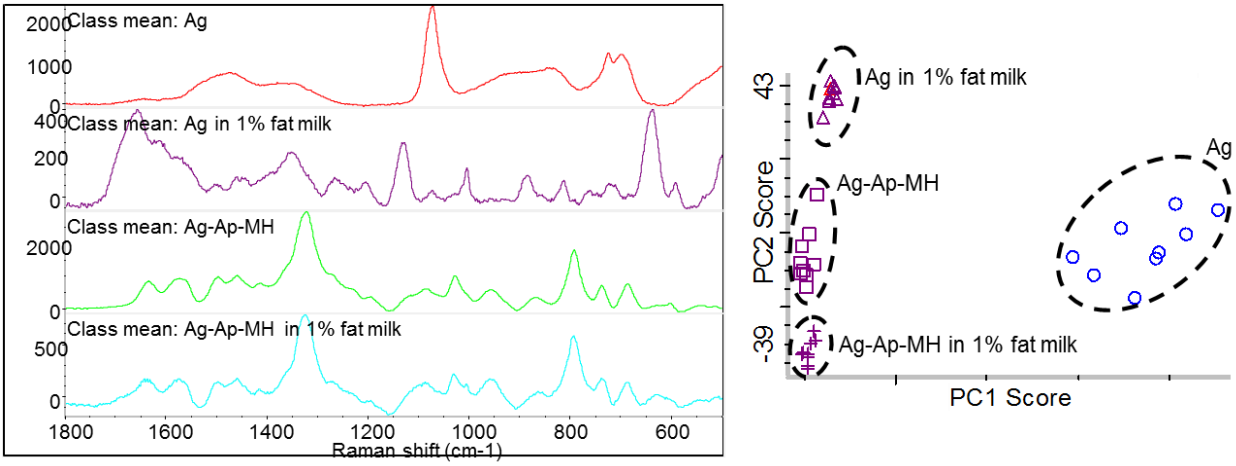

Figure 4.5 SERS spectra and principal component analysis (PCA) plots showing the influence of 1% fat milk on Ag dendrites and aptamer-modified Ag dendrites.

4.4.3 Specificity of aptamer-modified SERS substrate

In order to illustrate the specificity of the capture of target bacteria using the aptamer-SERS method, two different aptamers were tested. First, the salmonella specific aptamer was used and compared against a negative control and a different bacterium (i.e. listeria). As we can see from **Fig 4.6**, there was a statistical difference in the Raman spectra, or to be more precise, an increase in aptamer peak intensity around 1080 and 1580 cm^{-1}. There was a slight decrease in the aptamer peak intensity at both Raman shifts for listeria, which could be due to nonspecific layered coverage. This result is similar to adding food components (non-specific components) onto the SERS substrate. The increase in Raman peak intensity when salmonella was present could be due to a 3-dimensional

conformational change of the aptamer due to capture of its target, which may have caused certain parts of the aptamer to become closer to the Ag dendrites (< 10 nm).

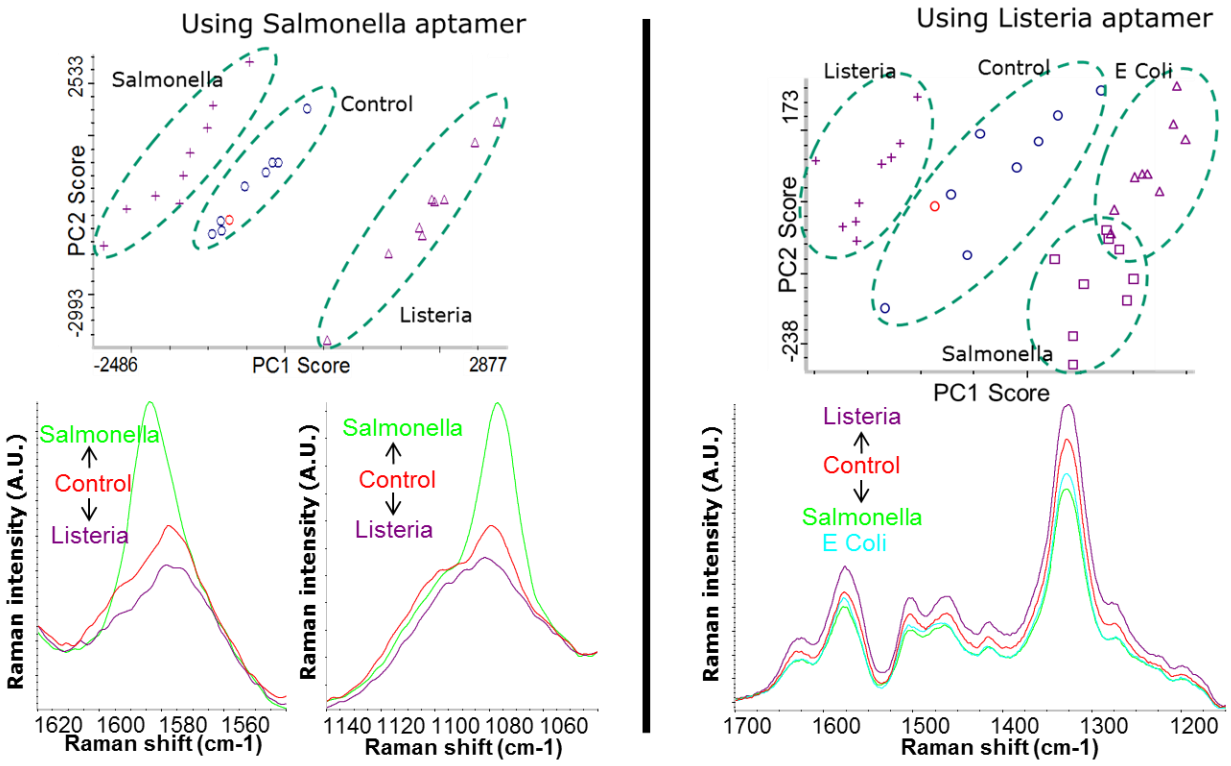

Figure 4.6 Specificity of salmonella aptamer and listeria aptamer based on the signals given by SERS analysis.

In a similar fashion, when a listeria specific aptamer was used, there was an increase in aptamer Raman peaks when listeria was added whereas a slight drop in Raman peaks when other bacteria (i.e. Salmonella and E. Coli) was added. These results suggest the high specificity of aptamer to capture their specific target bacteria.

4.4.4 Detection Limit of the aptamer-based SERS method

Fig. 4.7 shows the SERS spectra of salmonella enteritidis at different concentrations using aptamer modified Ag dendrites. Based on the second derivative SERS spectra and the 3-D principal component analysis graph, the limit of detection was found to be 10^7 cfu/mL in 1% milk which was diluted by one-tenth. Compared to other established bacteria detection methods, this may be considered high. This could be due to the large size of the bacteria (5-10 µm) and the far distance of it from the Ag nanoparticles, thus making SERS enhancement weak.

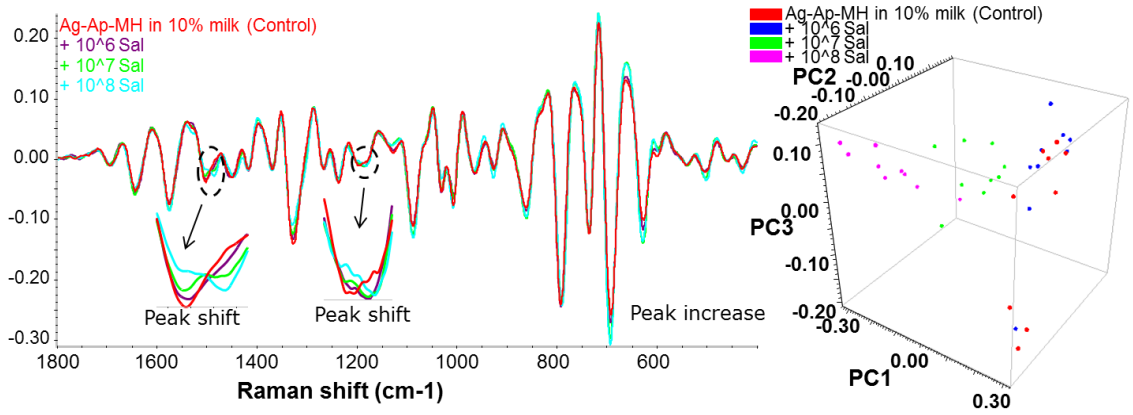

Figure 4.7 The limit of detection of aptamer based SERS on the detection of bacteria (i.e. Salmonella enteritidis).

We also attempted to lower the detection limit using Raman mapping to see if there were any spots that had significantly higher Raman peak intensity changes (Fig 11). Unfortunately, there were no significant differences in Raman peak intensities at 10^3 – 10^6 cfu/mL. Thus, this method can only be used to detect higher concentrations of bacteria.

4.5 Conclusions

The label free, aptamer-based SERS method was successfully developed to detect bacteria in food matrix. The Raman spectral profile had little influence from food matrix and only lowered Raman peak intensities. On the other hand, the addition of target bacteria increased the aptamer related Raman peaks, which can be seen by both the spectra and principal component analysis. More work should be conducted to lower the detection limit of this technique in order to use it as a sensitive detection tool. However, overall, this method serves as a model for the rapid detection of bacteria in complex solutions such as milk using aptamer-based SERS.

Supplementary Figures

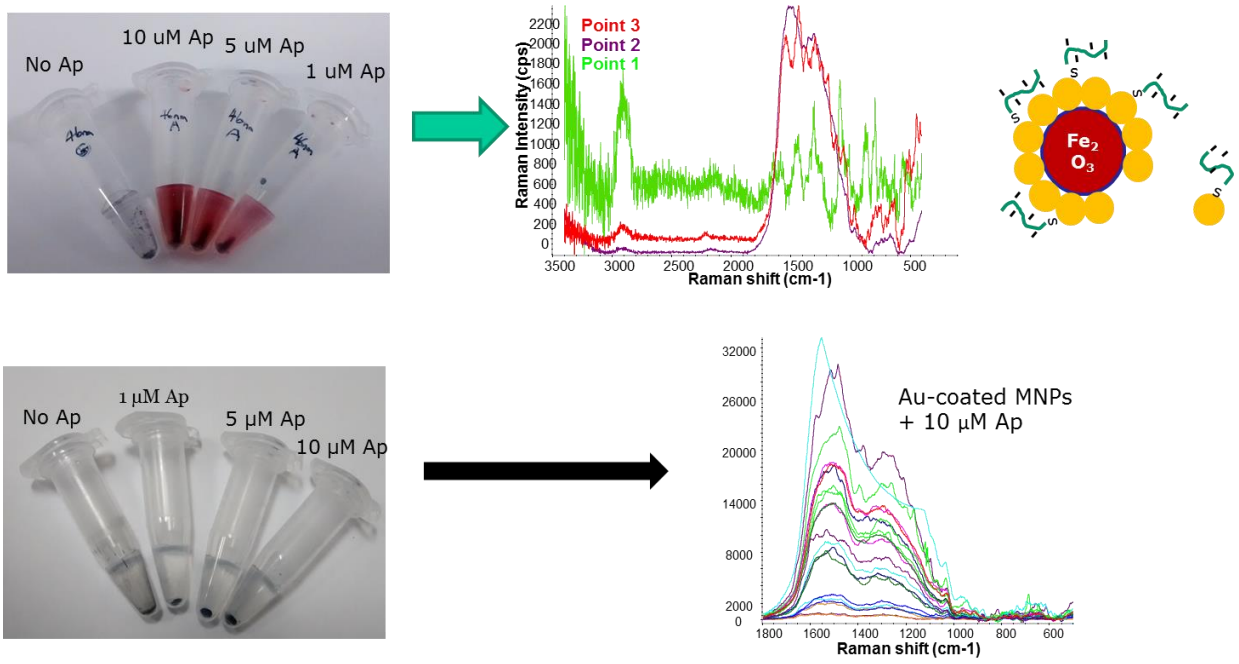

Figure 4.8 Irregularities in reproducibility seen in both gold nanoparticles coated magnetic nanoparticles (above) and gold coated magnetic nanoparticles below.

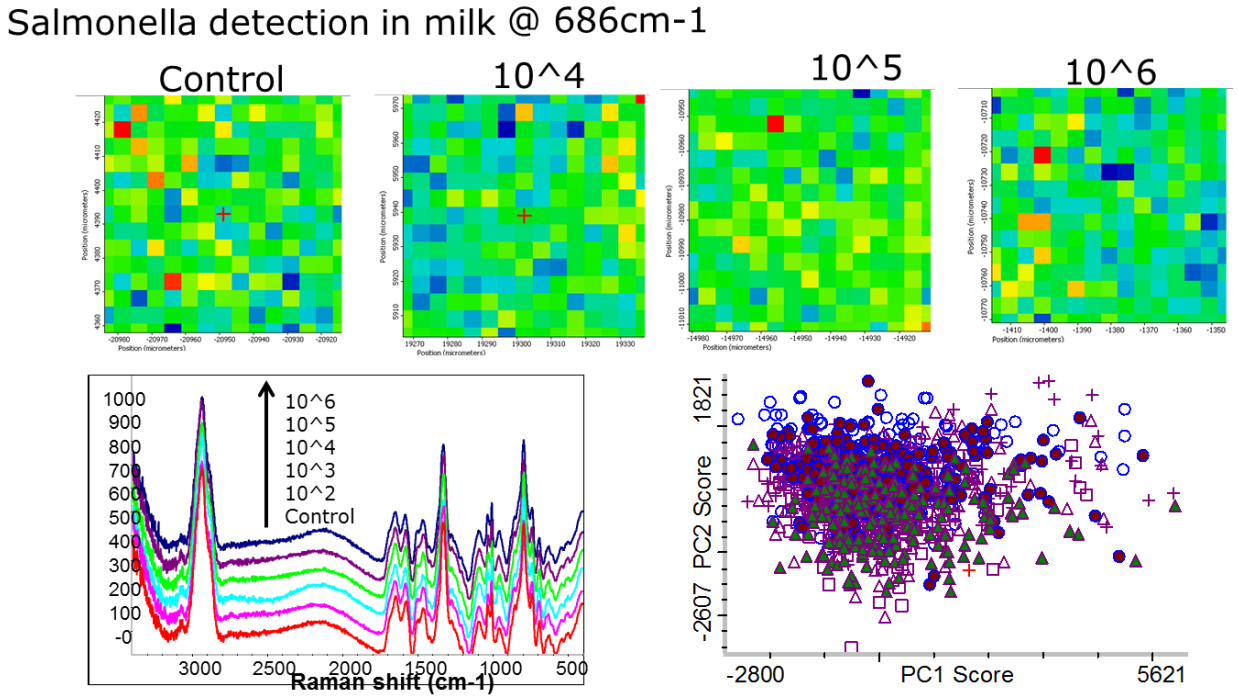

Figure 4.9 Raman map of salmonella enteritides at different concentrations using aptamer modified Ag dendrites.

CHAPTER 5

UNDERSTANDING THE COMPETITIVE INTERACTIONS IN THE APTAMER−GOLD NANOPARTICLE BASED COLORIMETRIC ASSAYS USING SURFACE ENHANCED RAMAN SPECTROSCOPY (SERS)[4]

5.1 Abstract

Aptamer−gold nanoparticles (AuNPs) based colorimetric assays have become increasingly popular as a viable rapid detection method, but the molecular interactions governing the mechanism and successful interpretation of the color changes has not been explored well. The objective of this study was to evaluate the competitive interactions that occur in this detection assay at the molecular level by employing surface enhanced Raman spectroscopy (SERS). The SERS signals of molecules in close proximity to AuNPs were exploited to give information on AuNPs surface coverage as well as ssDNA aptamer conformational changes during target capture. Two antibiotics, ampicillin and kanamycin, and their respective aptamers, were used in this study. Results indicate the reason for the lack of AuNPs aggregation with ampicillin could be due to a stronger binding affinity of AuNPs to the ampicillin than to the aptamer. Kanamycin, on the other

[4] Pang, Shintaro, and Lili He. 2016. "Understanding the Competitive Interactions in the Aptamer−Gold Nanoparticle Based Colorimetric Assays Using Surface Enhanced Raman Spectroscopy (SERS)." Anal. Methods (January 20). doi:10.1039/C5AY03158C.

hand, induced AuNPs aggregation to produce color change and the SERS data indicate a stronger binding affinity of kanamycin to the aptamer compared to the AuNPs as well as aptamer conformational changes. The use of SERS can be a potential tool to rapidly screen and validate the aptamer and target interaction for application of aptamer−gold nanoparticles (AuNPs) based colorimetric assays.

5.2 Introduction

Gold nanoparticles (AuNPs) are popular detection probes because they are able to produce a range of colors, caused by the shift of surface plasmon resonance (SPR) upon aggregation.[100] Target induced AuNPs aggregation has been widely applied in a variety of AuNPs based colorimetric assays for rapid sensing of ions (e.g. Hg^{2+}), small molecules (e.g. cocaine), complex molecules (e.g. proteins) and even cells.[101–104] One of the main advantages of using this kind of assay is the ability to detect changes with the naked eye. In addition, if an accurate and quantitative result is desired, a relatively inexpensive and commonly available spectrophotometer can be used to analyze a range of absorbance wavelength with precise optical density values. On the other hand, a major limitation hindering the application of many modes of AuNPs based colorimetric assays is the tendency for nonspecific interactions that can significantly alter the aggregation status of AuNPs. Indeed, a considerable number of papers have been dedicated to overcoming the nonspecific interactions, or biofouling, of AuNPs in the colorimetric detection assays.[105,106]

In order to reduce the non-specificity of AuNPs based colorimetric assays, aptamers have been employed as target specific bio-capture agents. Aptamers are single stranded oligonucleotides that are artificially synthesized to capture its target. They have many benefits as a target capture agent due to the ease in reproducibility for synthesis, versatility in labelling, immobilizing, signaling and regenerating.[68,69] Furthermore, recent technological advancements have made it faster and cheaper to create new aptamers.[107,108] However, the most compelling reason for choosing aptamers as opposed to other target capture agents (e.g. antibodies) is its ability to capture virtually any target, including small molecules (e.g. toxic chemicals).[95,103,109–117] One of the common strategies for applying ssDNA in the AuNPs based assay is to adsorb ssDNA onto AuNPs surfaces to stabilize the AuNPs. The flexibility of the ssDNA aptamer to partially uncoil its bases allows the negative charge of the phosphate backbone to be sufficiently distant so that van der Waals forces between the bases and the gold is strong enough to cause the ssDNA to stick to the gold.[118] When a target is later introduced into the mixture, the aptamer will bind to the target, which can cause the aptamer to de-attach from AuNPs due to conformational change in its tertiary structure. Hence, the AuNPs becomes prone to aggregation by neutralization of the surface charge with salts added later.

Despite the numerous benefits of using aptamers in a detection method such as the AuNPs based colorimetric assay, there are several limitations that can hinder the

successful implementation of this method. For example, aptamers are often selected in a buffer environment with a defined concentration of salts and pH, and thus, work optimally in those conditions, which happen to be critical factors contributing to the aggregation of AuNPs.[95] Hence, premature AuNPs aggregation may occur if sample solution matrix environment can significantly destabilize the AuNPs. Another challenge is the variable affinity of different aptamer sequences to AuNPs. For example, dT was found to have a much lower binding affinity to AuNPs than dG, dC, and dA., hence an aptamer sequence with more dTs may have lower binding affinity to AuNPs.[119] The same study also showed the length of oligonucleotides was able to significantly affect the stability of AuNPs. Lastly, there is still a possibility of other molecular interactions in the colorimetric assay that can significantly alter the results

In this study, we aim to understand the competitive interactions between AuNPs, aptamers, and targets in the aptamer-AuNPs based colorimetric assay described above. Two aptamers for the food-related antibiotics, ampicillin and kanamycin, respectively[111,114] were chosen for this study. Several key factors are considered and investigated. Firstly, a critical step to ensure the reliability and sensitivity of the detection assay is the optimization of the concentration ratio of AuNPs to aptamer. A lower than optimal AuNPs:aptamer concentration ratio will lead to false positives because the AuNPs will not be covered fully whereas a higher than optimal concentration ratio will lead to false positives. Secondly, for reliable application, the aptamer must have a stronger binding affinity to the target than to the AuNPs. Thirdly, it is equally important

that the target has a stronger binding affinity to the aptamer than to the AuNPs. If it was the other way around, the method will be unreliable and potentially give false results.

Here, we applied surface enhanced Raman spectroscopy (SERS) to investigate these competitive interactions. SERS is a combination of Raman spectroscopy and nanotechnology. Raman spectroscopy is capable of molecular fingerprint specificity for every distinct molecule that is being analyzed. Noble metallic nanosubstrates are essential in the enhancement of these Raman signals, attributed to the electromagnetic and charge transfer mechanisms. AuNPs are excellent SERS nanosubstrates when aggregated together and the chemical signatures of analytes staying in close proximity get mostly enhanced, and hence, the use of SERS not only requires little sample preparation, but allows for quick analysis of the surface interactions occurring between AuNPs, aptamer and/or target.

To the best of our knowledge, this is the first study that is conducted to understand the competitive interactions of molecules involved in the aptamer-AuNPs based colorimetric assay. The procedure and results from this study not only help us understand the interactions that occur in the molecular level, but also give us an analytical framework for future studies that may require understanding of competitive interactions in a complex system.

5.3 Materials and Methods

5.3.1 Chemicals and Reagents

Chloroauric acid ($HAuCl_4$), was purchased from Sigma Aldrich (St. Louis, MO, USA). Tetrasodium citrate, potassium phosphate monobasic, potassium phosphate dibasic, sodium chloride, ampicillin and kanamcycin and were purchased from Fisher Scientific (Pittsburg, PA, USA). ssDNA aptamers were purchased as lyophilized powder (salt-free) through Eurofins MWG Operon (Huntsville, AL, USA). Double distilled water was obtained from MicroPure system UV/UF (Fisher Scientific, Pittsburg, PA, USA) and was used throughout the experiment.

5.3.2 Synthesis of citrate-stabilized AuNPs

13 nm diameter AuNPs, as used in many aptamer-based colorimetric assays[95,103,109–117], were synthesized using a citrate reduction method. [94,95,120] Prior to synthesis, glassware were soaked in aqua regia (3 parts HCl, 1 part HNO_3), rinsed copiously with double distilled water and dried. Then, in a 250 ml beaker, 100 ml of 1 mM $HAuCl_4$ solution was heated on a hot plate with vigorous stirring using a magnetic stir bar. When the aqueous 1 mM $HAuCl_4$ solution started to boil, 10 ml of 38.8 mM trisodium citrate was quickly added and allowed to continuously boil for 20 min. During the boil, the color of the mixture turned from pale yellow to colorless, then to dark red. After 20 min, the mixture was taken off the hot plate and cooled to room temperature in a clean, closed lid container. TEM was performed to verify the size and

consistency of the AuNPs (13 $\pm$ 1.1 nm) (**Fig. 7**). The AuNPs concentration was then determined using Beer's Law with an extinction coefficient of 1.39 X 10^8 M^{-1}, resulting in calculated value of 17 nM.[121]

5.3.3 Aptamer preparation

ssDNA aptamer specific to ampicillin and kanamycin were obtained from literature[111,114]. The ampicillin specific aptamer (AMP17) sequence was 5'-GCGGGCGGTTGTATAGCGG-3'while the kanamycin specific aptamer (Ky2) sequence was 5'- TGGGGGTTGAGGCTAAGCCGA-3'. Prior to use, the aptamers were dissolved in 10 mM potassium phosphate buffer (pH 8.0), heated to 95 °C for 2 min and cooled to room temperature for 1 h in order to ensure the proper, 3-dimensional ssDNA conformation. The aptamer solution was then further diluted with buffer to various concentrations for analysis.

5.3.4 Procedure of aptamer-AuNPs based colorimetric assay

In a 96-well microplate, 40 µL of AuNPs was first mixed and incubated with 60 µL of 600 nM aptamer solution for 5 min. Then, 60 µL of target at various concentrations (final: 0, 30, 300, 600, 1200 nM) were added and mixed with the aptamer-AuNPs solution for 5 min. After incubation, 40 µL of 500 mM NaCl solution was added to induce AuNPs aggregation and the mixture was left for another 5 min to equilibrate. Pictures were taken and absorbance spectra (i.e. wavelength range: 450-750 nm) were

measured using a SpectraMax M2e UV-vis spectrophotometer (Molecular Devices, Sunnyvale, CA, USA). Finally, the absorbance ratio (620/520) was calculated to quantify the degree of AuNPs aggregation for each sample. Each sample was conducted in triplicates.

5.3.5 SERS study of molecular interactions in matrix

One of the main advantages of using SERS to study molecular interactions is the ability to analyze samples in situ. Since little or no sample preparation is required, it can be analyzed rapidly without the limitation of time lag and destruction of samples. In this study, 1 µL of each sample mixture obtained from the aptamer-AuNPs-based colorimetric assay were deposited onto a gold-coated slide and left on a counter for a few minutes to dry. Then, the samples were analyzed using a DXR Raman spectro-microscope (Thermo Scientific, Waltham, MA, USA).

OMNIC^{TM} software version 9.1 was used to control the DXR Raman spectro-microscope. The sample surface was first focused using a 50x microscope objective lens, then ten spots were randomly selected within the region of aggregated AuNPs to maximize Raman enhancement effects. Aggregated AuNPs were mainly formed around the sample coffee ring and were characterized by dark, black spots.

Raman instrumentation parameters used include a 780 nm laser excitation wavelength connected to a 50 µm slit width aperture, which produced a 4.7–8.7 cm^{-1} spectral resolution and 3.1 µm spot diameter. The laser power used was set at 5 mW with an integration time of 2 s per spot. The spectral range analyzed was 400 - 3000 cm^{-1}.

After collecting all the spectra, the data was inputted into TQ Analyst software (Thermo Scientific, Waltham, MA, USA) for statistical analysis. First, all the spectra gathered from different spots in each sample were averaged, and then normalized using the full spectral range (i.e. 400-3000 cm^{-1}) in order to reduce peak intensity variations attributed to Raman enhancement differences. Then, second derivative transformation and smoothing were applied so as to reduce spectral noise and to separate any overlapping bands. Finally, the principal component analysis (PCA) function was used to quantitatively compare the differences between several sets of spectra. This function is primarily used to focus the spectral data analysis onto the most dominant features, thereby removing random variations that are of less significance. The extent of variation between different samples is then measured based on how far the sample spots are from each other on the PCA plot. For example, if the spots representing "A" is clustered away from spots representing "B", then we can conclude that these two samples are significantly different from each other ($p<0.05$). On the other hand, if "A" and "B" spots overlap each other, then they are not significantly different from each other. Hence, this

type of discriminant analysis is useful to determine the extent of variation between different sample spectra.

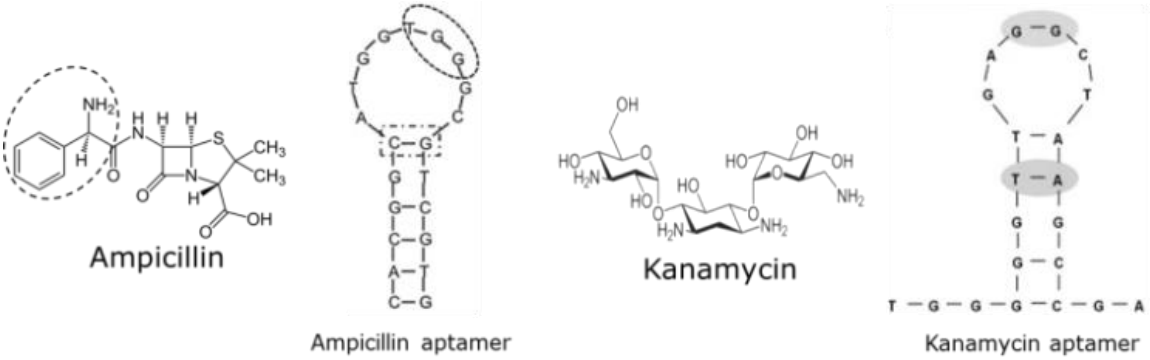

Figure 5.1 Chemical structures of target antibiotics and aptamers used (i.e. circled regions on aptamer structures indicate conserved motifs) [aptamers obtained from Song et. al.[111,114] Used with permission from Elsevier]

5.4 Results and Discussion

5.4.1 Target-Aptamer Interactions

To understand the competitive interactions in the aptamer-AuNPs colorimetric assay, it is important to first understand the basic mechanism for target-aptamer interactions. The underlying molecular interaction between aptamers and their target is largely due to hydrogen bonding, electrostatic interactions, stacking of aromatic rings and van der Waals interaction.[108] They typically follow an induced fit model, whereby the aptamer changes its 3-dimensional structure to interact fully with their target. Their secondary structure is also characterized by stems, internal loops, bulges, hairpins, tetra loops,

pseudoknots, triplicates, kissing complexes, or G-quadruplex; these specific structures influences the binding sites of the target.

The chemical structure of ampicillin and kanamycin, together with the secondary structure of ssDNA aptamers specific to these two compounds are shown in **Fig. 5.1**.

Ampicillin is a β-lactam antibiotic, and is characterized by a β-lactam ring in its molecular structure. Its side chain (circled) contains a primary amine functional group and a benzene ring. Interestingly, the ampicillin aptamer was reported to be highly specific to the ampicillin side chain, as other β-lactam antibiotics with similar chemical structures such as amoxicillin (i.e. additional hydroxyl group) and benzylpenicillin (i.e. lacks primary amino group) had significantly lower binding affinity to the aptamer (AMP17).[114] The aptamer sequence responsible for the binding of ampicillin was also reported to be "-GGT(T)-" in the loop region as well as "-GC-" base pairing (circled) at the joint of a loop and stem.[114]

Kanamycin is an aminoglycoside antibiotic, and is characterized by amino-modified glycoside groups in its molecular structure. Similar antibiotic structures such as kanamycin b (i.e. one hydroxyl group replaced by an amine) and tobramycin (i.e. one hydroxyl group replaced by an amine and another hydroxyl group removed) were shown to have similar binding affinity to the kanamycin aptamer (Ky2).[111] Other antibiotics with relatively different chemical structures such as ampicillin (i.e. penicillin),

streptomycin (i.e. aminoglycoside) and sulfadimethoxine (i.e. sulfonamide) were reported to have significantly less affinity to the aptamer.[111] This suggests that this aptamer sequence may be broad-specific for kanamycin and its derivatives. The "-TGGA"- motif (circled) was also found in a stem and loop structure in every aptamer candidates, hence it was concluded that this structure was primarily responsible for the capture of kanamycin.[111]

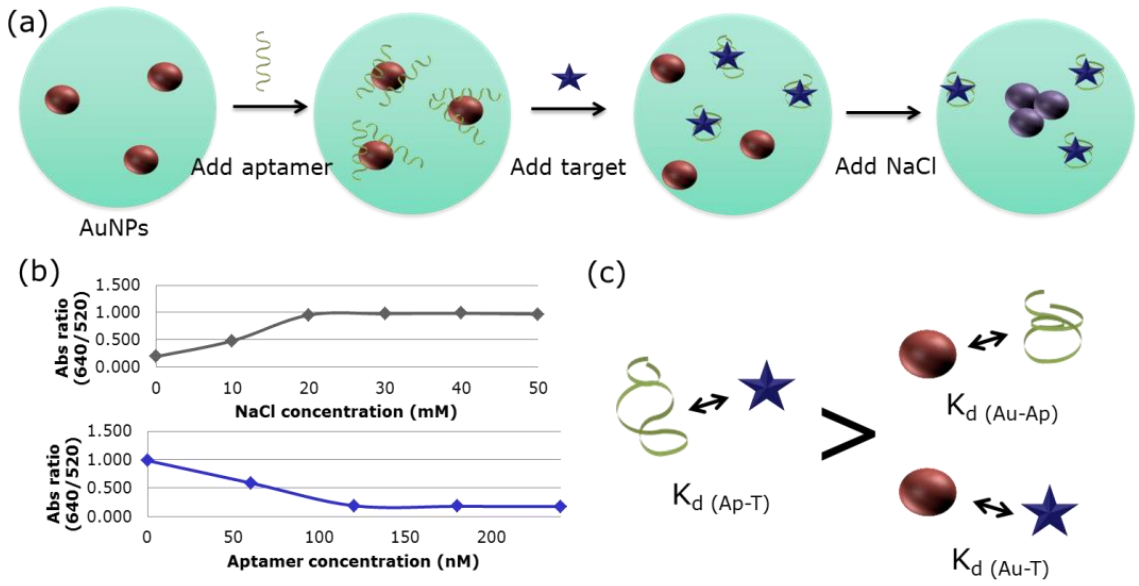

Figure 5.2(a) Schematic Illustration of a suitable aptamer-based colorimetric assay; (b) Optimization of aptamer and NaCl concentrations using absorbance ratio (i.e. 640/520); (c) Relative binding affinity (Kd) requirements for successful implementation of the aptamer-based colorimetric assay (Ap = aptamer; T = target; Au = gold nanoparticle)

5.4.2 Optimization of Concentration-Ratios

In order to study competitive interactions in the aptamer-AuNP based colorimetric assay, it is important to optimize the detection assay to best represent the implementation

of this method. The use of the right concentrations of each component in the aptamer-AuNP based colorimetric assay is crucial to not only improve sensitivity, but to also prevent false colorimetric results. **Fig. 5.2a** shows a schematic illustration of the aptamer-AuNP based colorimetric assay.

The first important optimization step is the concentration of NaCl added to induce the aggregation. NaCl is used in this assay to neutralize the surface charge caused by citrate-capped (i.e. negatively charged) AuNPs. Adding too little NaCl will cause insufficient neutralization of the surface charge of AuNPs, hence it will not induce aggregation (i.e. change color) even if aptamers were not bound to the AuNPs. If too much NaCl is added, it can potentially neutralize the surface charge of ssDNA aptamers, and thus cause AuNPs to get close enough for a color change, even though steric hindrance can prevent full aggregation. Our results show that 30 mM NaCl was optimal for the full aggregation of AuNPs without aptamer (Fig. 2b), and hence this concentration was used for subsequent experiments in this study.

The second optimization step in this assay requires knowledge of how much aptamer to add to AuNPs. If insufficient aptamer is added, the AuNPs will be partially exposed and will be more sensitive to AuNPs aggregation. On the other hand, if there is an oversaturated amount of aptamer, the AuNPs will more likely still be covered by aptamer even after target addition as the target will preferentially bind to the aptamers not bound to AuNPs, hence a false negative result can occur. **Fig. 5.2b** shows the absorbance ratio

(640/520) of the samples decreasing as more aptamer is added to AuNPs until an optimum concentration (i.e. 180 nM), where it begins to remain constant even after more aptamer addition.

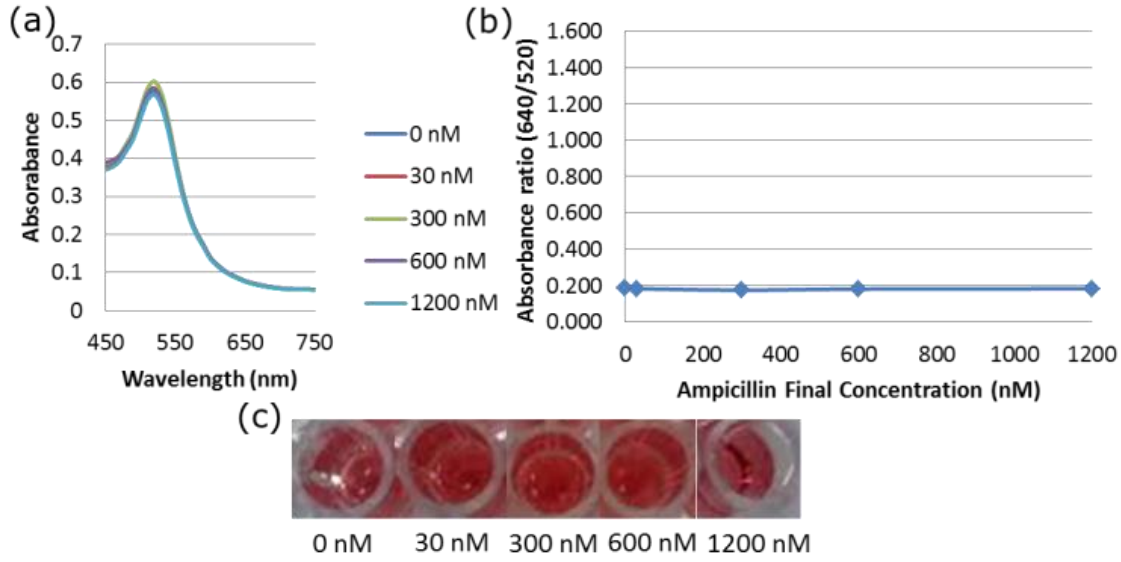

Figure 5.3(a) UV-vis absorbance of aptamer-based colorimetric samples with various ampicillin concentrations; (b) Absorbance ratio (640/520) based on UV-vis absorbance; (c) Optical image of aptamer-based colorimetric samples with increasing concentrations of ampicillin (left to right).

5.4.3 Competitive Interactions Influencing the Detection of Ampicillin

Fig. 5.2c shows the key competitive interactions and their relative affinities to each other in order to have a reliable aptamer-AuNPs colorimetric assay. Briefly, the relative binding affinity between aptamer and target must be stronger than the aptamer-AuNPs and the target-AuNPs interactions. The detection of ampicillin was used as the first example for investigating these competitive interactions. To do this, ampicillin was tested

at several concentrations that represented a range of aptamer:target concentration ratios (i.e. 16:1, 2:1, 1:1, and 1:2). The absorption spectrums of these samples are shown in **Fig. 5.3a**.

Surprisingly, the absorption peak for all target concentration samples was 520 nm, which is representative of a wine-red color (**Fig. 5.3c**). **Fig. 5.3b** shows the absorption ratio vs ampicillin concentration graph, where the higher the absorption ratio, the more aggregation of AuNPs has occurred. This result showed no significant difference ($p<0.05$) in the aggregation status of these samples.

SERS was then used to elucidate the surface chemistry of AuNPs. **Fig. 5.8** shows the full raw SERS spectra of all the samples analyzed. In order to interpret the SERS data, the second derivative SERS spectra after smoothing and normalization was used to reduce spectral noise and to focus on changes caused by the addition of ampicillin. **Fig. 5.4** includes the second derivative SERS spectra and principal component analysis (PCA) 3-D graph of samples analyzed at a lower (i.e. 30 nM) and higher (600 nM) ampicillin concentration.

At the lower ampicillin concentration, it is evident that the AuNPs surface coverage is dominated by peaks attributed to the binding of aptamers. The PCA graph shows a statistical similarity between the “Aptamer only” sample (i.e. AuNPs mixed only with

aptamer) and the "Aptamer+Ampicillin (30 nM)" sample (i.e. AuNPs mixed with aptamer and 30 nM ampicillin). The SERS spectra at higher ampicillin concentrations, however, show a different result. A quick observation of the spectra shows a huge difference between the "Aptamer only" and the "Aptamer + Ampicillin (600nM)" samples, but a very close resemblance between the "Aptamer + Ampicillin (600nM)" and "Ampicillin only (600nM)" samples. The PCA graph confirms this observation and thus, we can conclude that the AuNPs surface was almost fully covered with ampicillin and furthermore, displaced the aptamer previously bound to the AuNPs.

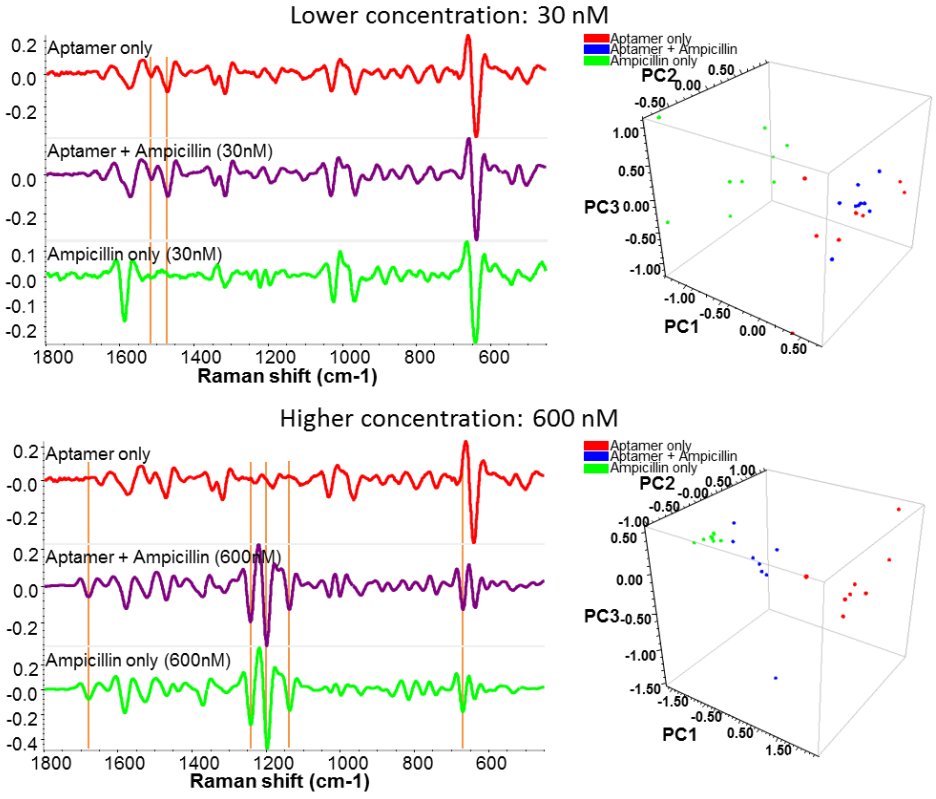

Figure 5.4 Second derivative SERS spectra and principal component analysis chart of aptamer-based colorimetric samples at low (i.e. 30 nM) and high (600 nM)

ampicillin concentrations. Aptamer and ampicillin peaks are represented by orange lines on the spectra. Other specific peaks can be located by referring to Fig. 8.

From the SERS results (i.e. structure), the colorimetric results (i.e. function) can be better explained. In this case, the SERS results showed that in these sample matrices, the AuNPs-ampicillin interaction was stronger than the AuNPs-aptamer and ampicillin-aptamer interactions, so that the ampicillin can replace the aptamer on the AuNPs. From the molecular structure of ampicillin, we speculate the interaction between ampicillin and AuNPs is primarily through the Au-S bond, which is very strong and commonly used for surface modification of Au.[122,123] After ampicillin has covered the AuNPs surface, the addition of salt was unable to induce aggregation due to the steric repulsion of the ampicillin molecules. It is also possible some aptamers were still attached to the ampicillin even after ampicillin covered the AuNPs, as some little aptamer signals were observed in the SERS spectra of the "Aptamer + Ampicillin (600nM)" sample, and thus provide additional repulsive charge/hindrance to prevent AuNPs aggregation. In this scenario, because of the proximity of the aptamer from the AuNPs was further than the ampicillin, the signals of the aptamer was much weaker than the ampicillin. In either case, however, the competitive interactions and their relative affinity to each other do not meet the assay criteria to obtain desired results in the aptamer-AuNPs based colorimetric assay.

5.4.4 Competitive Interactions Influencing the Detection of Kanamcyin

To better understand the competitive interactions influencing the detection of analyte in the aptamer-AuNPs colorimetric assay, kanamycin was used as the second target with its specific aptamer sequence. **Fig. 5.5a** shows the colorimetric results as kanamycin concentration was added from 0 to 1200 nM.

As the concentration of kanamycin increased, the absorption peak wavelength shifted from 520 nm to approximately 640 nm, which corresponds to the visual color change from red to blue (**Fig. 5.5c**). The absorption ratio (640/520) increased from 0.2 to 1.4 when the kanamycin concentration was increased from 0 to 600 nM, with a linear, concentration-dependent curve from 30 to 600 nM ($R^2 = 0.994$) (**Fig. 5.5b**). These colorimetric results show the successful aggregation of AuNPs due to kanamycin introduction.

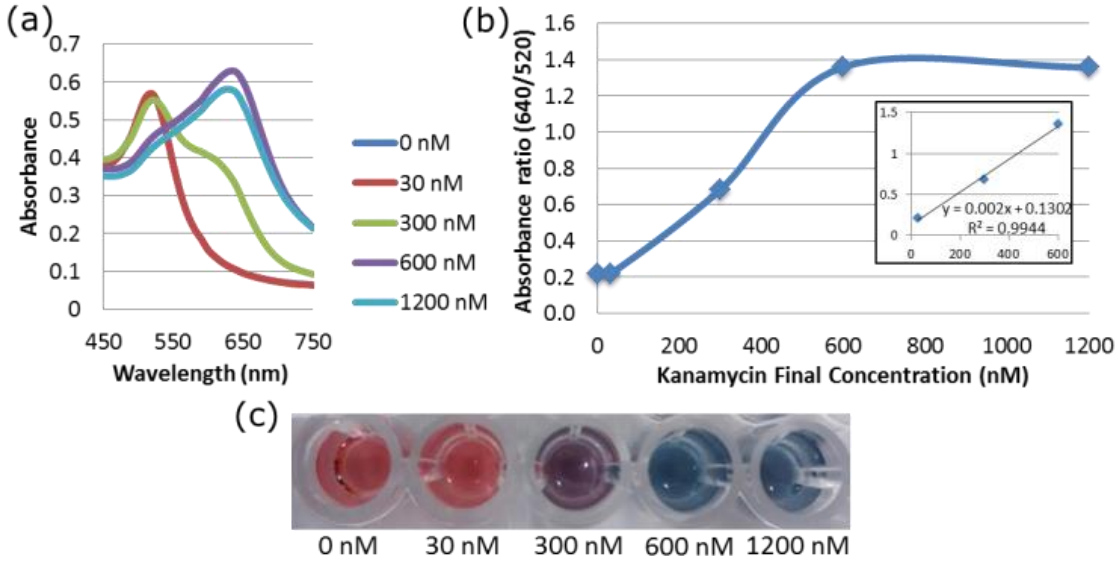

Figure 5.5 (a) UV-vis absorbance of aptamer-based colorimetric samples with various kanamycin concentrations; (b) Absorbance ratio (620/520) based on UV-vis absorbance; (c) Optical image of aptamer-based colorimetric samples with increasing concentrations of kanamycin (left to right).

The raw SERS spectra of kanamycin at different concentrations in the aptamer-AuNPs based colorimetric assay are found in **Fig. 5.9**. The spectra in **Fig. 5.6** use the same data and provide information on the surface coverage of AuNPs in this assay. At lower kanamycin concentrations (i.e. 30 nM), the "Aptamer + Kanamycin (30nM)" sample's spectral profile was not the same as the "Aptamer only" sample's, although there were several peaks that were similar to each other. The "Kanamycin only" sample's spectral profile was also not the same as the "Aptamer + Kanamycin (30nM)" sample's, but had some similar peaks. This suggests that the aptamer and kanamycin were both present on or near the surface of AuNPs, possibly due to the interaction between aptamer

and kanamycin. The PCA graph shows the "Aptamer + Kanamycin (30nM)" sample spectra had a PC1 score between the "Aptamer only" sample and the "Kanamycin only (30 nM)" sample, which strengthens this claim. In addition, the enhanced peak at 997 cm^{-1} for "Aptamer + Kanamycin (30nM)" is possibly another indication of an interaction between aptamer and kanamcyin.

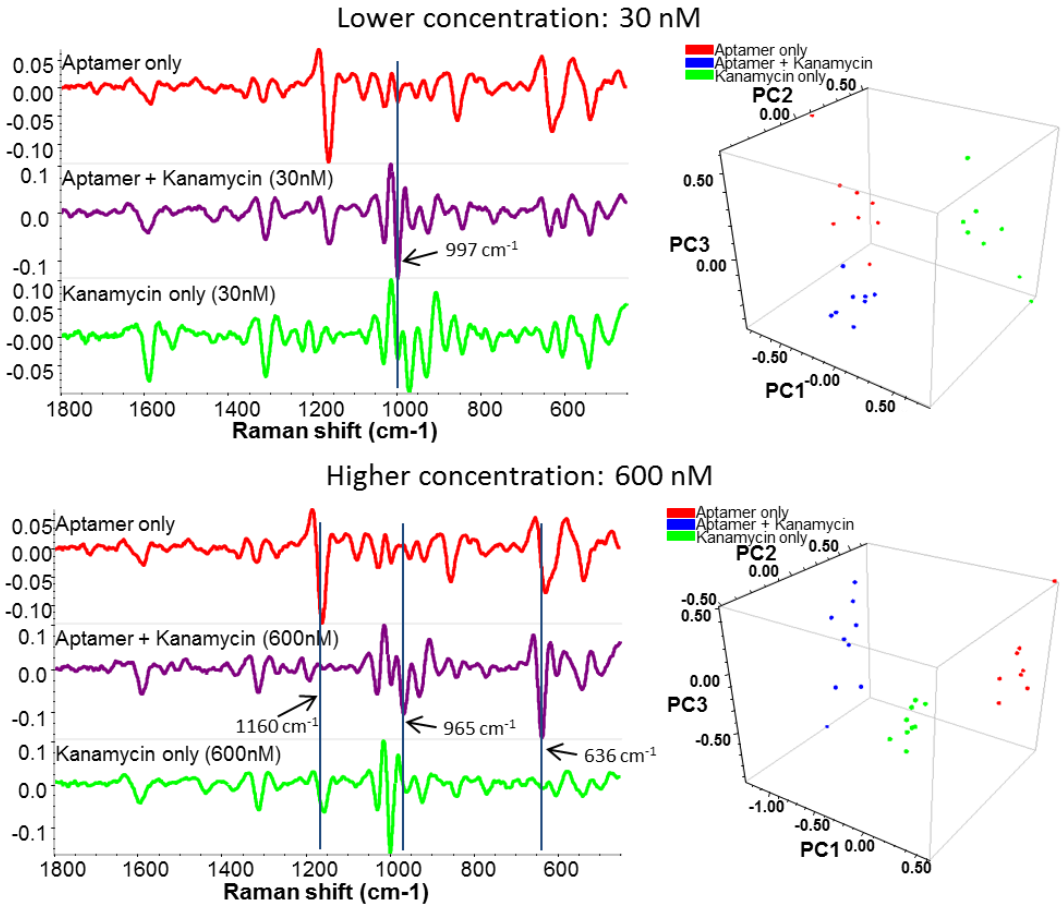

Figure 5.6 Second derivative SERS spectra and principal component analysis chart of aptamer-based colorimetric samples at low (i.e. 30 nM) and high (600 nM) kanamycin concentrations. Aptamer and kanamycin peaks are represented by dotted lines on the spectra. Other specific peaks can be located by referring to Fig. 5.9.

At the higher kanamycin concentration (600 nM), the "Aptamer + Kanamycin (600nM)" sample's spectral profile was still not the same as the "Aptamer only" or "Kanamycin only (600nM)" sample's. However, the spectral profile of "Aptamer + Kanamycin (600nM)" was different from "Aptamer + Kanamycin (30nM)". The changes that occurred could be due to the wrapping of kanamycin by the aptamer, thus producing conformational changes that can be detected by SERS. For example, the aptamer peak at 1160 cm^{-1} disappeared on "Aptamer + Kanamycin (600nM)". At 965 cm^{-1}, a new peak was seen on "Aptamer + Kanamycin (600nM)", whereas a shift in the aptamer peak was spotted at 636 cm^{-1} on "Aptamer + Kanamycin (600nM)". These SERS results suggest that the aggregation of AuNPs was due to the stronger affinity of aptamer binding to the kanamycin than the affinity of the kanamycin to the AuNPs, as seen in the case of ampicillin and its aptamer. The lack of resemblance of the "Kanamycin only (600nM)" sample's spectral profile to "Aptamer + Kanamycin (600nM)" also suggests that the affinity of kanamycin binding to AuNPs was weaker than the affinity of aptamer to kanamycin. Hence, the aptamer-AuNPs based colorimetric assay using the kanamycin aptamer and its target meets the criteria to successfully interpret the colorimetric results.

5.5 Conclusions

With the increasing popularity of aptamer-AuNPs based colorimetric assay, it is important to understand the underlying factors that contribute to the success of this detection method. This study was able to evaluate the competitive interactions present in

the aptamer-AuNPs colorimetric assay using SERS to ensure the correct interpretation of the colorimetric results. The interaction between aptamer and target must be stronger than the interaction between AuNPs and aptamer as well as the interaction between AuNPs and target. In addition, SERS was employed as a simple and rapid (<30 min) method to investigate surface chemistry of AuNPs at the molecular level in order to ensure reliable colorimetric detection. Future studies would involve the investigation of the colorimetric assay in a complex matrix such as food.

Supplementary Figures

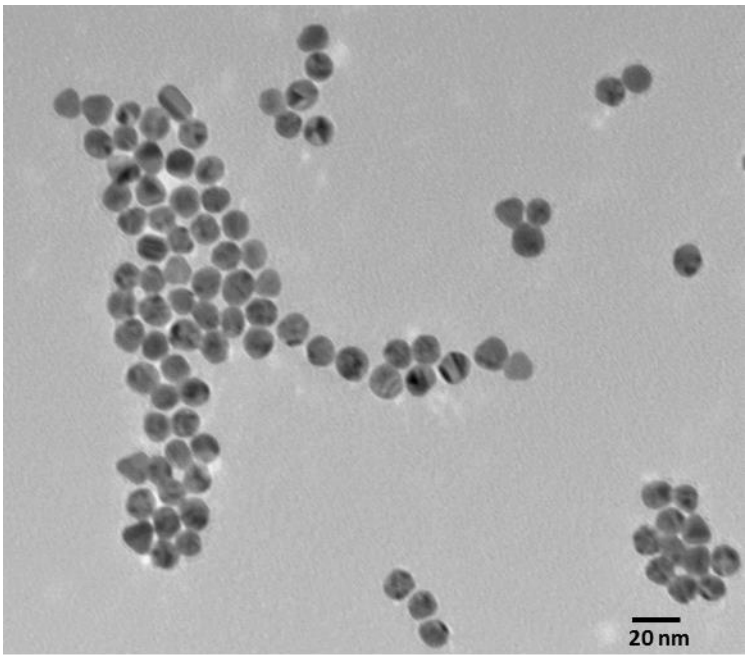

Figure 5.7 TEM image of synthesized AuNPs with an average diameter of 13 nm.

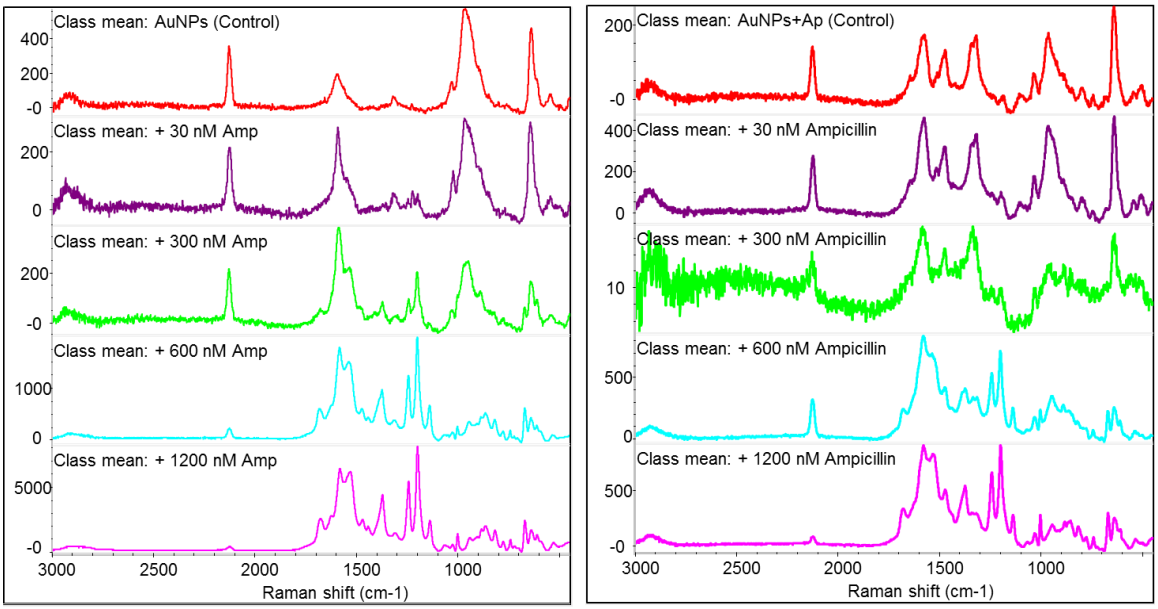

Figure 5.8 Raw SERS spectra of ampicillin at different concentrations (0, 30, 300, 600, 1200 nM) mixed with AuNPs or Aptamer + AuNPs

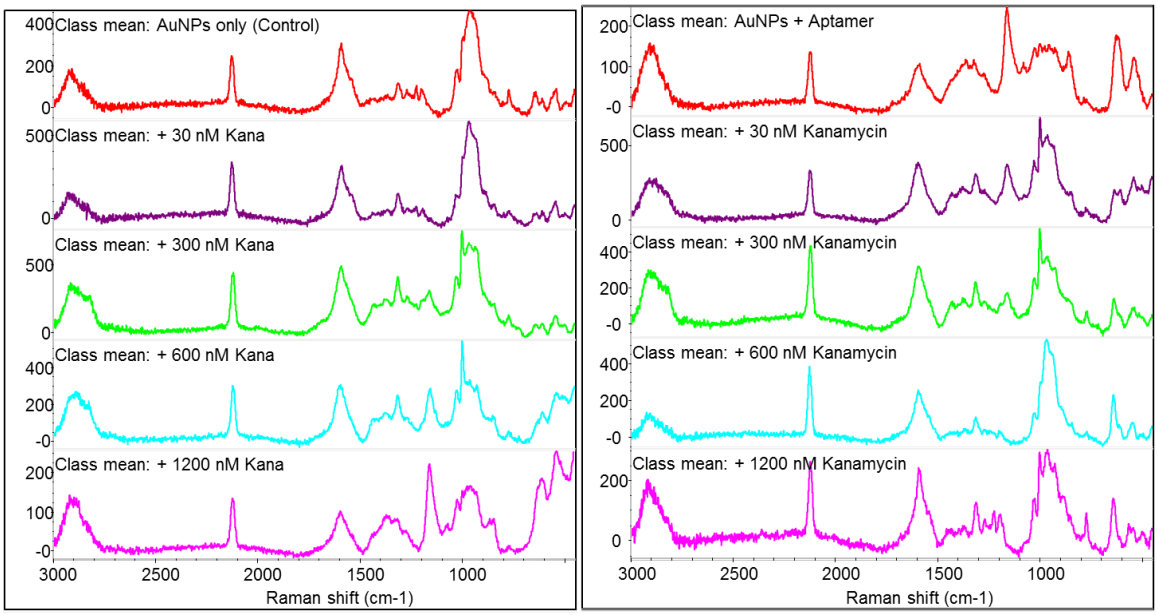

Figure 5.9 Raw SERS spectra of kanamycin at different concentrations (0, 30, 300, 600, 1200 nM) mixed with AuNPs or Aptamer + AuNPs.

CHAPTER 6

SELECTION OF APATMERS USING GOLD NANOPARTICLES-ASSISTED SELEX FOR THE DETECTION OF FOOD CONTAMINANTS

6.1 Abstract

Biosensors are a popular, rapid analytical tool for detecting food contaminants. However, a crucial factor that limits its expanded use is the lack of versatile and effective bio-capture agents to detect a wider variety of food contaminants. Aptamers are artificially engineered oligonucleotides that have great potential to satisfy this need, as they can be designed to have strong binding affinity to many types of food contaminants, including toxic and immunogenic molecules, ions and even bacterial cells. Unfortunately, the protocol for selecting aptamers is still somewhat complicated and requires highly specialized equipment, which may explain why there are still not many selected aptamers available. Therefore, the objective of this study was to develop a simpler protocol that could be used to expand the library of selected aptamer for food contaminants. To do this, we explored the feasibility of using gold nanoparticles as a non-specific ssDNA binding agent to control the release of ssDNA and subsequent capture of target analytes, i.e. ampicillin, in the sample system. A modified SELEX (i.e. systematic evolution of ligands by exponential enrichment) protocol was adapted in order to finish one round of SELEX cycle. Our results showed that gold nananoparticles are capable of monitoring the capture efficiency of the random ssDNA library pool to the target analyte. A significant hurdle in

the aptamer development process was to retrieve sufficient ssDNA after PCR amplification for the next round of SELEX. After attempting different methods to separate the dsDNA, d-PAGE was chosen as the most effective method. Future studies should focus on repeating the SELEX cycle multiple times. By doing so, we anticipate the ssDNA library pool to be narrowed down to a few, highly target-specific aptamer sequence, which can then be characterized to pick out the best aptamer.

6.2 Introduction

The increase in world population and subsequent need for a larger food supply has created a demand for more efficient ways to monitor food safety. Current epidemiological data shows 1 out of 6 Americans or approximately 48 million Americans being infected with foodborne diseases annually, resulting in 128,000 hospitalizations and 3,000 deaths (CDC 2011 estimates). One way to reduce the occurrence of these health deteriorating cases is to develop a robust detection method that is capable of scanning a larger representation of food that is supplied to consumers and accurately deliver results. Currently, the FDA only analyses about 3,500 – 4000 samples per year out of the billions of tons of food crops produced domestically and imported, thus there is great potential to expand the sampling population by developing rapid and reliable detection methods.

Among rapid detection methods that have become increasingly popular in recent years, antibody and enzymatic dependent assays, such as enzyme linked immunosorbent assays (ELISA) and gold immunochromatography assays (GICA), have emerged as one of the more commonly used rapid screening methods for tackling food safety issues. Although these methods have overcome certain limitations of traditional detection technologies (i.e. HPLC, GC/LC-MS) such as expensive equipment and long analysis time, other challenges still persist. For example, antibodies are difficult to produce for toxicants and nonimmunogens, especially for small molecules. The ethical use of using animals to produce these antibodies persists and subsequently, the cost of producing them is still very high. As a result, there has been a growing trend to discover other specific target capture agents to overcome these challenges. Among them, aptamers have evolved to become of one of the more popular alternatives.

Aptamers are a group of synthetic oligonucleotides (i.e. ssRNA and ssDNA) that are designed specifically to capture a target analyte with high binding affinity. Unlike DNA probes, the ability of aptamers to capture its target is not dependent on complementary DNA sequences, but influenced largely by numerous intermolecular interactions including complementarity in the geometrical shape, stacking interactions of aromatic rings and the nucleobases of the aptamers, electrostatic interactions between charged groups, van der Waals interactions, and hydrogen bonding [124]. When a target analyte is present, the aptamer experiences unique folding and 3-D conformational change. These

physical changes are characterized by stems, internal loops, bulges, hairpins, tetra loops, pseudoknots, triplicates, kissing complexes, or G-quadruplex. The binding affinity of target to aptamer is typically in the nanomolar range, and is comparable to other biological capture agents such as antibodies. In addition, there are several merits of using aptamers over antibodies (Table 6.1).

Table 6.1 List of characteristic differences between aptamers and antibodies

Factor	Aptamers	Antibodies
Working environment	Flexible; Thermostable; Can be regenerated easily	Limited; Difficult to regenerate after denaturation
Production process	Efficient and rapid (using PCR)	Time consuming and costly (using in vivo systems)
Types of targets	Almost any molecules, including toxins and nonimmunogens	Constrained by immune response of in vivo systems
Target sites	Aptatopes can be engineered at specific sites by the investigator	Animal immune system control epitope sites
Chemical modification	Can be easily modified with wide variety of labeling molecules	Limited modification flexibility

The main advantage related to food safety is that it can be designed to capture a wide range of target analytes, including toxicants and immunogens that are hard to produce for antibodies. Other notable advantages include the flexibility and easiness of preparing and modifying the aptamer for immobilization, longer shelf life and the capability of being stable in nonphysiological environments (e.g. low pH, high ionic strength, etc).

Another reason for the increasing popularity of aptamers is due to the technological advancement in the creation of new and more efficient aptamers. This

fundamental process is called systematic evolution of ligands by exponential enrichment (SELEX), and can be categorized into five critical steps: (1) **Design, (2) Selection, (3) Partition, (4) Amplification and (5) Acquisition (Fig. 6.1)**.

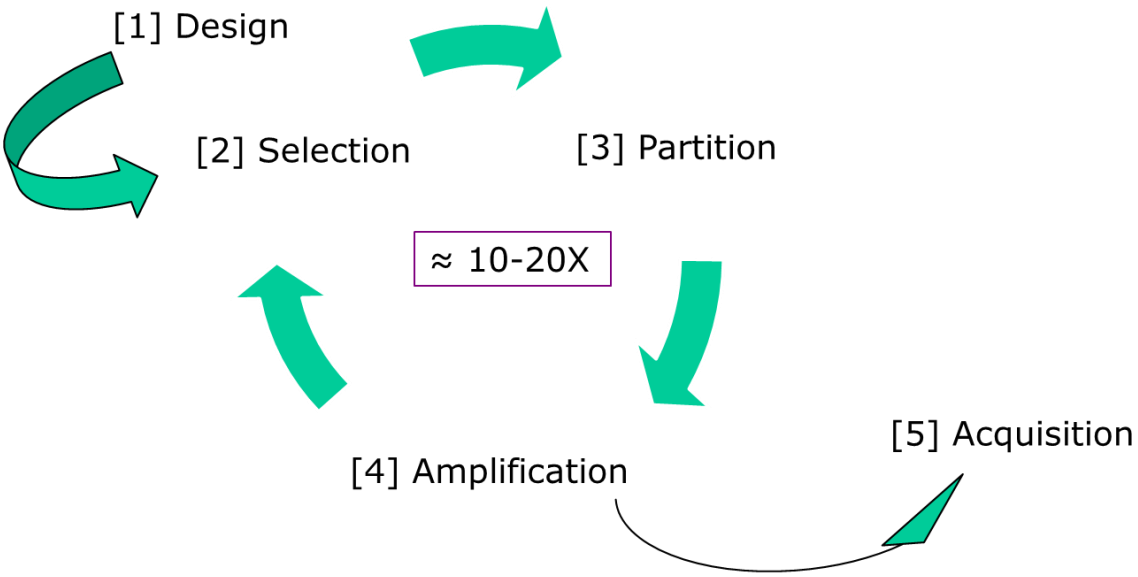

Figure 6.1 Description of the SELEX process.

[1] In the design step, the starting DNA library pool (typically 10^{15} different sequences) is determined, including the constant length (complementary to primers), random length (to give a possible maximum number of total sequences), positioning of constant and random sequences, and modification at the 3' and/or 5' end. Primer sequences are also determined to ensure optimal conditions for binding and subsequent selection. The type of buffer to use and ideal conditions for target capture that is compatible with oligonucleotides is also determined.

[2] The next step is the selection process, where the oligonucleotide is exposed to the target. In this step, concentration ratios, incubation times and environment are carefully monitored and optimized to give the ideal capture efficiency. Another important element to note in this process is the reduction of nonspecific binding to other materials such as the solid support, if any. In order to reduce this type of binding, a counter selection step could be employed to remove all oligonulceotides that will bind to the solid support before the final step (i.e. acquisition) of obtaining an aptamer.

[3] The third step is partitioning, which is the separation of the bound target-aptamer from the unbound target and oligonucleotide sequences. This has been achieved using various number of ways, including filtration, centrifugation, magnetic separation, chromatographic separation, and electrophoretic separation. An important element during the partitioning step is also the elution of the bound oligonucleotides from the target. This can be achieved by adding ethanol to precipitate the oligonucleotide and subsequently centrifuging the mixture to obtain the precipitate. Other ways of elution include heating, changing the ionic strength or pH, or using other types of denaturing agents such as urea, sodium dodecyl sulfate (SDS) and/or ethylenediamine tetraacetic acid (EDTA). During partitioning, an important element is quantifying the proportion of bound and

unbound oligonucleotides to monitor the binding efficiency of the DNA pool tested. This has been done by tagging the DNA pool with fluorescent or radioactive dyes and effectively measuring the bound DNA concentration using a spectrophotometer. Alternatively, the unbound ssDNA concentration can be quantified.

[4] The next step is amplification. In this step, ssRNA is amplified using RT-PCR or in the case of ssDNA, PCR. This will produce dsDNA. In order to separate the complementary strand from the sense strand, the reverse primer can be tagged with biotin or thiol group to bind to a solid support while the sense strand is released into the supernatant using a denaturing agent, which breaks the hydrogen bonds between the sense-antisense strands. The sense strand concentration is then measured and mixed together with appropriate amounts of target to go through another round of the selection process. The SELEX cycle, i.e. steps [2]-[4], is repeated until the proportion of target-bound oligonucleotides to unbound oligonucleotide remains high and stable for consecutive cycles, after which the acquisition step takes place.

[5] In the acquisition stage, the target bound oligonucleotide is amplified one last time with unmodified primers. Then, the DNA sequence is identified by cloning and sequencing of the selected clones. Typically, more than 50 sequences are

chosen for sequencing and analyzed after. Regions of homologous sequences differing by only a few bases may represent important parts of the aptamer for target binding. These sequence analysis can be performed using software programs such as DIALIGN and CLUSTAL. Secondary structural analysis of the aptamer can also be analyzed using "m-fold" software. The secondary structure is predicted based on free energy minimization algorithm. The potential binding sites of the target can then identified, which is often found in the stem-loop or G-quadruplex structures. Lastly, the acquired aptamer sequences are individually tested for binding affinity and specificity in a defined environment to obtain their dissociation constants for future method applications.

The first aptamers were selected in 1990 by two separate labs[54,125], which gave the fundamental procedural basis of obtaining new aptamers, now known as SELEX. Over the last 25 years, the SELEX method has evolved to obtain aptamers for different types of applications. Although aptamers have been studied mainly for biomedical and pharmaceutical applications, the selection and characterization of aptamers relevant to food safety has begun to emerge and has been noted by several researchers in recent years[126,127]. However, all of them agree that the development of aptamers for food safety applications is limited and is still in its infancy. In an industry where investments in high risk technology development are constrained by minimal budget, it is essential to provide new and cost-effective ways to explore that technology. Although numerous

SELEX variations have been published over the past two decades, there are still limited resources available for food industry to explore new aptamer development for food safety applications. With our previous success in the development of aptamer-based detection methods, this study attempted to focus on the development of a new type of SELEX method that would not only be cost-effective, but would provide the food industry and governmental agencies with a suitable method that would work for its applied field (i.e. food matrix). Specifically, we attempted todevelop a gold nanoparticle-assisted SELEX method that can potentially be used to develop aptamers in a simple and effective way.

6.3 Materials and Method

6.3.1 Materials

All chemicals were purchased through Fisher Scientific unless otherwise noted. DNA oligonucleotides were purchased from Eurofins OWG. PCR kits were obtained from New England Biolabs. Cloning Kits were obtained from Invitrogen. Micropure water (Fisher Scientific) was autoclaved before use. Citrate capped gold nanoparticles 13 nm in size was synthesized using the method as described by Grabar and Freeman [94,95].

6.3.2 Design

The initial DNA library pool contained 18 base pairs each in the two primer regions and a centralized random sequence of 30 base pairs with possibilities of A, T, G,

C in each base. The forward primer (FP) sequence was: 5'-CGT ACG GAA TTC GCT AGC-3' while the reverse primer (RP) sequence was: 5'- CAC GTG GAG CTC GGA TCC-3'. This sequence gave a possible maximum of 10^{18} sequences. The primer sequences were chosen based on the reported success of developing other aptamers with it [128]. The melting temperature of these primers, T_m, were as follows: FP – 59.9 °C; RP – 64.5 °C. The GC contents of the primers were as follows: FP – 55.6%; RP – 66.7%. The reverse primer was modified with a biotin label on the 5'end. The purification levels of the ssDNA purchased were salt-free and came in 1 µmole aliquots that was prepared as a 100 µM stock solution before further dilution. Before aptamer selection, the ssDNA solution was heated to 95℃ for 5 mins, then immediately cooled in an ice-water bath for a few minutes.

6.3.3 Selection

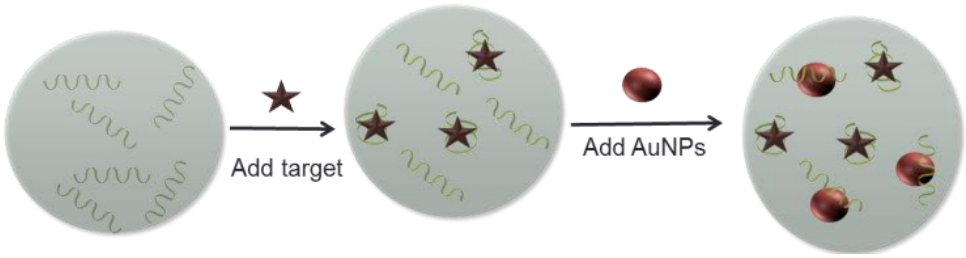

Figure 6.2 Schematic Illustration of the aptamer selection process using AuNPs

The first requirement for this step is to have at least 10^{14} random sequences available for the selection pool. 100 µL of 2µM of this sequence in water was mixed with

equimolar ratio of target (i.e. ampicillin-100 µL in water) for 1 h at room temperature with constant shaking using an orbital shaker that rotated at 24 rpm. 100 µL of 5 nM AuNPs (in citrate buffer) was then added to the mixture and incubated for an additional 1 h (**Fig 6.2**). 2 µM aptamer concentration was chosen because it was the minimum concentration that prevented aggregation of AuNPs when 10 µL of a 75 mM NaCl solution was added (i.e. this was the minimum NaCl concentration that caused maximum aggregation of AuNPs without ssDNA). This is another important optimization step because the aggregation of AuNPs after adding NaCl will be used as an indicator later on to determine the ratio of target bound ssDNA to unbound ssDNA.

6.3.4 Partition

After incubation, the mixture was centrifuged at 10,000 X g for 15 minutes in order to separate the ssDNA coated AuNPs from the supernatant (**Fig 6.3**). After centrifugation, 200 µL of the supernatant was transferred to a separate tube. This solution contained the target bound ssDNA. 1 µL of the remaining AuNPs was dropped onto a gold slide and analyzed under Raman microscope to verify the presence of AuNPs bound ssDNA.

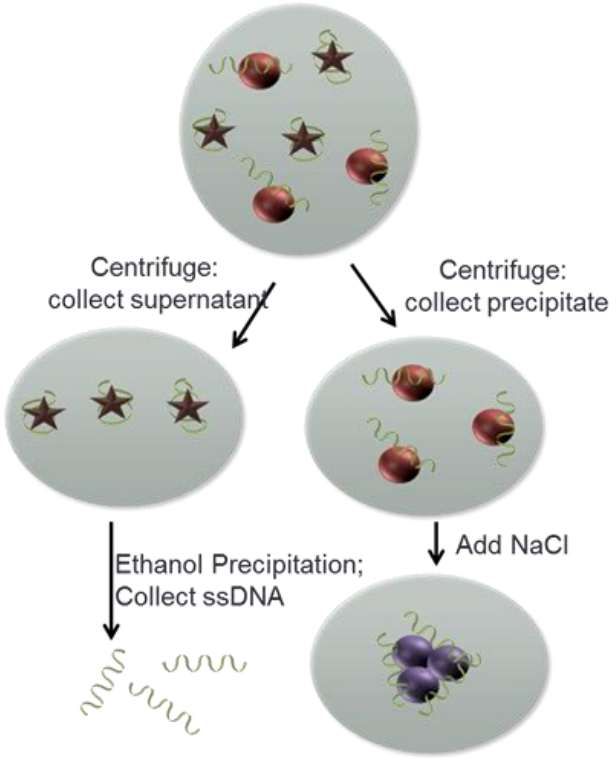

Figure 6.3 Partitioning of target bound/unbound ssDNA and their subsequent step.

The Raman instrument parameters and data analysis protocol used was based on Pang and others 2014 [44]. The target bound ssDNA solution then subjected to ethanol precipitation. Briefly the ssDNA-target solution was mixed with 20 µL of 3 M sodium

acetate, pH 5.2, followed by 440 µL of cold 100% ethanol. After mixing thoroughly, the mixture was placed in ice for 20 min. Then the solution tube was centrifuged at 20,000 X g for 10 min at 4°C. The supernatant was slowly decanted, then 1 mL of 70% ethanol was mixed in and centrifuged again at 20,000 for 10 min. The supernatant was removed again and the precipitate was left to air dry for approximately 5 min. The dried ssDNA pellet was then reconstituted with 50 µL double distilled water and the ssDNA concentration was then measured using Nanodrop 2000c.

6.3.5 Amplification

PCR optimization and amplification was performed based on modification of Sefah et al 2010 [128]. First, the optimization of PCR was performed using a two-step process. In the first step, ten PCR cycles were performed by adding 45 µL of ssDNA sample template into the PCR cocktail (**Table 6.2**) with a standard PCR protocol (**Table 6.3**).

Table 6.2 PCR cocktail used in the first step of PCR optimization

Reagents	Volume	Final Concentration
Autoclaved water	32.7 µL	
10x PCR buffer	10 µL	1x
dNTP mix (10 mM)	2 µL	200 µM
Taq Polymerase	0.3 µL	
Forward Primer (10 µM)	5µL	0.5 µM
Reverse Primer (10 µM)	5µL	0.5 µM
Total	55 µL	

Table 6.3 PCR protocol used in the first step of PCR optimization

Step	Temp (°C)	Time (s)
Hot Start	95	150
Amplification (10x)		
Denaturation	95	30
Annealing	56.3	30
Extension	72	30
Final Extension	72	180
Hold	4	∞

The second step of the PCR optimization was performed by adding 5 µL of the PCR product from the first PCR optimization step into five PCR tubes each containing PCR cocktail (**Table 6.4**).

Table 6.4 PCR cocktail used in the second step of PCR optimization

Reagents	Volume	Final Concentration
Autoclaved water	33.85 µL	
10x PCR buffer	5 µL	1x
dNTP mix (10 mM)	1 µL	200 µM
Taq Polymerase	0.15 µL	
Forward Primer (10 µM)	2.5 µL	0.5 µM
Reverse Primer (10 µM)	2.5 µL	0.5 µM
Total:	45 µL	

A sixth PCR cocktail was prepared without ssDNA template (i.e. buffer as a replacement) to be used as the negative control. The six prepared PCR tubes were placed in the thermal cycler and amplification was performed using the same procedure outline above (**Table 6.3**). However, one sample was taken out after 4 cycles, 8 cycles, 12 cycles, 16 cycles and 20 cycles respectively. The negative control sample was taken out after 20 cycles.

The 6 samples and one DNA ladder (50 bp ladder – furthest band at 25 bp) were run using agarose gel electrophoresis. 3% agarose gel was prepared with Midori green (Bulldog, NH, USA) as the DNA staining dye and 1x TBE as the buffer. The power supply used to run the gel was 100V for 40 mins. 6x loading dye were added to PCR sample at 1:6 concentration ratios before inserting into gel holes. Then, the gel electrophoresis was run. After the procedure, UV light at long wavelength (365 nm) was shone over the gel and a picture was taken using an 8 MP camera to identify the number of PCR cycles that produced the clearest DNA band.

After determining the optimized number of PCR cycles, the remaining sample from the first PCR optimization step was amplified accordingly. This was followed by the separation of ssDNA from its complementary strand (**Fig 6.4**).

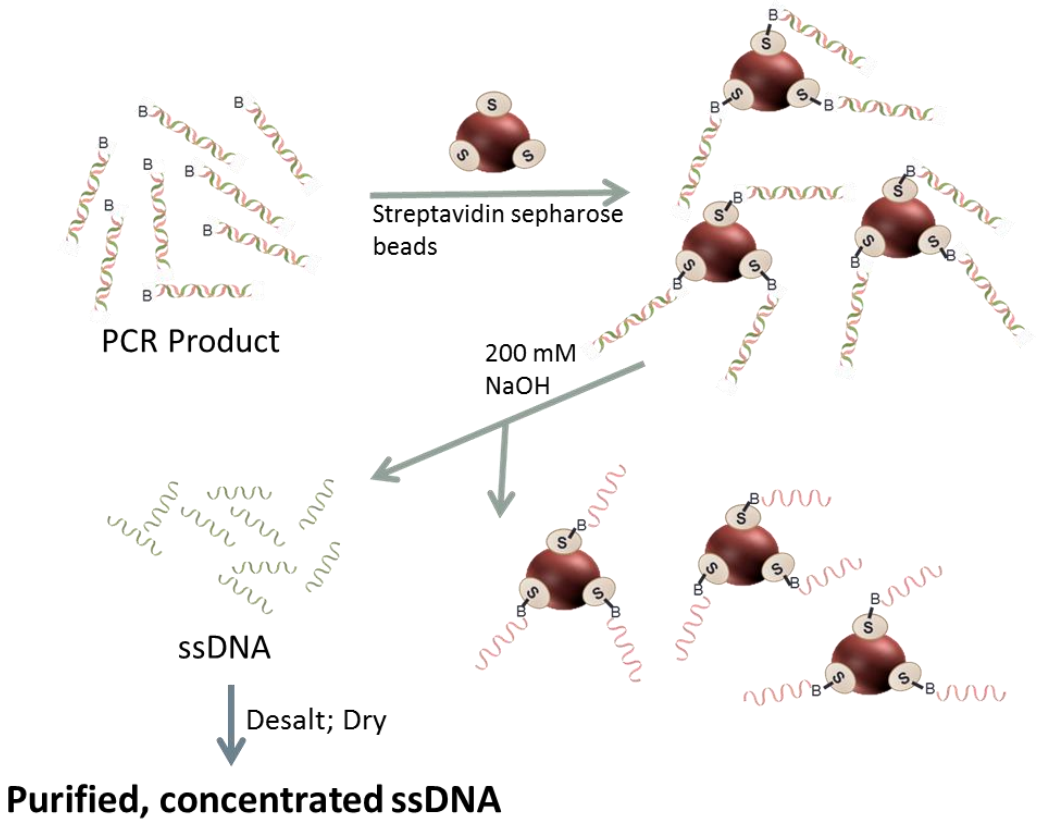

Figure 6.4 Schematic Illustration of the separation of dsDNA after PCR amplification

To do this, the amplified dsDNA was first conjugated onto streptavidin-coated sepharose beads through the biotin labeled antisense strand with the following setup: On one end of a DNA synthesis column, a filter (that came with the "DNA synthesis column") was fitted. The plunger was removed from a 10 ml sterile syringe and the syringe was placed into the other end of the DNA synthesis column. The setup was placed on a clamp. 200 µL of streptavidin sepharose beads were added into the syringe by aiming at the middle of the hole in the bottom. Then the plunger was used to slowly

press down the liquid until it started to drain. Once the liquid was all drained out, the plunger was pushed all the way. 2.5 mL water was then added to the syringe and the plunger was pressed again to drip out the water slowly. Then, the sample was passed through the column. The eluate was collected with the same centrifuge tube and this process was repeated three times.

Next, a freshly prepared 200 mM NaOH solution was used as a denaturing agent to release the ssDNA complementary strand from the biotin-labeled anti-sense strand. This was done by adding 500 µL of NaOH solution into the syringe and slowly pushing the plunger down to collect the supernatant. (Be careful not to push the plunger too hard).

The final step was to desalt the collected ssDNA. One NAP5 column was prepared by draining out all the liquids vertically on a clamp. Then, 15 ml of water was added to rinse the column. 500 µL of the eluted ssDNA was then placed in the column and allowed to drain into a tube. Then, the sample was concentrated for 3 hours on a SpeedVac. The ssDNA concentration was then determined using Nanodrop 2000c.

6.4 Results and Discussion

6.4.1 Optimization of target capture and separation

For the gold nanoparticle-assisted SELEX to operate optimally, it is important to have the right amount and concentration ratio of ssDNA, target (i.e. ampicillin) and AuNPs.

This will not only maximize the number of possible target-specific aptamers available, but will also help to improve the monitoring of target capture efficiency. For instance, if there are more ssDNA molecules than the maximum amount capable of binding to AuNPs, then there is no way to find out if the ssDNA molecules not bound to AuNPs were actually captured by target after AuNPs were separated out. Therefore, the optimal volume and concentration of ssDNA was determined (**Fig 6.5**).

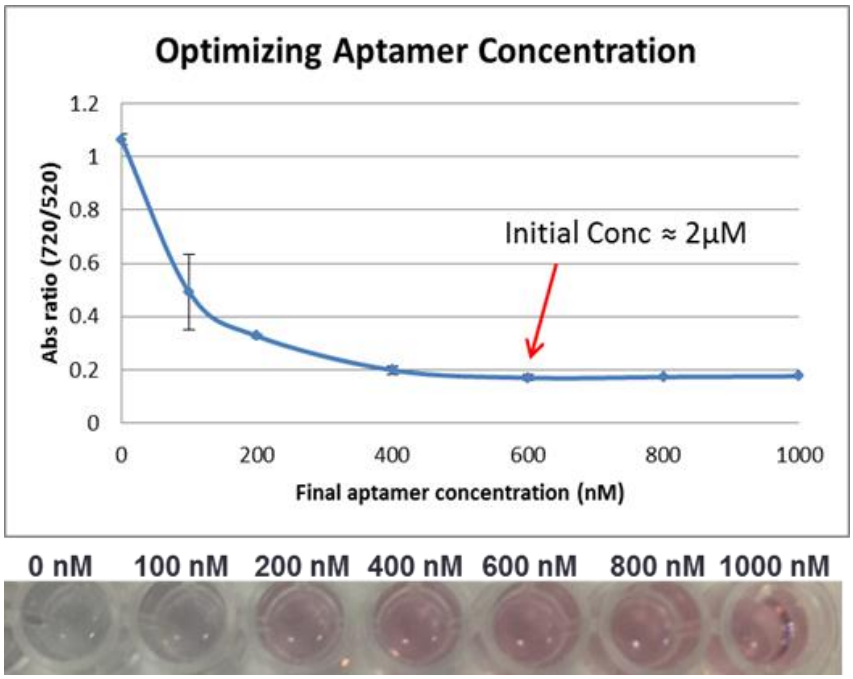

Figure 6.5 Absorabance ratio (720/520) and color of gold nanoparticles exposed to different concentrations of ssDNA after the addition of 75 mM NaCl.

In order to use a manageable volume for this study, 100 µL of ssDNA was used. Since the optimal ssDNA concentration was 2 µM, the total number of possible ssDNA sequences in this sample was approximately 10^{14} sequences, which is comparable to the starting amount of many SELEX procedures[108].

Another important optimization step was to separate the target bound ssDNA from the rest of the sample mix. This was performed using centrifugation at different speeds and time. The optimal centrifugation condition was determined to be 10,000 X g for 15 minutes. Other speeds and times were tested but the lower the speed and time, the less effective was the separation. The presence of ssDNA on AuNPs was monitored using surface enhanced Raman spectroscopy (**Fig 6.6**). As ssDNA can produce strong Raman peaks when attached to AuNPs, we can potentially use this as a monitoring tool to measure the amount of ssDNA that is left on the surface of AuNPs.

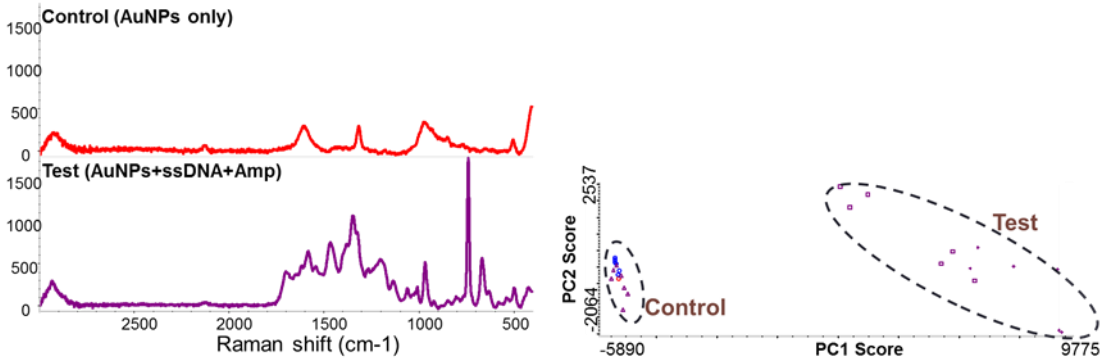

Figure 6.6 SERS spectra and principal component analysis score of the supernatant after AuNPs-based SELEX selection.

Alternatively, the aggregation status of AuNPs after adding NaCl can also be used to calculate the proportion of ssDNA that is bound to AuNPs after target addition and centrifugation by using a standard curve such as the one presented in **Fig 6.5**.

6.4.2 Amplification and Extraction of ssDNA

Prior to the amplification of all extracted ssDNA, the optimization of PCR cycles is an important step in SELEX in order to maintain the purity and accuracy of the ssDNA sequences being replicated. Hence, the target extracted ssDNA was first subjected to a preparative PCR step to partially increase each ssDNA sequence population. The results show that 10+16 cycles produced the sharpest and clearest band (**Fig 6.7**). Beyond that, the DNA band began to become blurred, suggesting mutation or production of side products.

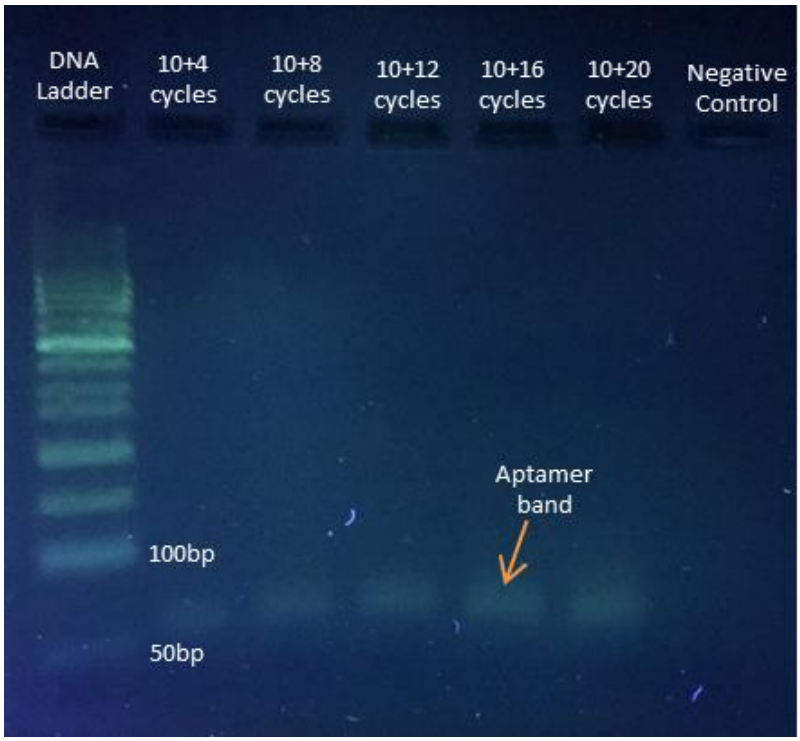

Figure 6.7 Agarose gel results showing DNA bands at the appropriate distance corresponding to its length. Also, 10+16 cycles is shown to have the clearest peak.

When all the ssDNA had undergone PCR, the products (i.e. dsDNA) were initially conjugated onto streptavidin coated sepharose beads and subjected to alkaline denaturation to extract the sense strand ssDNA sequences. However, we found that our alkaline denaturation step was unable to release the ssDNA strand we wanted. We confirmed this hypothesis by first comparing the DNA gel of the sample mix right after PCR and right after sample mix was added to beads to verify that the DNA was bound to streptavidin sepharose beads. Then, we checked the ssDNA concentration of the eluted ssDNA after alkaline denaturation (i.e. 200 mM NaOH) using Nanodrop (i.e. absorption peak at 260 nm). Little to no ssDNA was detected (<2 ng/µL). An electrophoreses gel run also indicated no DNA.

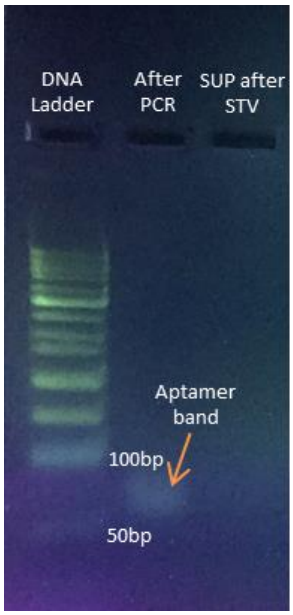

Figure 6.8 Agarose electrophoresis gel image of DNA library (50 bp ladder), DNA products after PCR, and supernatant (SUP) after streptavidin (STV) beads exposure.

In order to overcome the problem of extracting ssDNA, several tests were done. First, the denaturing agent solution used to elute ssDNA was modified using NaOH at 0.2, 0.5, 1, 2 and 5 M. Urea was also used at 5, 6,7,8 M. Unfortunately, none of these denaturing agents and concentrations worked. The next factor that was considered was the incubation time. Based on other studies, the release of ssDNA should be quick (i.e. within a few seconds), hence, the initial experiments were done by adding the denaturing agent to the DNA conjugated beads and slowly pushing the supernatant out of the column (i.e. approximately one minute). To increase the incubation time, the experiment was conducted in a centrifuge tube and the mixture of DNA conjugated beads and the denaturing agent was incubated for 0.5 or 2 hr. Another factor that was studied was the temperature. Initially, the experiment was conducted in room temperature, and hence, the incubation was conducted at 95C. In all of these tests, little to no ssDNA was detected (<2 ng/μL). At 95°C, an absorption peak appeared at 280 nm, suggesting the release of protein (i.e. streptavidin) in the sample system.

Since alkaline denaturation was not able to release ssDNA in this study, denatured polyacrylamide gel electrophoresis (dPAGE) was explored as an alternative extraction method (refer to Appendix B). dPAGE works on the principle of adding denaturing agent directly to PCR products and then separating the ssDNA based on their length. Therefore, the complementary strands must be different in base length. To test whether this method was capable of separating PCR products for our application, two ssDNA strands

complementary to each other, but one having an elongated sequence (i.e. extra 20 bases, all As) was separated using dPAGE (**Fig 6.8**).

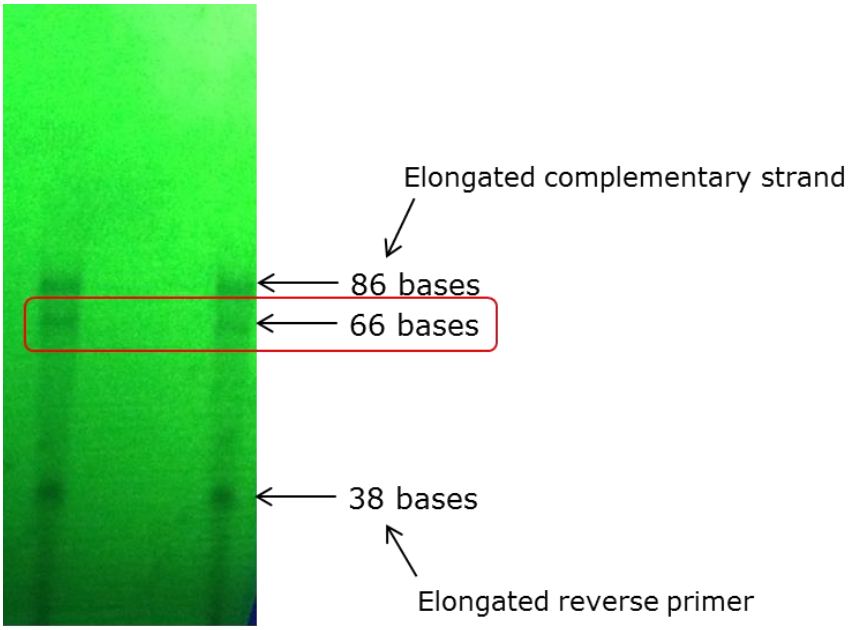

Figure 6.9 dPAGE gel showing three clear bands, representing ssDNA with 86, 66 and 38 base lengths respectively

The gel containing DNA bands were cut, crushed and soaked overnight at 37°C, after which the supernatant was collected and measured. The ssDNA concentrations were high enough for detection using Nanodrop as long as there was at least 239 ng of ssDNA present. In order to successfully finish one round of SELEX cycle, the extraction of ssDNA after PCR can be done using dPAGE. However, this requires that the reverse primer used have an elongated sequence that will not be fully replicated during PCR. This can be done by adding a hexaethylene glycol spacer between the elongated portion of the primer sequence and the parts that are complementary to the sense DNA strand.

6.4.3 Other considerations for using gold nanoparticles-assisted SELEX for the selection of aptamers

Once a full round of SELEX cycle is accomplished, the ssDNA concentration has to be adjusted to ensure optimal coverage of AuNPs. Then, the next round of SELEX cycle can continue. The number of SELEX cycles to be performed is dependent on the proportion of ssDNA that is bound to the target during the last round. If the proportion is similar to the previous round and is capable of causing AuNPs aggregation after adding a defined amount of NaCl, then the selection of aptamer sequences is assumed to be highly enriched. Then, the ssDNA pool is amplified using non-biotinylated primers and the eluted ssDNA can be cloned into the pGEM-T easy vectors provided by Promega. High efficiency, E. coli competent cells obtained from Promega can then be transformed using the vectors containing DNA fragments of interest. The successful transformation can then be verified using the bacterial colonies for PCR to amplify the inserts, and subsequently using a 3% agarose gel for electrophoresis. Several colonies can then be chosen at random for sequencing , after which the secondary structure can be analyzed using m-fold software to identify the sequences with the probability of the highest binding affinity using free energy minimization algorithm.

Another consideration to take with this SELEX procedure is the type of targets that can be compatible for the selection of aptamers. The aptamer selection mechanism relies on the fact that the target will have relatively lower binding affinity to the AuNPs

compared to non-specific binding of ssDNA to AuNPs. Furthermore, in order to use the AuNPs-colorimetric data to monitor the capture efficiency of ssDNA to target, the sample environment (i.e. pH, ionic strength) and target should not affect the aggregation of AuNPs. In our study, we suggest using both colorimetric data and SERS data to validate the proportion of ssDNA that is bound to AuNPs. We have shown through our previous studies that SERS is capable of monitoring the surface chemistry of AuNPs, and hence, there is still great potential in using the gold nanoparticle assisted SELEX method to monitor the selection of aptamers for various food contaminants.

6.5 Conclusion

This study has provided several breakthroughs in order to advance the development of gold nanoparticle-assisted SELEX. This includes designing the ssDNA library pool, figuring out the optimal concentrations of ssDNA and AuNPs to use, establishing methods for monitoring target capture efficiency of ssDNA, as well as the extraction procedure for collecting ssDNA after PCR. The successful selection of an aptamer using this protocol would require repetition of SELEX cycles and acquisition of aptamer candidates. Gold nanoparticle assisted SELEX continues to show great promise in bringing a simple procedure that the food industry might use to create more aptamers relevant to the detection of food contaminants and the realm of food safety.

CHAPTER 7

SUMMRARY AND OUTLOOK

The development and application of label-free, aptamer-based SERS for food contaminant detection was presented in this dissertation using three main ways. First, the fabrication of different aptamer-modified SERS substrates were explored together with the testing of different types of food contaminants ranging from small molecules (i.e. pesticides, antibiotics) and foodborne pathogens (i.e. salmonella, listeria). These studies show that label-free aptamer-based SERS has great potential for becoming a standard rapid detection tool for a wide range of food contaminants in food matrix. Although the accuracy and specificity of target analyte detection was improved from traditional SERS, future work can be focused on improving the sensitivity (i.e. limit of detection) of this method. In order to do this, attempts could be made to get the target analyte to be closer to the SERS substrate (< 10 nm) by picking aptamer sequences of shorter length or with a specific 3-D configuration. Another way is to use aptamers with stronger binding affinity. Sandwich assays could also be explored to increase sensitivity as the SERS enhancement effect could be even greater if the target analyte was bound to several SERS substrates.

Another way that this dissertation described the development and application of label-free, aptamer-based SERS was through the integration of aptamer-based SERS with aptamer-assisted gold nanoparticle based colorimetric detection for the detection of food

related antibiotics, ampicillin and kanamycin. Our results were able to explain the competitive interaction between gold nanoparticles, aptamers and the target occurring at the molecular level based on the ability of SERS to study the surface chemistry of gold nanoparticles. Future work could also be done to integrate label-free, aptamer-based SERS with other detection methods including SPR (surface plasmon resonance) and AFM (atomic force microscopy). The integration of these rapid detection methods can help to complement the advantages of each analytical tool, which could provide solutions to analytical challenges that would otherwise be hard to resolve.

Another focus of this dissertation study was to develop a simple and cost-efficient SELEX method that would create aptamers relevant to food safety. Several important portions of the protocol was established, including the design of ssDNA library pool, the optimal concentrations of ssDNA and AuNPs to use, the establishment of methods for monitoring target capture efficiency of ssDNA, and the extraction procedure for collecting ssDNA after PCR. By continuing to develop the other components of this protocol, aptamers can potentially be developed in a simple and cost-efficient way, which will provide great potential for the advancement of label-free, aptamer-based SERS and other aptamer-based detection methods to detect food contaminants.

Many analytical methods have been studied and are continued to be studied for the detection of food contaminants. Our study has shown that label-free, aptamer-based

SERS has its advantages and limitations as described. We anticipate that this work will be a useful tool for researchers who are interested in developing this method as well as other techniques that have not yet been developed.

Appendix A

dPAGE for separating ssDNA from PCR product

Ethanol precipitation of DNA samples (2 h)

Supplies needed:

1.5 mL centrifuge tube, 1 per 0.5 ml PCR sample
3 M sodium acetate, pH 5.2, 45 uL per 0.5 mL sample
Pipets and tips (1mL and 50uL)
Vortex
100% Ethanol (cold), 1.25mL per sample
Centrifuge
70% ethanol (cold), 1mL per sample
Tube hot plate
1xTE buffer, pH 7.4

Method:

1. In every 1.5 mL centrifuge tube, add 500 uL of PCR product and 45 uL of 3M sodium acetate, pH 5.2 together. Vortex well.
2. Add 1.25 mL of 100% cold ethanol. Vortex well.
3. Place the sample tube in freezer for at least 1 h.

*During this time, you can prepare the gel-casting apparatus assembly and prepare the gel solution.

4. Centrifuge at maximum speed for 15 min. There should be a white precipitate at the bottom.
5. Remove supernatant with a pipette.
6. Add 1mL 70% cold ethanol and vortex sample.
7. Centrifuge at maximum speed for 10 min.
8. Remove supernatant with pipet and evaporate the ethanol completely using tube hot plate @ 40C. It should take about 10 min.
9. Add 20 uL of 1xTE buffer, pH 7.4 to DNA sample and mix with pipet tip.

Gel-casting apparatus assembly (30 min)

Supplies needed:
PAGE setup (plates, comb, gel setting station, clamp, foam pad)

Method:

1. Clean all PAGE setup thoroughly, especially the parts that will touch the gel. Wash with soapy water, then rinse with water, and lastly, with ethanol.
2. Prepare the PAGE setup as follows:

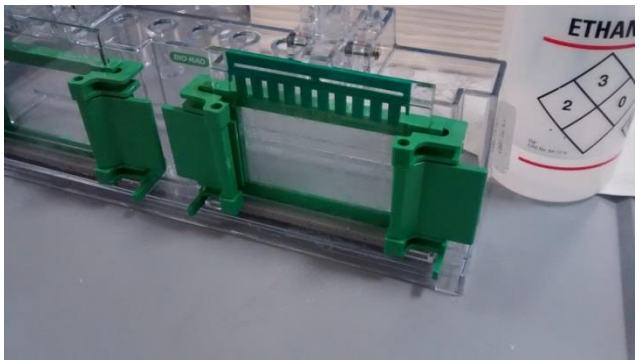

Prepare gel solution (1 h)

Supplies needed:
50 mL centrifuge tube
Hot water bath, set at 55C
Pipet and tips (10uL, 200uL, 1mL and 10mL)

Method:

1. Prepare the loading gel in a 50 mL centrifuge tube using the following recipe to make 20 mL (2 gels):

Chemicals	Volume
Acrylamide (30%)	6.6 mL
10x TBE	2 mL
Urea	9.6 g
dd H_2O	Add up to total 20 mL

2. Incubate for 5 min in a hot water bath that was pre-set at 55C. Then, cool the solution by placing under running cold water.

3. Add the following chemicals to loading gel solution to induce gelling, then immediately place loading gel solution into the space between plates using a 10 mL pipet.

Chemicals	Volume
APS (10%)	200 uL
TEMED	10 uL

4. Let the gel sit in the plate for 30 min.

Running the gel (3 hr)

1. Prepare 1.5 mL of 1xTBE by adding 150 mL of 10xTBE buffer in to 1350 mL of micropure water.
2. Unclamp the gel plates and place it in an electrophoresis plate which is contained in the PAGE running container.
3. Load the 1xTBE buffer into the container until the max line.
4. Prerun the gel for 45 min at 100 mV. While waiting, perform the next steps.
5. Prepare the formamide loading buffer (FLD) using the following recipe (there might be enough leftover from previous run in the fridge):

Chemicals	Volume
Formamide	950 uL
*0.5 M EDTA solution, pH 8.0	10 uL
Water	40 uL

To make 0.5 M EDTA solution, dissolve 9.305 g of EDTA in 45 mL water. Then, add 2.5 mL of 10 M NaOH. Measure pH of solution and add more NaOH if it is not at least 8.0 or did not dissolve the EDTA completely. It will take awhile to dissolve EDTA, > 10 min.

6. Mix 20 uL of FLD with the 20 uL DNA sample.
7. Using a tube hot plate, heat the sample at 95 C for 5 min, then place in ice immediately.
8. Pipet in and out the solutions surrounding the comb.
9. Load the samples. Load one of the comb with 10 uL loading dye to track the flow of gel.

10. Start the power supply at 120 mV for 90 min.

Crush and soak method (overnight)

1. Remove gel from the plates carefully using a pick. Cut the gel and insert into 1.5 mL centrifuge tube.
2. Use a pipette tip to crush the gel.
3. Add 25 uL of 1xTE buffer
4. Incubate tube @ 37C overnight.
5. After incubation, centrifuge @ low speed (5000 G) for 3 min
6. Transfer supernatant into a clean 0.6 mL tube
7. Measure the ssDNA concentration using Nanodrop.

Appendix B

PEER-REVIEWED MANUSCRIPTS THAT HAVE BEEN PREPARED AND/OR PUBLISHED DURING THIS PH.D. STUDY

[16] Pang, Shintaro, Panxue Wang, Juhong Chen and Lili He. 2016. "Label-free, aptamer based SERS detection of *salmonella enteritidis* and *listeria monocytogenes* for food safety applications." (Under Preparation).

[15] Pang, Shintaro and Lili He. 2016. "Recent Advances in Surface Enhanced Raman Spectroscopic (SERS) Detection of Synthetic Chemical Pesticides." *Trends in Analytical Chemistry* (Submitted and under review).

[14] Boushell, Victoria, **Shintaro Pang** and Lili He. 2016. "Aptamer Based SERS Detection of Lysozyme on a Food Handling Surface." *Journal of Food Science* (Submitted and under review).

[13] Chen, Juhong, **Shintaro Pang**, Lili He and Sam Nugen. 2016. "Highly Sensitive and Selective Detection of Nitrite Ions Using Fe_3O_4 Au Magnetic Nanoparticles by Surface-Enhanced Raman Spectroscopy." *Analytical Chemistry*. (Submitted and under review).

[12] Hou, Ruyan, Zhiyun Zhang, Tianxi Yang, **Shintaro Pang**, John Clark and Lili He. 2016. "Alteration of the non-systemic behavior of the pesticide ferbam on tea leaves by engineered gold nanoparticles." *Environmental Science & Technology* (Submitted and under review).

[11] Dornath, Paul, Stephen Ruzycky, **Shintaro Pang**, Lili He, Paul Dauenhauer and Wei Fan. 2016. "Adsorption-enhanced hydrolysis of Glucan Oligomers into Glucose over Three-Dimensionally Ordered Mesoporous Carbon Catalysts." *ACS Catalysis*. (Submitted and under review)

[10] Pang, Shintaro, and Lili He. 2016. "Understanding the Competitive Interactions in the Aptamer−Gold Nanoparticle Based Colorimetric Assays Using Surface Enhanced Raman Spectroscopy (SERS)." Anal. Methods (January 20). doi:10.1039/C5AY03158C.

[9] Pang, Shintaro, Changchu Ma, Naijie Zhang, and Lili He. 2015. "Investigation of the Solubility Enhancement Mechanism of Rebaudioside D Using a Solid

Dispersion Technique with Potassium Sorbate as a Carrier." Food Chemistry 174 (May 1): 564–70. doi:10.1016/j.foodchem.2014.11.113.

[8] Pang, Shintaro, Theodore P Labuza and Lili He. 2014. "Development of a Single Aptamer-based Surface Enhanced Raman Scattering Method for Rapid Detection of Multiple Pesticides." *The Analyst*. doi:10.1039/C3AN02263C.

[7] Wang, Panxue, **Shintaro Pang**, Juhong Chen, Lynne McLandsborough, Sam R Nugen, Mingtao Fan, and Lili He. 2016. "Label-Free Mapping of Single Bacterial Cells Using Surface-Enhanced Raman Spectroscopy." The Analyst (January 11). doi:10.1039/c5an02175h.

[6] Wang, Panxue, **Shintaro Pang**, Hua Zhang, Mingtao Fan, and Lili He. 2016. "Characterization of Lactococcus Lactis Response to Ampicillin and Ciprofloxacin Using Surface-Enhanced Raman Spectroscopy." Analytical and Bioanalytical Chemistry 408 (3) (January): 933–41. doi:10.1007/s00216-015-9184-2.

[5] Hou, Ruyan, **Shintaro Pang**, Lili He. 2015. "In situ SERS detection of multi-class insecticides on plant surfaces." Analytical Methods (June 29). doi: 10.1039/C5AY01058F

[4] Lang, Tingting, **Shintaro Pang**, Lili He. 2015. "Integration of colorimetric and SERS detection for rapid screening and validation of melamine in milk. " Analytical Methods (June 16). doi: 10.1039/C5AY00955C

[3] Zheng, Jinkai, **Shintaro Pang**, Theodore P Labuza, and Lili He. 2014. "Evaluation of Surface-Enhanced Raman Scattering Detection Using a Handheld and a Bench-Top Raman Spectrometer: A Comparative Study." Talanta 129 (November): 79–85. doi:10.1016/j.talanta.2014.05.015.

[2] Wijaya, Wisiani, **Shintaro Pang**, Theodore P Labuza, and Lili He. 2014. "Rapid Detection of Acetamiprid in Foods Using Surface-Enhanced Raman Spectroscopy (SERS)." Journal of Food Science 79 (4) (April): T743–7. doi:10.1111/1750-3841.12391.

[1] Zheng, Jinkai, **Shintaro Pang**, Theodore P Labuza, and Lili He. 2013. "Semi-Quantification of Surface-Enhanced Raman Scattering Using a Handheld Raman Spectrometer: a Feasibility Study." *The Analyst* 138 (23) (December 7): 7075–8. doi:10.1039/c3an01450a.

REFERENCES

[1] C. V. Raman, K.S. Krishnan, A new type of secondary radiation, Nature. (1928).

[2] M. Fleischmann, P.J. Hendra, A.J. McQuillan, Raman spectra of pyridine adsorbed at a silver electrode, Chem. Phys. Lett. 26 (1974) 163–166. doi:10.1016/0009-2614(74)85388-1.

[3] D. Cialla, A. März, R. Böhme, F. Theil, K. Weber, M. Schmitt, et al., Surface-enhanced Raman spectroscopy (SERS): progress and trends., Anal. Bioanal. Chem. 403 (2012) 27–54. doi:10.1007/s00216-011-5631-x.

[4] Y. Cao, J. Zhang, Y. Yang, Z. Huang, N.V. Long, C. Fu, Engineering of SERS Substrates Based on Noble Metal Nanomaterials for Chemical and Biomedical Applications, Appl. Spectrosc. Rev. 50 (2015) 499–525. doi:10.1080/05704928.2014.923901.

[5] K. Kneipp, Y. Wang, H. Kneipp, L. Perelman, I. Itzkan, R. Dasari, et al., Single Molecule Detection Using Surface-Enhanced Raman Scattering (SERS), Phys. Rev. Lett. 78 (1997) 1667–1670. doi:10.1103/PhysRevLett.78.1667.

[6] S. Nie, Probing Single Molecules and Single Nanoparticles by Surface-Enhanced Raman Scattering, Science (80-.). 275 (1997) 1102–1106. doi:10.1126/science.275.5303.1102.

[7] T. Winuprasith, M. Suphantharika, D.J. McClements, L. He, Spectroscopic studies of conformational changes of β-lactoglobulin adsorbed on gold nanoparticle surfaces., J. Colloid Interface Sci. 416 (2014) 184–9. doi:10.1016/j.jcis.2013.11.006.

[8] L. He, J. Zheng, T.P. Labuza, H. Xiao, A surface enhanced Raman spectroscopic study of interactions between casein and polymethoxyflavones, J. Raman Spectrosc. 44 (2013) 531–535. doi:10.1002/jrs.4229.

[9] K.V. Kong, Z. Lam, W.D. Goh, W.K. Leong, M. Olivo, Metal Carbonyl-Gold Nanoparticle Conjugates for Live-Cell SERS Imaging, Angew. Chemie. 124 (2012) 9934–9937. doi:10.1002/ange.201204349.

[10] J. Lin, R. Chen, S. Feng, Y. Li, Z. Huang, S. Xie, et al., Rapid delivery of silver nanoparticles into living cells by electroporation for surface-enhanced Raman spectroscopy., Biosens. Bioelectron. 25 (2009) 388–94. doi:10.1016/j.bios.2009.07.027.

[11] B.D. J. Fang, H. You, P. Kong, Y. Yi, X. Song, Dendritic Silver Nanostructure Growth and Evolution in Replacement Reaction, Cryst. Growth Des. 7 (2007) 864–867. doi:10.1021/cg0604879.

[12] M. Zhang, A. Zhao, H. Sun, H. Guo, D. Wang, D. Li, et al., Rapid, large-scale, sonochemical synthesis of 3D nanotextured silver microflowers as highly efficient SERS substrates, J. Mater. Chem. 21 (2011) 18817. doi:10.1039/c1jm12831k.

[13] S.E.J. Bell, M.R. McCourt, SERS enhancement by aggregated Au colloids: effect of particle size., Phys. Chem. Chem. Phys. 11 (2009) 7455–62. doi:10.1039/b906049a.

[14] W.W. Yu, I.M. White, A simple filter-based approach to surface enhanced Raman spectroscopy for trace chemical detection, Analyst. 137 (2012) 1168. doi:10.1039/c2an15947c.

[15] I.-H. Cho, P. Bhandari, P. Patel, J. Irudayaraj, Membrane filter-assisted surface enhanced Raman spectroscopy for the rapid detection of E. coli O157:H7 in ground beef., Biosens. Bioelectron. 64 (2015) 171–6. doi:10.1016/j.bios.2014.08.063.

[16] Y.-T. Li, L.-L. Qu, D.-W. Li, Q.-X. Song, F. Fathi, Y.-T. Long, Rapid and sensitive in-situ detection of polar antibiotics in water using a disposable Ag-graphene sensor based on electrophoretic preconcentration and surface-enhanced Raman spectroscopy., Biosens. Bioelectron. 43 (2013) 94–100. doi:10.1016/j.bios.2012.12.005.

[17] D. Li, D.-W. Li, J.S. Fossey, Y.-T. Long, Portable surface-enhanced Raman scattering sensor for rapid detection of aniline and phenol derivatives by on-site electrostatic preconcentration., Anal. Chem. 82 (2010) 9299–305. doi:10.1021/ac101812x.

[18] O. Péron, E. Rinnert, M. Lehaitre, P. Crassous, C. Compère, Detection of polycyclic aromatic hydrocarbon (PAH) compounds in artificial sea-water using surface-enhanced Raman scattering (SERS), Talanta. 79 (2009) 199–204. doi:10.1016/j.talanta.2009.03.043.

[19] A.J. van Hengel, Food allergen detection methods and the challenge to protect food-allergic consumers., Anal. Bioanal. Chem. 389 (2007) 111–8. doi:10.1007/s00216-007-1353-5.

[20] O. Stephan, S. Vieths, Development of a Real-Time PCR and a Sandwich ELISA for Detection of Potentially Allergenic Trace Amounts of Peanut (Arachis hypogaea) in Processed Foods, J. Agric. Food Chem. 52 (2004) 3754–3760. doi:10.1021/jf035178u.

[21] N.A. Abu Hatab, J.M. Oran, M.J. Sepaniak, Surface-enhanced Raman spectroscopy substrates created via electron beam lithography and nanotransfer printing., ACS Nano. 2 (2008) 377–85. doi:10.1021/nn7003487.

[22] W.W. Yu, I.M. White, Inkjet-printed paper-based SERS dipsticks and swabs for trace chemical detection., Analyst. 138 (2013) 1020–5. doi:10.1039/c2an36116g.

[23] C.H. Lee, L. Tian, S. Singamaneni, Paper-based SERS swab for rapid trace detection on real-world surfaces., ACS Appl. Mater. Interfaces. 2 (2010) 3429–35. doi:10.1021/am1009875.

[24] L.-L. Qu, D.-W. Li, J.-Q. Xue, W.-L. Zhai, J.S. Fossey, Y.-T. Long, Batch fabrication of disposable screen printed SERS arrays., Lab Chip. 12 (2012) 876–81. doi:10.1039/c2lc20926h.

[25] P.R. Stoddart, D.J. White, Optical fibre SERS sensors., Anal. Bioanal. Chem. 394 (2009) 1761–74. doi:10.1007/s00216-009-2797-6.

[26] F.L. Yap, P. Thoniyot, S. Krishnan, S. Krishnamoorthy, Nanoparticle Cluster Arrays for High-Performance SERS through Directed Self-Assembly on Flat Substrates and on Optical Fibers, ACS Nano. 6 (2012) 2056–2070. doi:10.1021/nn203661n.

[27] M. Sackmann, S. Bom, T. Balster, A. Materny, Nanostructured gold surfaces as reproducible substrates for surface-enhanced Raman spectroscopy, J. Raman Spectrosc. 38 (2007) 277–282. doi:10.1002/jrs.1639.

[28] L. He, M. Lin, H. Li, N.-J. Kim, Surface-enhanced Raman spectroscopy coupled with dendritic silver nanosubstrate for detection of restricted antibiotics, J. Raman Spectrosc. 41 (2010) 739–744. doi:10.1002/jrs.2505.

[29] M. Keating, Y. Chen, I.A. Larmour, K. Faulds, D. Graham, Growth and surface-enhanced Raman scattering of Ag nanoparticle assembly in agarose gel, Meas. Sci. Technol. 23 (2012) 084006. doi:10.1088/0957-0233/23/8/084006.

[30] Y.-H. Lee, S. Dai, J.P. Young, Silver-doped sol-gel films as the substrate for surface-enhanced Raman scattering, J. Raman Spectrosc. 28 (1997) 635–639. doi:10.1002/(SICI)1097-4555(199708)28:8<635::AID-JRS152>3.0.CO;2-0.

[31] S. Lee, J. Choi, L. Chen, B. Park, J.B. Kyong, G.H. Seong, et al., Fast and sensitive trace analysis of malachite green using a surface-enhanced Raman microfluidic sensor, Anal. Chim. Acta. 590 (2007) 139–144. doi:10.1016/j.aca.2007.03.049.

[32] D. Lee, S. Lee, G.H. Seong, J. Choo, E.K. Lee, D.-G. Gweon, et al., Quantitative Analysis of Methyl Parathion Pesticides in a Polydimethylsiloxane Microfluidic Channel Using Confocal Surface-Enhanced Raman Spectroscopy, Appl. Spectrosc. 60 (2006) 373–377.

[33] W. Wijaya, S. Pang, T.P. Labuza, L. He, Rapid detection of acetamiprid in foods using surface-enhanced Raman spectroscopy (SERS)., J. Food Sci. 79 (2014) T743–7. doi:10.1111/1750-3841.12391.

[34] Electronic Code of Federal Regulations, Acetamiprid; tolerances for residues, 2013.

[35] C.S. Shende, F. Inscore, A. Gift, P. Maksymiuk, S. Farquharson, <title>Analysis of pesticides on or in fruit by surface-enhanced Raman spectroscopy</title>, in: Y.-R. Chen, S.-I. Tu (Eds.), Opt. East, International Society for Optics and Photonics, 2004: pp. 170–176. doi:10.1117/12.569595.

[36] C. Shende, A. Gift, F. Inscore, P. Maksymiuk, S. Farquharson, <title>Inspection of pesticide residues on food by surface-enhanced Raman spectroscopy</title>, in: B.S. Bennedsen, Y.-R. Chen, G.E. Meyer, A.G. Senecal, S.-I. Tu (Eds.), Opt. Technol. Ind. Environ. Biol. Sens., International Society for Optics and Photonics, 2004: pp. 28–34. doi:10.1117/12.511941.

[37] K. Wong-ek, M. Horprathum, P. Eiamchai, P. Limnonthakul, V. Patthanasettakul, P. Chindaudom, et al., <title>Portable surface-enhanced Raman spectroscopy for insecticide detection using silver nanorod film fabricated by magnetron sputtering</title>, in: T. Vo-Dinh, J.R. Lakowicz (Eds.), SPIE BiOS, International Society for Optics and Photonics, 2011: pp. 791108–791108–11. doi:10.1117/12.874601.

[38] B. Liu, P. Zhou, X. Liu, X. Sun, H. Li, M. Lin, Detection of Pesticides in Fruits by Surface-Enhanced Raman Spectroscopy Coupled with Gold Nanostructures, Food Bioprocess Technol. 6 (2012) 710–718. doi:10.1007/s11947-011-0774-5.

[39] B. Liu, G. Han, Z. Zhang, R. Liu, C. Jiang, S. Wang, et al., Shell thickness-dependent Raman enhancement for rapid identification and detection of pesticide residues at fruit peels., Anal. Chem. 84 (2012) 255–61. doi:10.1021/ac202452t.

[40] L. Guerrini, S. Sanchez-Cortes, V.L. Cruz, S. Martinez, S. Ristori, A. Feis, Surface-enhanced Raman spectra of dimethoate and omethoate, J. Raman Spectrosc. 42 (2011) 980–985. doi:10.1002/jrs.2823.

[41] D. Liu, W. Chen, J. Wei, X. Li, Z. Wang, X. Jiang, A highly sensitive, dual-readout assay based on gold nanoparticles for organophosphorus and carbamate pesticides., Anal. Chem. 84 (2012) 4185–91. doi:10.1021/ac300545p.

[42] Y. Xie, G. Mukamurezi, Y. Sun, H. Wang, H. Qian, W. Yao, Establishment of rapid detection method of methamidophos in vegetables by surface enhanced Raman spectroscopy, Eur. Food Res. Technol. 234 (2012) 1091–1098. doi:10.1007/s00217-012-1724-9.

[43] C. Yao, F. Cheng, C. Wang, Y. Wang, X. Guo, Z. Gong, et al., Separation, identification and fast determination of organophosphate pesticide methidathion in tea leaves by thin layer chromatography–surface-enhanced Raman scattering, Anal. Methods. 5 (2013) 5560. doi:10.1039/c3ay41152d.

[44] S. Pang, T.P. Labuza, L. He, Development of a single aptamer-based surface enhanced Raman scattering method for rapid detection of multiple pesticides., Analyst. (2014). doi:10.1039/c3an02263c.

[45] L. He, T. Chen, T.P. Labuza, Recovery and quantitative detection of thiabendazole on apples using a surface swab capture method followed by surface-enhanced Raman spectroscopy., Food Chem. 148 (2014) 42–6. doi:10.1016/j.foodchem.2013.10.023.

[46] X. Tang, W. Cai, L. Yang, J. Liu, Highly uniform and optical visualization of SERS substrate for pesticide analysis based on Au nanoparticles grafted on dendritic α-Fe2O3., Nanoscale. 5 (2013) 11193–9. doi:10.1039/c3nr03671e.

[47] J.F. Li, Y.F. Huang, Y. Ding, Z.L. Yang, S.B. Li, X.S. Zhou, et al., Shell-isolated nanoparticle-enhanced Raman spectroscopy., Nature. 464 (2010) 392–5. doi:10.1038/nature08907.

[48] T. Lang, S. Pang, L. He, Integration of colorimetric and SERS detection for rapid screening and validation of melamine in milk, Anal. Methods. 7 (2015) 6426–6431. doi:10.1039/C5AY00955C.

[49] A.D. Ellington, J.W. Szostak, Selection in vitro of single-stranded DNA molecules that fold into specific ligand-binding structures., Nature. 355 (1992) 850–2. doi:10.1038/355850a0.

[50] C. Tuerk, L. Gold, Systematic evolution of ligands by exponential enrichment: RNA ligands to bacteriophage T4 DNA polymerase, Science (80-.). 249 (1990) 505–510. doi:10.1126/science.2200121.

[51] R. Welz, R.R. Breaker, Ligand binding and gene control characteristics of tandem riboswitches in Bacillus anthracis, RNA. 13 (2007) 573–582. doi:10.1261/rna.407707.

[52] M. Mandal, B. Boese, J.E. Barrick, W.C. Winkler, R.R. Breaker, Riboswitches Control Fundamental Biochemical Pathways in Bacillus subtilis and Other Bacteria, Cell. 113 (2003) 577–586. doi:10.1016/S0092-8674(03)00391-X.

[53] D.L. Robertson, G.F. Joyce, Selection in vitro of an RNA enzyme that specifically cleaves single-stranded DNA., Nature. 344 (1990) 467–8. doi:10.1038/344467a0.

[54] A.D. Ellington, J.W. Szostak, In vitro selection of RNA molecules that bind specific ligands, Nature. 346 (1990) 818–822.

[55] B. Jin, L. Xie, Y. Guo, G. Pang, Multi-residue detection of pesticides in juice and fruit wine: A review of extraction and detection methods, Food Res. Int. 46 (2012) 399–409. doi:10.1016/j.foodres.2011.12.003.

[56] M. Anastassiades, S. Lehotay, D. Štajnbaher, Quick, easy, cheap, effective, rugged, and safe (QuEChERS) approach for the determination of pesticide residues, in: 18th Annu. Waste Test. Qual. Symp. Proceeding, Arlington, VA, 2002: pp. 231–241.

[57] J. Lee, H.K. Lee, Fully automated dynamic in-syringe liquid-phase microextraction and on-column derivatization of carbamate pesticides with gas chromatography/mass spectrometric analysis., Anal. Chem. 83 (2011) 6856–61. doi:10.1021/ac200807d.

[58] M. a Martínez-Uroz, M. Mezcua, N. Belmonte Valles, a R. Fernández-Alba, Determination of selected pesticides by GC with simultaneous detection by MS (NCI) and μ-ECD in fruit and vegetable matrices., Anal. Bioanal. Chem. 402 (2012) 1365–72. doi:10.1007/s00216-011-5552-8.

[59] J.S. Punzi, M. Lamont, D. Haynes, R.L. Epstein, USDA Pesticide Data Program: Pesticide Residues on Fresh and Processed Fruit and Vegetables, Grains, Meats, Milk, and Drinking Water, Outlooks Pest Manag. 16 (2005) 131–137. doi:10.1564/16jun12.

[60] L. Wang, Q. Zhang, D. Chen, Y. Liu, C. Li, B. Hu, et al., Development of a Specific Enzyme-Linked Immunosorbent Assay (ELISA) for the Analysis of the Organophosphorous Pesticide Fenthion in Real Samples Based on Monoclonal Antibody, Anal. Lett. 44 (2011) 1591–1601. doi:10.1080/00032719.2010.520391.

[61] Z.-L. Xu, H. Deng, X.-F. Deng, J.-Y. Yang, Y.-M. Jiang, D.-P. Zeng, et al., Monitoring of organophosphorus pesticides in vegetables using monoclonal antibody-based direct competitive ELISA followed by HPLC–MS/MS, Food Chem. 131 (2012) 1569–1576. doi:10.1016/j.foodchem.2011.10.020.

[62] X. Hua, L. Wang, G. Li, Q. Fang, M. Wang, F. Liu, Multi-analyte enzyme-linked immunosorbent assay for organophosphorus pesticides and neonicotinoid insecticides using a bispecific monoclonal antibody, Anal. Methods. 5 (2013) 1556. doi:10.1039/c3ay26398c.

[63] C.D. Ercegovich, R.P. Vallejo, R.R. Gettig, L. Woods, E.R. Bogus, R.O. Mumma, Development of a radioimmunoassay for parathion., J. Agric. Food Chem. 29 (1981) 559–63.

[64] J.C. Hall, R.J.A. Deschamps, K.K. Krieg, Immunoassays for the detection of 2,4-D and picloram in river water and urine, J. Agric. Food Chem. 37 (1989) 981–984. doi:10.1021/jf00088a035.

[65] Y. Guo, J. Tian, C. Liang, G. Zhu, W. Gui, Multiplex bead-array competitive immunoassay for simultaneous detection of three pesticides in vegetables, Microchim. Acta. 180 (2013) 387–395. doi:10.1007/s00604-013-0944-4.

[66] S. White, Biosensors for Food Analysis, in: L. Nollet (Ed.), Handb. Food Anal. Second Ed. -3 Vol. Set, CRC Press, 2004: pp. 2133–2148.

[67] H. Im, K.C. Bantz, N.C. Lindquist, C.L. Haynes, S.-H. Oh, Vertically oriented sub-10-nm plasmonic nanogap arrays., Nano Lett. 10 (2010) 2231–6. doi:10.1021/nl1012085.

[68] J.-W. Chen, X.-P. Liu, K.-J. Feng, Y. Liang, J.-H. Jiang, G.-L. Shen, et al., Detection of adenosine using surface-enhanced Raman scattering based on structure-switching signaling aptamer., Biosens. Bioelectron. 24 (2008) 66–71. doi:10.1016/j.bios.2008.03.013.

[69] Y. Dong, Y. Xu, W. Yong, X. Chu, D. Wang, Aptamer and its Potential Applications for Food Safety, Crit. Rev. Food Sci. Nutr. (2013) 130524060823006. doi:10.1080/10408398.2011.642905.

[70] L. He, E. Lamont, B. Veeregowda, S. Sreevatsan, C.L. Haynes, F. Diez-Gonzalez, et al., Aptamer-based surface-enhanced Raman scattering detection of ricin in liquid foods, Chem. Sci. 2 (2011) 1579. doi:10.1039/c1sc00201e.

[71] L. Wang, X. Liu, Q. Zhang, C. Zhang, Y. Liu, K. Tu, et al., Selection of DNA aptamers that bind to four organophosphorus pesticides., Biotechnol. Lett. 34 (2012) 869–74. doi:10.1007/s10529-012-0850-6.

[72] M. Li, J. Zhang, S. Suri, L.J. Sooter, D. Ma, N. Wu, Detection of adenosine triphosphate with an aptamer biosensor based on surface-enhanced Raman scattering., Anal. Chem. 84 (2012) 2837–42. doi:10.1021/ac203325z.

[73] F. Barahona, C.L. Bardliving, A. Phifer, J.G. Bruno, C. a. Batt, An Aptasensor Based on Polymer-Gold Nanoparticle Composite Microspheres for the Detection of Malathion Using Surface-Enhanced Raman Spectroscopy, Ind. Biotechnol. 9 (2013) 42–50. doi:10.1089/ind.2012.0029.

[74] L. He, T. Rodda, C.L. Haynes, T. Deschaines, T. Strother, F. Diez-Gonzalez, et al., Detection of a foreign protein in milk using surface-enhanced Raman spectroscopy coupled with antibody-modified silver dendrites., Anal. Chem. 83 (2011) 1510–3. doi:10.1021/ac1032353.

[75] K.G.M. Laurier, M. Poets, F. Vermoortele, G. De Cremer, J.A. Martens, H. UjI-i, et al., Photocatalytic growth of dendritic silver nanostructures as SERS substrates., Chem. Commun. (Camb). 48 (2012) 1559–61. doi:10.1039/c1cc14727g.

[76] L. He, B. D Deen, A.H. Pagel, F. Diez-Gonzalez, T.P. Labuza, Concentration, detection and discrimination of Bacillus anthracis spores in orange juice using aptamer based surface enhanced Raman spectroscopy., Analyst. 138 (2013) 1657–9. doi:10.1039/c3an36561a.

[77] T.M. Herne, M.J. Tarlov, Characterization of DNA Probes Immobilized on Gold Surfaces, J. Am. Chem. Soc. 119 (1997) 8916–8920. doi:10.1021/ja9719586.

[78] K.A. Peterlinz, R.M. Georgiadis, T.M. Herne, M.J. Tarlov, Observation of Hybridization and Dehybridization of Thiol-Tethered DNA Using Two-Color Surface Plasmon Resonance Spectroscopy, J. Am. Chem. Soc. 119 (1997) 3401–3402.

[79] P. Sandstrom, M. Boncheva, B. Akerman, Nonspecific and Thiol-Specific Binding of DNA to Gold Nanoparticles, Langmuir. 19 (2003) 7537–7543.

[80] S. Park, K. a. Brown, K. Hamad-Schifferli, Changes in Oligonucleotide Conformation on Nanoparticle Surfaces by Modification with Mercaptohexanol, Nano Lett. 4 (2004) 1925–1929. doi:10.1021/nl048920t.

[81] A. Wijaya, S.B. Schaffer, I.G. Pallares, K. Hamad-Schifferli, Selective Release of Multiple DNA Oligonucleotides from Gold Nanorods, ACS Nano. 3 (2009) 80–86. doi:10.1021/nn800702n.

[82] P. Jayapal, G. Mayer, A. Heckel, F. Wennmohs, Structure-activity relationships of a caged thrombin binding DNA aptamer: insight gained from molecular dynamics simulation studies., J. Struct. Biol. 166 (2009) 241–50. doi:10.1016/j.jsb.2009.01.010.

[83] W.S. Ross, C.C. Hardin, Ion-Induced Stabilization of the G-DNA Quadruplex: Free Energy Perturbation Studies, J. Am. Chem. Soc. 116 (1994) 6070–6080. doi:10.1021/ja00093a003.

[84] M. McKeague, M.C. Derosa, Challenges and opportunities for small molecule aptamer development., J. Nucleic Acids. 2012 (2012) 748913. doi:10.1155/2012/748913.

[85] Foodsafety.gov, Bacteria and Viruses, (n.d.).

[86] K. Yamada, W. Choi, I. Lee, B.-K. Cho, S. Jun, Rapid detection of multiple foodborne pathogens using a nanoparticle-functionalized multi-junction biosensor., Biosens. Bioelectron. 77 (2016) 137–43. doi:10.1016/j.bios.2015.09.030.

[87] S.M. Yoo, S.Y. Lee, Optical Biosensors for the Detection of Pathogenic Microorganisms., Trends Biotechnol. 34 (2015) 7–25. doi:10.1016/j.tibtech.2015.09.012.

[88] S.P. Ravindranath, Y. Wang, J. Irudayaraj, SERS driven cross-platform based multiplex pathogen detection, Sensors Actuators B Chem. 152 (2011) 183–190. doi:10.1016/j.snb.2010.12.005.

[89] N. Duan, B. Chang, H. Zhang, Z. Wang, S. Wu, Salmonella typhimurium detection using a surface-enhanced Raman scattering-based aptasensor., Int. J. Food Microbiol. 218 (2016) 38–43. doi:10.1016/j.ijfoodmicro.2015.11.006.

[90] H. Zhang, X. Ma, Y. Liu, N. Duan, S. Wu, Z. Wang, et al., Gold nanoparticles enhanced SERS aptasensor for the simultaneous detection of Salmonella typhimurium and Staphylococcus aureus, Biosens. Bioelectron. 74 (2015) 872–877. doi:10.1016/j.bios.2015.07.033.

[91] J. Zheng, L. He, Surface-Enhanced Raman Spectroscopy for the Chemical Analysis of Food, Compr. Rev. Food Sci. Food Saf. 13 (2014) 317–328. doi:10.1111/1541-4337.12062.

[92] O.S. Kolovskaya, A.G. Savitskaya, T.N. Zamay, I.T. Reshetneva, G.S. Zamay, E.N. Erkaev, et al., Development of bacteriostatic DNA aptamers for salmonella., J. Med. Chem. 56 (2013) 1564–72. doi:10.1021/jm301856j.

[93] N. Duan, X. Ding, L. He, S. Wu, Y. Wei, Z. Wang, Selection, identification and application of a DNA aptamer against Listeria monocytogenes, Food Control. 33 (2013) 239–243. doi:10.1016/j.foodcont.2013.03.011.

[94] K. Grabar, R. Freeman, Preparation and Characterization of Au Colloid Monolayers, Anal. …. 67 (1995) 1217–1225. doi:0003-2700/95/0367-0735.

[95] A. Chen, X. Jiang, W. Zhang, G. Chen, Y. Zhao, T.M. Tunio, et al., High sensitive rapid visual detection of sulfadimethoxine by label-free aptasensor., Biosens. Bioelectron. 42 (2013) 419–25. doi:10.1016/j.bios.2012.10.059.

[96] M.R. Rasch, K. V. Sokolov, B.A. Korgel, Limitations on the Optical Tunability of Small Diameter Gold Nanoshells, Langmuir. 25 (2009) 11777–11785. doi:10.1021/la901249j.

[97] T.C. Preston, R. Signorell, Growth and optical properties of gold nanoshells prior to the formation of a continuous metallic layer., ACS Nano. 3 (2009) 3696–706. doi:10.1021/nn900883d.

[98] P. Wang, S. Pang, J. Chen, L. McLandsborough, S.R. Nugen, M. Fan, et al., Label-free mapping of single bacterial cells using surface-enhanced Raman spectroscopy., Analyst. (2016). doi:10.1039/c5an02175h.

[99] B. Guven, N. Basaran-Akgul, E. Temur, U. Tamer, I.H. Boyaci, SERS-based sandwich immunoassay using antibody coated magnetic nanoparticles for Escherichia coli enumeration., Analyst. 136 (2011) 740–8. doi:10.1039/c0an00473a.

[100] Y. Sun, Y. Xia, Gold and silver nanoparticles: A class of chromophores with colors tunable in the range from 400 to 750 nm, Analyst. 128 (2003) 686. doi:10.1039/b212437h.

[101] J.-S. Lee, M.S. Han, C.A. Mirkin, Colorimetric Detection of Mercuric Ion (Hg2+) in Aqueous Media using DNA-Functionalized Gold Nanoparticles, Angew. Chemie. 119 (2007) 4171–4174. doi:10.1002/ange.200700269.

[102] J. Zhang, L. Wang, D. Pan, S. Song, F.Y.C. Boey, H. Zhang, et al., Visual cocaine detection with gold nanoparticles and rationally engineered aptamer structures., Small. 4 (2008) 1196–200. doi:10.1002/smll.200800057.

[103] H. Wei, B. Li, J. Li, E. Wang, S. Dong, Simple and sensitive aptamer-based colorimetric sensing of protein using unmodified gold nanoparticle probes., Chem. Commun. (Camb). (2007) 3735–7. doi:10.1039/b707642h.

[104] C.D. Medley, J.E. Smith, Z. Tang, Y. Wu, S. Bamrungsap, W. Tan, Gold nanoparticle-based colorimetric assay for the direct detection of cancerous cells., Anal. Chem. 80 (2008) 1067–72. doi:10.1021/ac702037y.

[105] S.C.B. Gopinath, T. Lakshmipriya, K. Awazu, Colorimetric detection of controlled assembly and disassembly of aptamers on unmodified gold nanoparticles., Biosens. Bioelectron. 51 (2014) 115–23. doi:10.1016/j.bios.2013.07.037.

[106] S.P. Jeong, S.M. Kang, D. Hong, H.-Y. Lee, I.S. Choi, S. Ko, et al., Immobilization of Antibody on a Cyclic Olefin Copolymer Surface with Functionalizable, Non-Biofouling Poly[Oligo(Ethylene Glycol) Methacrylate], J. Nanosci. Nanotechnol. 15 (2015) 1767–1770. doi:10.1166/jnn.2015.9335.

[107] J. Wu, Y. Zhu, F. Xue, Z. Mei, L. Yao, X. Wang, et al., Recent trends in SELEX technique and its application to food safety monitoring, Microchim. Acta. 181 (2014) 479–491. doi:10.1007/s00604-013-1156-7.

[108] Y.S. Kim, M.B. Gu, Advances in aptamer screening and small molecule aptasensors., Adv. Biochem. Eng. Biotechnol. 140 (2014) 29–67. doi:10.1007/10_2013_225.

[109] L. Li, B. Li, Y. Qi, Y. Jin, Label-free aptamer-based colorimetric detection of mercury ions in aqueous media using unmodified gold nanoparticles as colorimetric probe., Anal. Bioanal. Chem. 393 (2009) 2051–7. doi:10.1007/s00216-009-2640-0.

[110] Y.S. Kim, J.H. Kim, I.A. Kim, S.J. Lee, J. Jurng, M.B. Gu, A novel colorimetric aptasensor using gold nanoparticle for a highly sensitive and specific detection of oxytetracycline., Biosens. Bioelectron. 26 (2010) 1644–9. doi:10.1016/j.bios.2010.08.046.

[111] K.-M. Song, M. Cho, H. Jo, K. Min, S.H. Jeon, T. Kim, et al., Gold nanoparticle-based colorimetric detection of kanamycin using a DNA aptamer., Anal. Biochem. 415 (2011) 175–81. doi:10.1016/j.ab.2011.04.007.

[112] Y. Zheng, Y. Wang, X. Yang, Aptamer-based colorimetric biosensing of dopamine using unmodified gold nanoparticles, Sensors Actuators B Chem. 156 (2011) 95–99. doi:10.1016/j.snb.2011.03.077.

[113] C.-C. Chang, S.-C. Wei, T.-H. Wu, C.-H. Lee, C.-W. Lin, Aptamer-based colorimetric detection of platelet-derived growth factor using unmodified gold nanoparticles., Biosens. Bioelectron. 42 (2013) 119–23. doi:10.1016/j.bios.2012.10.072.

[114] K.-M. Song, E. Jeong, W. Jeon, M. Cho, C. Ban, Aptasensor for ampicillin using gold nanoparticle based dual fluorescence–colorimetric methods, Anal. Bioanal. Chem. 402 (2012) 2153–2161. doi:10.1007/s00216-011-5662-3.

[115] Y. Peng, L. Li, X. Mu, L. Guo, Aptamer-gold nanoparticle-based colorimetric assay for the sensitive detection of thrombin, Sensors Actuators B Chem. 177 (2013) 818–825. doi:10.1016/j.snb.2012.12.004.

[116] C.-C. Huang, Y.-F. Huang, Z. Cao, W. Tan, H.-T. Chang, Aptamer-modified gold nanoparticles for colorimetric determination of platelet-derived growth factors and their receptors., Anal. Chem. 77 (2005) 5735–41. doi:10.1021/ac050957q.

[117] S.-J. Chen, Y.-F. Huang, C.-C. Huang, K.-H. Lee, Z.-H. Lin, H.-T. Chang, Colorimetric determination of urinary adenosine using aptamer-modified gold nanoparticles., Biosens. Bioelectron. 23 (2008) 1749–53. doi:10.1016/j.bios.2008.02.008.

[118] H. Li, L. Rothberg, Colorimetric detection of DNA sequences based on electrostatic interactions with unmodified gold nanoparticles., Proc. Natl. Acad. Sci. U. S. A. 101 (2004) 14036–9. doi:10.1073/pnas.0406115101.

[119] J.J. Storhoff, R. Elghanian, C.A. Mirkin, R.L. Letsinger, Sequence-Dependent Stability of DNA-Modified Gold Nanoparticles, Langmuir. 18 (2002) 6666–6670. doi:10.1021/la0202428.

[120] J. Liu, Y. Lu, Preparation of aptamer-linked gold nanoparticle purple aggregates for colorimetric sensing of analytes., Nat. Protoc. 1 (2006) 246–52. doi:10.1038/nprot.2006.38.

[121] W. Haiss, N.T.K. Thanh, J. Aveyard, D.G. Fernig, Determination of size and concentration of gold nanoparticles from UV-vis spectra., Anal. Chem. 79 (2007) 4215–21. doi:10.1021/ac0702084.

[122] H. Grönbeck, A. Curioni, W. Andreoni, Thiols and Disulfides on the Au(111) Surface: The Headgroup−Gold Interaction, J. Am. Chem. Soc. 122 (2000) 3839–3842. doi:10.1021/ja993622x.

[123] W. Andreoni, A. Curioni, H. Gronbeck, Density functional theory approach to thiols and disulfides on gold: Au(111) surface and clusters, Int. J. Quantum Chem. 80 (2000) 598–608. doi:10.1002/1097-461X(2000)80:4/5<598::AID-QUA9>3.0.CO;2-W.

[124] T. Hermann, Adaptive Recognition by Nucleic Acid Aptamers, Science (80-.). 287 (2000) 820–825. doi:10.1126/science.287.5454.820.

[125] L.C. Bock, L.C. Griffin, J.A. Latham, E.H. Vermaas, J.J. Toole, Selection of single-stranded DNA molecules that bind and inhibit human thrombin, Nature. 355 (1992) 564–566.

[126] Y. Dong, Y. Xu, W. Yong, X. Chu, D. Wang, Aptamer and its Potential Applications for Food Safety, Crit. Rev. Food Sci. Nutr. (2013) 130524060823006. doi:10.1080/10408398.2011.642905.

[127] S. Amaya-González, N. de-los-Santos-Alvarez, A.J. Miranda-Ordieres, M.J. Lobo-Castañón, Aptamer-based analysis: a promising alternative for food safety control., Sensors (Basel). 13 (2013) 16292–311. doi:10.3390/s131216292.

[128] K. Sefah, D. Shangguan, X. Xiong, M.B. O'Donoghue, W. Tan, Development of DNA aptamers using Cell-SELEX., Nat. Protoc. 5 (2010) 1169–85. doi:10.1038/nprot.2010.66.